HYDROGEOLOGICAL CHARACTERIZATION OF A LEGACY WASTE STORAGE SITE AND THE CHALLENGE OF COMMUNICATING UNCERTAINTY

A Thesis Submitted to the
College of Graduate and Postdoctoral Studies
In Partial Fulfillment of the Requirements
For the Degree of Masters of Science
In the Department of Civil, Geological and Environmental Engineering
University of Saskatchewan
Saskatoon
Canada

By

COLLEEN STEELE

PERMISSION TO USE

In presenting this thesis/dissertation in partial fulfillment of the requirements for a Postgraduate degree from the University of Saskatchewan, I agree that the Libraries of this University may make it freely available for inspection. I further agree that permission for copying of this thesis/dissertation in any manner, in whole or in part, for scholarly purposes may be granted by the professor or professors who supervised my thesis/dissertation work or, in their absence, by the Head of the Department or the Dean of the College in which my thesis work was done. It is understood that any copying or publication or use of this thesis/dissertation or parts thereof for financial gain shall not be allowed without my written permission. It is also understood that due recognition shall be given to me and to the University of Saskatchewan in any scholarly use which may be made of any material in my thesis/dissertation.

Disclaimer

Reference in this thesis/dissertation to any specific commercial products, process, or service by trade name, trademark, manufacturer, or otherwise, does not constitute or imply its endorsement, recommendation, or favoring by the University of Saskatchewan. The views and opinions of the author expressed herein do not state or reflect those of the University of Saskatchewan, and shall not be used for advertising or product endorsement purposes.

Requests for permission to copy or to make other uses of materials in this thesis/dissertation in whole or part should be addressed to:

Head of the Department of Civil, Geological and Environmental Engineering
57 Campus Drive
University of Saskatchewan
Saskatoon, Saskatchewan S7N 5A9Canada

OR

Dean
College of Graduate and Postdoctoral Studies
University of Saskatchewan
116 Thorvaldson Building, 110 Science Place
Saskatoon, Saskatchewan S7N 5C9 Canada

ABSTRACT

Analytical groundwater and contaminant transport models rely on estimates of hydrogeological parameters that can range from two to three orders of magnitude. The effect parameter variability has on the results of groundwater and contaminant transport modelling was assessed for a legacy nuclear waste storage site in southern Ontario.

Site specific hydrogeological parameters were estimated from groundwater measurements collected and hydraulic response testing completed at the Site. A 2D groundwater flow and contaminant transport model was developed and three hundred and seventy-five scenarios were modelled by manipulating hydraulic conductivity, dispersivity, and recharge estimates. The results indicate hydraulic conductivity, dispersivity, and recharge all effect contaminant breakthrough times and under/overestimate breakthrough by up to 50 years.

The results of the sensitivity analysis exemplify and confirm that models are only ever tools to test potential outcomes and are limited in their ability to predict future scenarios. The model developed for the Site offers one line of evidence that advective transport of contaminants below waste storage area would be slow, but the model ignores the stratigraphic heterogeneity and geochemical processes that would influence the rate and distance contaminants travel.

The inherent uncertainty of modelling results prompted research into how people interpret and respond to scientific uncertainty. There is a need for the ongoing research into the communication of scientific estimations and depoliticizing scientific results. Questions into how trust effects public buy-in and how to educate without overwhelming the public remain unanswered. Further research into how to effectively communicate scientific results and the inherent uncertainty is needed.

ACKNOWLEDGEMENTS

I would like to thank my supervisor, Dr. Grant Ferguson, for his guidance, encouragement, and enduring patience. Much respect, appreciation, and inspiration is owed to Dr. Ferguson. Thank you for allowing me to learn and fail forward during this process.

I would also like to thank my co-supervisor, Dr. Andrew Ireson, for his thoughtful and critical feedback throughout my degree. I am grateful to my committee members, Dr. Lee Barbour and Dr. Matt Lindsay, for their ability to ask tough questions that aided in my research and to my external examiner, Dr. Robert Patrick, whose feedback was invaluable and much appreciated.

Thank you to my parents for teaching me to not leave things unfinished, to my friends for thoughtful conversations and good laughs, and to my partner, Adrien, whose love and support sustains me. Finally, a world of love and thanks is owed to my little bug, Emerson, whose arrival into this world gave me the motivation to finish this thesis.

TABLE OF CONTENTS

PERMISSION TO USE ..... **i**

ABSTRACT ..... **ii**

ACKNOWLEDGEMENTS ..... **iii**

Chapter 1: Introduction **1**

1.1 Site Description and Background **1**

1.2 Research Objectives **5**

Chapter 2: Literature Review **6**

2.1 Legacy Nuclear Waste Storage Facilities **6**

2.2 Contaminants of Interest **8**

2.2.1 Uranium 8

2.2.2 Arsenic 10

2.3 Groundwater Flow **10**

2.4 Contaminant Transport **11**

2.4.1 Advection 11

2.4.2 Diffusion 12

2.4.3 Dispersion 13

2.5 Groundwater Modelling **13**

2.6 Uncertainty and Public Policy **16**

Chapter 3: Methods **21**

3.1 Historical Review **21**

3.2 Site Description **21**

3.3 Data Collection and Analysis **26**

3.4 Water Level Measurements **26**

3.5 Hydraulic Response Testing **27**

3.6 Groundwater Modelling **27**

3.7 Finite Element Method **30**

3.7.1 Modelling Parameters and Scenarios 33

Chapter 4: Results 29
4.1 Water Level Measurements 29
4.2 Hydraulic Response Testing 33
4.3 Groundwater Modelling and Contaminant Transport 33
4.4 Calibration 34
4.5 Base Case Results 36
Chapter 5: Discussion 48
5.1 Groundwater and Contaminant Transport Modelling 48
5.2 Communicating Uncertainty 50
Chapter 6: Conclusion 52
References 54
Appendix A 63
Appendix B 95

FIGURES

Figure 1.1 – Location of Chalk River Laboratories (Adapted from Cao et al, 2011). 2
Figure 1.2 – 2005 Lidar Survey of WMAF (Killey, 2013). 4
Figure 3.1 – Topographical map of WMAF showing groundwater elevations and cross section locations (Killey, 2013). 23
Figure 3.2 – Stratigraphy along cross section C-C' (Killey, 2013). 24
Figure 3.3 – Stratigraphy along cross section Z-Z' (Killey, 2013). 25
Figure 3.4 – Stratigraphy along cross section Y-Y' (Killey, 2013). 25
Figure 3.5 – Location of installed pressure transducers and hydraulic response tests 26
Figure 3.6 – Conceptual model of WMAF. 31
Figure 3.7 – Model domain showing stratigraphic units. 34
Figure 4.1 – Groundwater levels within the vicinity of WMAF (Killey, 2015). 30
Figure 4.2 – Groundwater level measurement from August 2014 to October 2015. 32
Figure 4.3 – Comparison of the simulated and observed potentiometric elevations across the modelled profile. 35
Figure 4.4 – Simulated potentiometric elevation for the base case scenario. 37
Figure 4.5 – Base case simulated concentration at 5 years. 38
Figure 4.6 – Base case simulated concentration at 10 years. 38
Figure 4.7 – Base case simulated concentration at 25 years. 39
Figure 4.8 – Base case simulated concentration at 50 years. 39
Figure 4.9 – Base case simulated concentration at 100 years. 39
Figure 4.10 – Node locations within the modelling mesh used for analysis. 40
Figure 4.11 – Base case breakthrough time at 16 locations along the contaminant pathway. 40
Figure 4.12 – Breakthrough times along the contaminant pathway showing the influence of hydraulic conductivity. 41
Figure 4.13 – Breakthrough times along the contaminant pathway showing the influence of dispersivity. 42
Figure 4.14 – Breakthrough times along the contaminant pathway showing the influence of the recharge. 43

Figure 4.15 – Breakthrough times along the contaminant pathway showing the influence of hydraulic conductivity excluding unrealistic breakthrough times. 45
Figure 4.16 – Breakthrough times along the contaminant pathway showing the influence of dispersivity excluding unrealistic breakthrough times. 46
Figure 4.17 – Breakthrough times along the contaminant pathway showing the influence of the recharge excluding unrealistic breakthrough times. 47

TABLES

Table 1.1 – Inventory of waste received at WMAF (Killey, 2013). 2
Table 3.1 – Monitoring well stratigraphy 34
Table 3.2 – Modelling Parameters 27
Table 3.3 – Modelling Parameters for Scenarios 28
Table 4.1 – Manual groundwater measurement taken August 2014. 31
Table 4.2 -- Hydraulic response testing results 33
Table 4.3 – Hydraulic Parameters for Scenarios 34
Table 4.4 – Recharge conditions. 35
Table 4.5 – Statistical analysis of predicted and observed head elevations. 36
Table 4.6 – Base case modelling parameters. 37

CHAPTER 1. INTRODUCTION

Legacy waste storage sites can present a challenge for environmental managers. Too often past containment strategies have proved to be ineffective and have led to the contamination of surface and groundwater resources (Um et al., 2009; Muldoon et al., 2009; Gillogly, 2017). The transport of contaminants is typically driven by aqueous transport processes which may be slow in unsaturated materials but can dramatically increase in saturated zones (van der Kamp, 1994). In order to protect water quality and manage contaminated sites effectively, the drivers and controls on groundwater flow and chemistry need to be understood.

The purpose of this thesis is to characterize the hydrogeology and contaminant transport at the Canadian Nuclear Laboratories' (CNL) Chalk River Laboratories (CRL), Waste Management Area F (WMAF) site (Figure 1.1). A 2D numerical model was developed to simulate groundwater flow and contaminant transport at WMAF. A literature review was completed to gain insight into how people engage with groundwater models and the role uncertainty plays in environmental policy.

1.1 Site Description and Background

WMAF was established at CRL in the late 1970s. Between 1976 and 1979, approximately 119,000 tonnes of contaminated soils was transported to WMAF from various sources in Ontario (Killey et al., 1985). This waste consisted of radionuclide contaminated soils and municipal building materials, such as brick, wood, and concrete. Table 1.1 summarizes the quantity of contaminants present in the material placed at WMAF. These quantities were estimated from samples taken at source locations; later investigations have shown that the quantities present at WMAF were initially overestimated and are present at much lower concentrations (Killey, 2015).

Figure 1.1 – Location of Chalk River Laboratories (Adapted from Cao et al, 2011).

Table 1.1 – Inventory of waste received at WMAF (Killey, 2013).

Source	Description	Mass (tonnes)	Radium (GBq)	Arsenic (tonnes)	Uranium (tonnes)
Port Hope, Ontario	U-refinery waste in silt till soil	95100	110	4.2 - 13	0.5 - 1.5
Rideau Road, Ottawa, Ontario	Niobium smelting slag & organic soil	17400	260	64	64
Albion Road, Ottawa, Ontario	Niobium smelting slag, soil	4780	110	13.8	13.8
Mono Mills, Ontario	Radium paint waste in silt till	1530	< 37	-	-
Total		118810	515	4.2 - 13	79

The contaminated materials were transported to site by truck and placed along a topographic flat between a bedrock high and elevated dune (Figure 1.2) (Killey, 2013; Killey, 2015). The water table at this location was deep enough to ensure it remained below the waste materials. The last of the contaminated soils were transported to site in 1979. The waste was graded and overlain by 0.3 m of silty clay, 1 m of sand, and 0.15 m of topsoil (Killey et al., 1985; Killey, 2015). The clay cover was designed to limit infiltration from passing through the waste materials and transporting contaminants to the water table. The high permeability sand placed above the clay cover was meant to keep the clay saturated and prevent fracturing. Unfortunately, within the first year of the cover installation, site monitoring indicating increased moisture contents within the waste materials attributed to cracking within the clay cover.

In 1983 and 1993, extensive site investigations were carried out to determine the implications of the clay cover failure. The results indicated iron hydroxide coatings present in natural sandy sediments were effectively slowing the subsurface transport of uranium and arsenic through sorption. Annual groundwater sampling at WMAF confirmed that the contaminants of interest have yet to reach the water table (Killey et al., 1985; Killey, 2015). Samples taken down gradient of the waste have < 1 ug/L of arsenic, < 1.3 ug/L of uranium, and no radium has been detected to date (Killey, 2013).

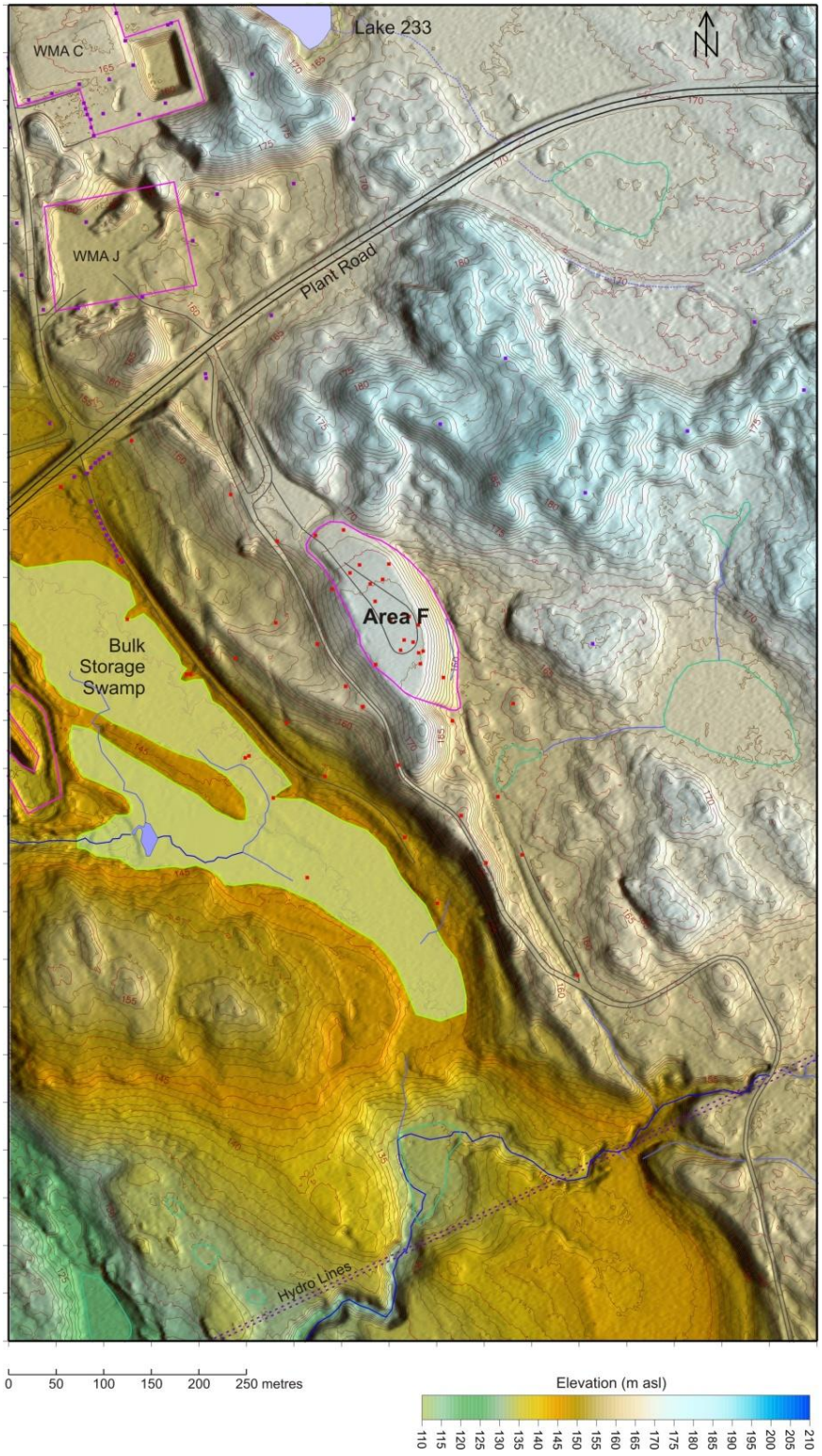

Figure 1.2 – 2005 Lidar Survey of WMAF (Killey, 2013).

1.2 Research Objectives

The main objective for this thesis is to build an understanding of potential subsurface contaminant transport scenarios and explore how people respond to scientific uncertainty. The hypothesis is that the variability of hydraulic parameters makes it difficult to model groundwater flow without a large degree of uncertainty.

Testing the impact of hydraulic parameter variability on groundwater modelling involved the development of a 2D groundwater flow and transport model for WMAF. A number of potential scenarios were generated based on parameter uncertainty and temporal and spatial configurations. Research was conducted to better understand how people understand and respond to scientific uncertainty and how this shapes environmental policy. Policy decisions need to include both scientific study and public involvement; the need for interdisciplinary discussions and collaboration is becoming increasingly important.

CHAPTER 2. LITERATURE REVIEW

This chapter provides context to the research conducted at WMAF and summarizes the relevant literature pertaining to nuclear waste storage, uranium and arsenic geochemistry, groundwater flow, contaminant transport, and public perceptions of uncertainty.

2.1 Legacy Nuclear Waste Storage Facilities

The Manhattan Project in the United States spurred a concerted effort to produce uranium and plutonium resources for the production of nuclear weapons. The largest of the sites developed under the Manhattan Project are the Hanford site in Washington, United States and Oak Ridge in Tennessee, United States. These sites were active until the early 1970s and house large quantities of legacy nuclear waste that continue to pose environmental remediation challenges (Crowley, 2002). Following the cold war, technological advancements in the nuclear industry were concentrated on energy production as an alternative to oil and gas (Gillogly, 2017). The early development of nuclear reactors and power plants was done without much thought or planning of long-term waste management and under little or no regulatory control (Deregel, 2008; Gillogly, 2017). As a result, disposal often led to contamination detrimental to human, ecological, and environmental receptors (Gillogly, 2017).

The challenge with legacy nuclear waste storage facilities is two-fold: we know more now than they did in the past and containment systems do not have an infinite lifespan. Estimating the physical distribution of groundwater contaminants with time is a weighty challenge for hydrogeologists and environmental managers, particularly with radioactive waste where the source terms may persist for tens of thousands of years (Gillham et al., 1982).

Environmental remediation and the study of contaminant transport hinges on the source, pathway, and receptor framework. Typically, the least financially and environmentally costly method of preventing contaminant transport is securing the source. Failing that, cutting off the pathways for contaminant migration to reach a receptor, presents the secondary point of intervention. Once a contaminant reaches receptors, remediation becomes more difficult and costly due to the extent of the area effected and increased potential of risk and/or harm. In the context of legacy nuclear waste, given the lack of planning involved in waste disposal, remediation typically requires intervention all along the source, pathway, receptor lineage. Two sites that illustrate the complexity involved in

remediating legacy nuclear waste are the former Hanford Site in Washington, United States and the Gunnar Mine site in Saskatchewan, Canada.

Historically, the nuclear waste generated at the Hanford Site was deposited directly into the ground, where contaminants have been found migrating into groundwater and surface water systems, or into storage containers that are now leaking (Abbotts et al., 2008; Lichtenstein, 2004). Remediation at the Hanford site involves removal and/or treatment of contaminant sources, cutting off migration pathways, and treating water resources downstream to reduce the impact of contaminants to humans, ecological receptors, and the environment (Abbotts et al., 2008). The Hanford site is the largest superfund site in the United States with most recent remediation estimates ranging from approximately $323B to $677B (Cary, 2019).

Gunnar Mine, located on Lake Athabasca in northern Saskatchewan, operated as a uranium mine and mill from 1957 to 1964. At the time of closure, decommissioning activities were limited to flooding the open pit mine by removing the berm between the open pit and Lake Athabasca and capping the underground shaft. Mine tailings, buildings, and mining infrastructure were largely abandoned with little consideration to future environmental risks (Muldoon, 2009). Radionuclide hazards are present on site in the former mill area, tailings ponds, waste rock piles, and flooded pit. Remediation is currently underway at Gunnar Mine and consists of demolition and removal of asbestos laden buildings, removal and/or treatment of high level biological and chemical hazards, capping underground shaft access, and covering tailings and waste rock areas to restrict contaminant transport and support revegetation (O'Kane, 2015; SRC 2019). The original estimate for remediation and reclamation of Gunnar Mine was approximately $25M, but the latest cost was estimated at $280M (MacPherson, 2019).

The Hanford and Gunnar Mine sites are illustrative of the scientific challenges posed by legacy nuclear waste remediation made further difficult due to the political, economic, regulatory implications. Political and regulatory influences on the local, provincial/state, and federal levels impact the timeline, expenditure, and endpoint objectives that both help and hinder the remediation of legacy nuclear waste sites (Lichtenstein, 2004; MacPherson, 2019; O'Kane, 2008). The effort and expense to remediate legacy industrial sites is immense and reclamation is best planned and budgeted for prior to development (Schamm, 2016).

2.2 Contaminants of Interest

This subsection summarizes the aqueous geochemistry of Uranium and Arsenic which are the primary contaminants of interest at WMAF.

2.2.1 Uranium

Uranium is a naturally occurring actinide metal mineral found in geological formations and an important constituent of groundwater. The presence of uranium in groundwater can be attributed to both natural processes, such as the dissolution of uranium-bearing minerals, and anthropogenic activities such as mine milling operations, nuclear industries, phosphate fertilizer production, and coal combustion. Low concentrations of uranium in drinking water can have detrimental impacts on humans and other species due to the toxicity of the metal. The maximum acceptable concentration for uranium, based on the Guidelines for Canadian Drinking Water Quality, is 0.02 mg/L. This signifies the importance of preventing uranium from entering groundwater systems, particularly from anthropogenic sources.

The transport of uranium from anthropogenic sources in groundwater systems is affected by geochemical aqueous complexation, sorption and exchange, redox processes, and precipitation-dissolution. An understanding of these processes can be a useful component in determining effective containment and/or remediation methods at a particular site.

Like other actinide metals uranium can be present at oxidation states ranging from trivalent uranium to hexavalent uranium (Fein at al. 2013). The most stable and soluble form of uranium in groundwater is hexavalent uranium. This is due to the rapid oxidation of trivalent uranium in groundwater, the rapid disproportionation of pentavalent uranium, and the insoluble nature of tetravalent uranium. The high solubility of hexavalent uranium in comparison to tetravalent uranium provides the basis for many uranium remediation schemes where the question becomes: how do we promote the reduction of hexavalent uranium to tetravalent uranium?

Fein et al. (2013) presented the tetravalent and hexavalent hydrolysis reactions used to model fractionation of uranium species. The modeled hydrolysis results for tetravalent uranium and hexavalent uranium are indicative of how these two oxidation states differ in terms of chemical behavior. The hydrolysis of hexavalent uranium, as discussed by Fein et al. (2013), indicates that $U(OH)_2^{2+}$ dominates at the lower end of the pH scale (pH<5) and $U(OH)_4$ dominates at high pH. Based on previous studies, Fein et al. (2013) stated that the fractional distribution of uranium does

not depend on the total concentration present; no polynuclear aqueous tetravalent uranium species are expected. This differs for the hydrolysis of hexavalent uranium, where an increased concentration of total uranium leads to a different distribution of species. Fein et al. (2013) explains that there is weaker hydrolysis of hexavalent uranium at low pH and the free uranyl ion dominates the system, regardless of the total uranium concentration. At higher pH, the fractionation is dependent on the total uranium concentration available. At near neutral pH with a lower total concentration of hexavalent uranium, aqueous UO_2OH^+ and UO_2OH^{2+} species dominate the system. At higher hexavalent uranium concentrations with near neutral pH, $(UO_2)_3OH^{5+}$ is the dominant species.

A remaining gap in research on uranium speciation is the effect of temperature (Fein et al., 2013). The thermodynamic constants used in the hydrolysis reactions would not be valid at elevated temperatures due to the changes in enthalpy and entropy. The high heat that is typically associated with nuclear fuel repositories emphasizes the need for continued research into uranium aqueous speciation at elevated temperatures.

The transport of uranium in groundwater systems is determined by the constituents present in the system and by concentration, pH, oxidation state, redox potential, and other geochemical factors. Hexavalent uranium is the dominant aqueous species in groundwater systems and the strong bonds formed in carbonate complexes further increases the stability of hexavalent uranium in aqueous form (Barnett et al., 2002; Fein at al. 2013; Guillaumont et al., 2003; Kubicki et al., 2009). The sorption of uranium typically occurs between the pH range of 3 and 9 through a mixture of cation exchange and inner sphere cation/anion bonds. (Barnett et al., 2002; Catalano et al., 2005; Dong et al., 2005; Fein et al., 2013). Sorption, as previously discussed, is hindered by the presence of carbonates and calcium within a system. The reduction of hexavalent uranium through redox is often a coupled reaction with iron. It was also found that an iron-rich surface provides the necessary catalyst in the redox reaction (Behrends et al., 2005; Bots et al., 2008; Charlet et al., 1998; Crane et al., 2011; Liger et al., 1999; Schindler et al., 2013). Understanding microscale precipitation-dissolution can provide insight into the natural processes occurring in sediments. The kinetics involved in precipitation-dissolution reactions is an area that requires further research. (Schindler et al., 2013; Zachara et al., 2013).

2.2.2 Arsenic

Arsenic is a naturally occurring metalloid found in our atmosphere, sediments, groundwater, and surface water. The mobilization of arsenic can be attributed to natural processes, such as weathering and erosion, and anthropogenic activities such as mining and production of pesticides, herbicides, crop desiccants, and wood preservation (Smedley, 2002). Arsenic impacted groundwater can have severe detrimental effects on human health and is a particular concern for countries such as Bangladesh, India, China, Chile, and Argentina where drinking water resources have high concentrations of arsenic. The maximum acceptable concentration for arsenic, based on the Guidelines for Canadian Drinking Water Quality, is 0.010 mg/L.

While arsenic can exist within groundwater systems at varying oxidation states, it typically appears as trivalent arsenite and pentavalent arsenate (Smedley, 2002). Arsenic has a relatively high mobilization rate under a wide range of redox conditions, making it a comparatively problematic oxyanion-forming elements (Smedley, 2002; Phuong et al., 2012). Pentavalent arsenate dominates under oxidizing conditions and mobilizes at high pH, while trivalent arsenite appears in reducing environments (Smedley, 2002; Dixit, 2003). The most widely researched mechanisms for arsenic mobilization, include "microbial reduction of pentavalent arsenate, reductive dissolution of iron oxyhydroxide phases, and competition of solutes for sorption sites on iron oxides." (Dixit, 2003).

An important factor in the occurrence of arsenic in groundwater is desorption/dissolution from iron oxides (Smedley, 2002; Dixit, 2003). Sorption of arsenic to iron oxides occurs at surface sites and tend to be rapid reactions. High concentrations of arsenic within groundwater has been linked to the reductive dissolution of iron oxides and desorption of arsenic (Smedley, 2002). Reducing environments have a considerable effect on arsenic concentrations in groundwater water due to the reductive dissolution and desorption from iron oxides, aluminum oxides, and clay minerals (Smedley, 2002). Both arsenate and arsenite are mobile in the presences of iron oxides and affinity depends on pH, the iron oxide characteristics, and presence of sorption site competitors such as phosphate (Dixit, 2002).

2.3 Groundwater Flow

Groundwater flow is driven by mechanical, thermal, or chemical energy gradients that exist in nature (Fetter, 2001). Groundwater flows through interconnected, open spaces within sediments or rocks and follows the past of least resistance. Darcy's law is fundamental to hydrogeology and

describes fluid flow in porous media. Darcy observed that the difference in hydraulic head, the amount of energy available at a particular location, created a gradient that determines the direction and velocity of fluid flow (Schwartz et al., 2003). Darcy's equation for flow is written as

$$Q = -kiA \quad (2.1)$$

where: Q=discharge (m^3/s)

k=hydraulic conductivity (m/s)

i=hydraulic gradient ($\Delta H/\Delta x$)

A=cross sectional area (m^2)

Within heterogeneous porous media, groundwater flow has both longitudinal and transverse components (Fetter, 2001; Schwartz et al., 2003). Typically, the horizontal length of a continuous stratigraphic unit is greater than the vertical thickness. The direction of groundwater flow within stratigraphic units of a hydrogeological system depends on the hydraulic conductivity of the unit and the surrounding units (Fetter, 2001; Schwartz et al., 2003). Within stratigraphic units of high hydraulic conductivity, i.e. aquifers, groundwater typically flows horizontally. In units with low hydraulic conductivity, such as clay or shale, groundwater flow has a greater vertical component and travel through the stratigraphic unit towards a unit with higher conductivity.

2.4 Contaminant Transport

Groundwater contaminant transport is the study of how dissolved mass enters groundwater systems, how that mass moves through saturated porous media, and what chemical processes occur as that mass encounters other solutes or the porous medium (Schwartz et al., 2003). Contaminant transport encompasses both the physical processes that determine how a solute moves and the chemical and biological processes that define how that solute may change (Schwartz et al., 2003). The three physical mass transport processes within groundwater systems are advection, diffusion, and dispersion.

2.4.1 Advection

Advection is defined as the process by which dissolved solutes are transported by groundwater flow (Fetter, 2001). The direction and rate of mass transport is linked directly to the direction and rate of groundwater flow. As such, Darcy's Law is used to estimate the average linear velocity of advecting contaminants.

$$v = -\frac{K}{n_e} i \qquad (2.2)$$

where: v = velocity (m/s)

K = hydraulic conductivity (m^2/s)

i =hydraulic gradient ($\Delta H/\Delta x$)

n_e= effective porosity

In porous media with high hydraulic conductivity, advection plays an important role in contaminant transport. Diffusion and advection can occur together, but depending on the composition of porous media, one of the processes will dominate and determine the rate at which contaminants travels (Gillham et al., 1982).

2.4.2 Diffusion

Diffusion is defined as the process by which dissolved solutes move through water from areas of high concentration to low concentration (Fetter, 2001). Fick's Laws describe the process of diffusion. Fick's' First Law is applicable for mass flux under steady state conditions:

$$F = -D(\frac{dC}{dx}) \qquad (2.3)$$

where: F = mass flux of solute per unit area per unit time

D = diffusion coefficient (m^2/s)

C = concentration (g/m^3)

x = distance (m)

Ficks' Second Law is applicable when the mass concentration is changing with time:

$$\frac{dC}{dt} = D(\frac{d^2C}{dx^2}) \qquad (2.4)$$

where: D = diffusion coefficient (m^2/s)

C = concentration (g/m^3)

x = distance (m)

t = time (s)

Solutes can move through porous media by diffusion alone, regardless of fluid flow (Fetter, 2001). In porous media with very low hydraulic conductivity, diffusion dominates contaminant transport and solutes may move at a faster rate than that of groundwater (Fetter, 2001, Barbour et al., 2011).

2.4.3 Dispersion

Dispersion is the process by which solute concentrations are diluted as they move through porous media due to mixing (Fetter, 2001). Groundwater velocities will vary within porous media depending on the size and availability of interconnected pore space. Within a pore space, groundwater will move faster at the centre than along the edges and will move faster in large pores versus smaller pores. Groundwater velocities will also vary depending on the length of the flow path around media. The variance in groundwater flow velocities results in mixing and solute distribution along the flow path (Fetter, 2001). Dispersion occurs both in the direction of groundwater flow (longitudinally) and normal to the direction of groundwater flow (transverse). Hydrodynamic dispersion considers both mechanical mixing that occurs in contaminant transport and diffusion (Fetter, 2001).

$$D_L = a_L v_c + D' \qquad (2.5)$$

where: D_L = longitudinal hydrodynamic dispersion coefficient (m^2/s)

a_L = longitudinal dispersivity (m)

v_C = linear groundwater velocity (m/s)

D' = diffusion coefficient (m^2/s)

As mass is transported in groundwater, it spreads beyond the area estimated by the average groundwater velocity and causes "tailing" (Cherry et al., 1975). Dispersion explains the tailing seen in contaminant breakthrough curves (Schwartz, 2003).

2.5 Groundwater Modelling

As discussed in Barbour et al. (2004), modelling can be a powerful tool when used effectively. Models can aid in interpretation, design, and prediction, but it is important to recognize the limitations of modelling. In order for the modelling process to be useful, there needs to be a well-defined problem, a clear understanding of the physical processes, and a reasonable hypothesis. Lacking this, modelling can become a futile act illustrating very little useful information (Barbour et al., 2004, GEO-STUDIOS, 2001).

There are many different modelling approaches and objectives, so thoughtful consideration should be given to the process. Fetter (2001) provides two distinct objectives for modelling: to explain why a groundwater system is behaving in a particular way and to investigate what the groundwater system will do in the future. In a similar assertion, Schwartz et al., (2003) considers three applications for exploratory models: to match historical data, to review scenarios resulting from a policy decision, and to explore conceptual problems. The modelling proposed for WMAF is intended to investigate potential future scenarios.

Models will never fully capture the complexity of natural systems, but they can be useful tools (Fetter, 2001, Schwartz et al., 2003). The following modelling procedure was presented in Schwartz (2003):

1. Evaluate information available
2. If not enough information, acquire new data
3. Create a conceptual model
4. Create and run numerical model
5. Calibrate model, if calibration fails return to step 1
6. Verify model, if verification fails return to step 1
7. Summarize results

The Schwartz (2003) procedure guided the modelling process proposed for WMAF, with exception to the verification step. As Konikow (1992) asserts, models cannot be validated or verified, but rather tested and invalidated based on the original hypothesis. The modified Schwartz (2003) procedure used to guide the modelling process at WMAF is as follows:

1. Evaluate information available
2. If not enough information, acquire new data
3. Create a conceptual model
4. Create and run numerical model
5. Calibrate model, if calibration fails return to step 1
6. Test the hypothesis
7. Summarize results

Contaminant transport problems are more challenging to model than groundwater flow. The complexity of contaminant transport modelling in comparison to groundwater flow modelling is emphasized in Konikow (2011). The added difficulty arises because contaminant transport models depend on how well groundwater flow is defined, contaminants are characterized, and inevitably requires more assumptions to be made. Konikow (2011) describe four fundamental issues in contaminant transport modelling:

1. Conceptual Issues: the conceptual models of contaminant transport are typically based on Fick's law. The Fickian model may not be representative of the hydrodynamic-dispersion and there is a need for a better governing equation.
2. Numerical Issues: the numerical methods that are best for advection controlled transport may not be as useful diffusion controlled transport. Different types of transport may be dominant at different times and locations and the numerical method chosen for the entire domain, may not reflect this.
3. Parameter Estimation: parameters vary with time and space; there is a need for better methods for estimating parameters and their spatial and temporal uncertainty.
4. Model Complexity and Predictive Accuracy: increasing the complexity of a model may decrease the understandability and evaluation of the outcomes.

In 1983, Gorelick et al., emphasized the importance of understanding the impact of parameter uncertainty in models and how this affects both hydraulic and policy evaluations. Many of the issues highlighted in Gorelick (1983) remain a concern for modelers today. The uncertainty of hydrogeological parameters comes from the heterogeneity and anisotropy typically present in the geological structures (He et al., 2013). De Barros et al. (2012) points to the need for understanding how prediction goals, site characterization, and uncertainty are related and evaluated. The uncertainty present in estimating parameters may call for increased measurements and data collection locations. It is important to recognize that increased monitoring and sampling does not directly lead to increased certainty; practitioners must correlate what process they are trying to simulate and what data is relevant (De Barros et al., 2012). There are also cost considerations that cannot be ignored. Increased sampling to reduce parameter uncertainty may not provide sufficient added value in relation to cost.

Different techniques have been employed to aid in the estimation of hydrogeological parameters. Common field experiments that have been used in various subsurface media and at varying scales include slug or flowmeter tests, direct push-pull tests, tracer tests, and injection or pumping tests (Dafflon et al., 2011). Effectively estimating hydraulic parameters is dependent on the type of test used, scale considered, and hydraulic gradients present. Dafflon et al. (2011) found there can be a wide range of parameter estimates from a single test based on initial assumptions and using multiple estimation approaches may be helpful. Schulze-Makuch et al. (1997) examined the relationship between increased hydraulic conductivity estimates with increased aquifer test area. Schulze-Makuch et al. (1997) found that increased hydraulic conductivity estimates corresponded to the increased aquifer area tested during a single test and was independent of the test method. Further, scale dependence of hydraulic conductivity estimated during a single test was not affected by the test method; variability of hydraulic conductivities was attributed to aquifer heterogeneity and high conductivity zones within a low conductivity matrix (Schultz-Makuch et al., 1997).

Gillham et al. (1982) noted the difficulty in predicting future contaminant plumes stemmed from the inability to fully understand the physical and chemical processes that occur in groundwater. While advancement has been made in modelling technology that aids in estimating future contaminant transport paths, uncertainty persists in site specific models due to the complexity of our natural systems (Gillham et al., 1982). In the contaminant transport modelling process, it is important to recognize the weaknesses inherent in the model's conception and mathematics (Konikow, 2011). Models can be useful for estimating possible future outcomes and aid in decision making, but they are limited in terms of forecasting precision (Dougherty et al., 1993). The aim should be to get a suite of reasonable outcomes from a model, versus the 'right' answer.

2.6 Uncertainty and Public Policy

Uncertainty is inherent in all decisions regarding the future, but there is an unreasonable expectation that policy decisions based on scientific research be devoid of uncertainty (Oreskes et al., 1994). Part of this expectation may come from the language used in sharing the results of scientific studies, particularly in the case of models. Models are tools used to test and explore hypotheses, but terms such as predictive, verified, and validated give the public the perception that model are directly analogous to the physical environment (Konikow et al., 1992). While tools such as numerical models may be helpful in analyzing potential risks and consequences, it is naïve to

believe uncertainty can be eliminated. In the context of climate change, forecasting potential future states and evaluating future risk has become increasingly problematic. Milly et al. (2008) characterized a new era the world was entering where we can no longer assume that natural systems will fluctuate within a defined range based on historical data making modelling efforts increasingly fragile and subject to uncertain estimations.

The uncertainty, complexity, and lack of clear solutions to the issue of nuclear waste management shapes public attitudes and affects how policy is adopted. Uncertainty makes people skeptical. Trenberth (2010) described the incredible uncertainty that is present in climate change prediction and how difficult it is to translate this to the public. While the Trenberth (2010) study focused on climate change, but there are parallels that can be made to the issue of nuclear waste management. If the experts are unsure, how do we possibly tackle complex problems? The evidence of Lachapelle et al.'s (2011) study indicated the difficulty of gaining public trust and translating scientific uncertainty. Lachapelle et al. (2011) also illustrated how the public prioritizes problems and the effect of the 'worry basket.' When people are worried about the economy, their next meal, whether they have health care, violence at local and global scales, it makes it hard to move environmental issues to the top of their worry list. The risk of environmental degradation may also not feel as real as many of the other societal problems. Kaspersan (1996) provided an excellent account of how risk is manufactured and perceived by the public. Daily economic, political, and societal woes dramatically broadcasted every hour of every day can amplify the element of risk and prevent people from seeing issues clearly. While there is uncertainty in each of these, the perceived immediacy of the risk determines how likely the public is to engage and act, despite of the uncertainty.

Public attitudes have an obvious effect on policy. As Schneider (2006) described, we have entered a time of post normal science where risk assessment needs to consider what can happen, what are the odds, and how do we know. Scientific evidence will not provide the basis for public buy-in; there is a need for multidimensional and flexible policy (Karl et al., 2008). Unfortunately, adaptive policy requires a willingness to fail. Schneider (2006) made the risks for getting it wrong clear. Policy decisions can over adjust and be wrong or not adjust and have predictions come true. In the risk-adverse climate of most governance structures, there is little willingness to fail forward, go beyond the status quo, involve stakeholders, and address the complexity (Schneider, 2006; Brunner

2010; Camacho, 2009; Huitema et al., 2010; Norman et al., 2011). Policy change needs to take advantage of public attitudes and prepare for policy windows to open (Karl et al., 2008).

Nuclear waste is a contentious political issue. This is evidenced through the highly contested creation of a nuclear waste depository site at Yucca Mountain in Nevada, United States. The study of siting a nuclear waste depository at Yucca Mountains began in the late 1980s and since the initial proposal, there continues to be heated debate as to whether or not the project should move forward and heavy opposition mounted by Nevada citizens (Tollefson, 2011; Easley, 2012; Ewing et al., 2002). In the early 2000s, then President George H. W. Bush recommended the construction of the repository at Yucca, but in 2017, the Obama administration withdrew the application to progress the project without presenting any technical or scientific rationale as to why Yucca was not a viable option for the repository (Tollefson, 2011). Scientific uncertainty regarding future risk has plagued the Yucca mountain project and has resulted in cyclical debate with no clear end in sight.

There is inherent risk associated with nuclear waste, but much of the public concern is in response, as Kaspersan (1996) suggested, to amplification of this risk. Public perceptions are negative largely due to historical associations with nuclear weapons, catastrophic power plant failures, and failed waste management schemes (Slovic et al., 1991). Establishing trust in the nuclear industry is a difficult and enduring task; simply presenting the public with a technical rationale will do little to break down mistrust and ease fear. As Ramana (2013) found, there are both technical and social aspects to safety. Often technical solutions are presented to the public as rational and straightforward, but this approach dismisses the public's distrust or fear that the problem has been underestimated.

The debate around nuclear waste often hinges on what we define as safe. With nuclear waste, contaminants may persist in the environment for tens of thousands of years or longer. Given this, on what time scale is safety predicted and what is a reasonable design life for a waste disposal system? The Environmental Protection Agency in the United Sates set an initial requirement for the waste deposit at Yucca Mountain to ensure no radiation leakage for up to ten thousand years. This was later overturned by the federal courts who ruled the project must protect against radiation leakage for a million years (Scientific American 2008). This presents a clear challenge to scientists not only in a technical sense, i.e. how to you predict how the environment might change in a million years or design materials robust enough to withstand unlimited time and possible future conditions,

but also in a social sense: how can you ensure safety and/or achieve public support when the level of uncertainty is so great?

The importance of public perceptions was made abundantly clear in Fried et al. (2011) comparison of the communities of Port Hope and Kincardine in Ontario, Canada. Both Port Hope and Kincardine have nuclear waste storage facilities within or near their communities, but public attitudes differed. While the people in Kincardine associate the nuclear industry with progressivism and optimism, people in Port Hope associate the industry with environmental damage, regret, cover-ups and secrecy. There are a multitude of reasons why the opinions vary so greatly (Fried et al., 2011).

Eldorado Nuclear Limited (ENL) operated a radium and uranium refinery in Port Hope from the 1930s-1970s and produced low level radioactive waste. The impacted soil from the refinery was largely uncontained and discarded, often for free public use. In the late 1970s, efforts were made to reduce the level and amount of radioactive waste in Port Hope. Over 100,000 tonnes of contaminated soil was transported to CNL for storage at WMAF, but approximately 1.2 million cubic meters of impacted soil remained in Port Hope. Tension existed between industry and Port Hope citizens largely due to the distrust the citizens felt towards the nuclear industry due to the environmental damage they caused and the lack of open communication (Fried et al., 2011). In Kincardine, the waste storage site with established in the early 2000s and the waste was well contained and continually monitored. The waste was also located outside of the community, the citizens could see the economic benefits, and there was collaboration between industry and the community. The importance of communication and cooperative management has an important role. Effective waste management must involve a deconstruction of misconceptions while also providing transparent and accessible data to ensure trust and cooperation.

There has been progress made and nuclear waste management in Canada has seen large transformations in the last 50 years. There has been a notable shift from a top down governmental approach to a more inclusive, cooperative approach. The phased approach, offered by Canada's Nuclear Waste Management Organization (NWMO) Ethical and Social Framework, focuses on community involvement, consent, and support (Wilding, 2012; Johnson, 2007; Ramana, 2013; Fried et al., 2011). The progression of nuclear waste management in Canada is in response, not only to better scientific understanding, but also to understanding the importance of public

perceptions and trust. There is no debate that nuclear waste can be dangerous and must be safeguarded, the debate centers on how and where the waste is stored and will it be safe (Wilding, 2012). The current framework used by NWMO recognizes the importance of public engagement and is a step towards maintaining public trust and support. Despite this, the siting of nuclear waste depositories continues to be heavily debated in Canada with a vocal opposition who are unconvinced deep burial is a safe option (Sorensen, 2019; Turner, 2017). The questions remain, how do we define safety and on what timeline, how can scientific uncertainty be explained in a way that builds trust instead of diminishing it, and can people make confident decisions about nuclear waste management in light of scientific uncertainty?

CHAPTER 3. METHODS

This chapter provides an overview of the study area and a description of the methods used to collect and interpret hydrogeological data. A background review of finite element modelling, a summary of the analytical modelling approach used, and a description of the research conducted into public perceptions of uncertainty is also presented.

3.1 Historical Review

Prior to the site investigation in August 2014, a review of the historical data, compiled by CNL staff, was undertaken. This review involved tabulating past water level measurements, hydraulic parameters for distinct stratigraphic units, and site stratigraphy. Borehole logs and monitoring databases were provided by CNL and reviewed along with the following site reports:

- Killey, D. (2015). Hydrogeological and Contaminant Update at Waste Management Area F.
- Killey, D. (2013). Assessment of Contaminant Movement at Waste Management Area F,
- Killey, D. (2009). Technical Note: Limited Geological & Hydrogeological Investigation of the Proposed NDSS Site 4A.
- Killey, D., Young, J., Welch, S., Dal Bianco, R., King, K. (1993). Waste Management Area F: Arsenic, Radium, and Uranium Distributions 14 years after Emplacement.
- Killey, D., Myrand, D. (1985). The movement of water, Arsenic, and radium at a Chalk River waste management area 1979-1983.
- Gartner Lee Associates Ltd., (1977). Hydrogeological Study of Waste Management Area “F” Port Hope Disposal Site.

3.2 Site Description

CRL is located approximately 200 km northwest of Ottawa, Ontario on the southern shore of the Ottawa River. WMAF was established in 1976 when approximately 100,000 tonnes of radioactive waste material was transported to site for storage. The majority of the waste came from cleanup efforts undertaken at Port Hope in the late 1970s. WMAF is centrally located on CRL property within a small valley bounded to the west by a dune ridge and the east by a bedrock controlled slope (Killey, 2013). The bedrock controlled topographic high forms the local groundwater flow boundary in the northeast and local groundwater discharges to the bulk storage swamp in the southwest (Figure 3.1). Based on hydraulic conductivity and porosity estimates, groundwater

transit times range from 4 to 14 years from the water table below the waste to bulk storage swamp (Killey, 2013).

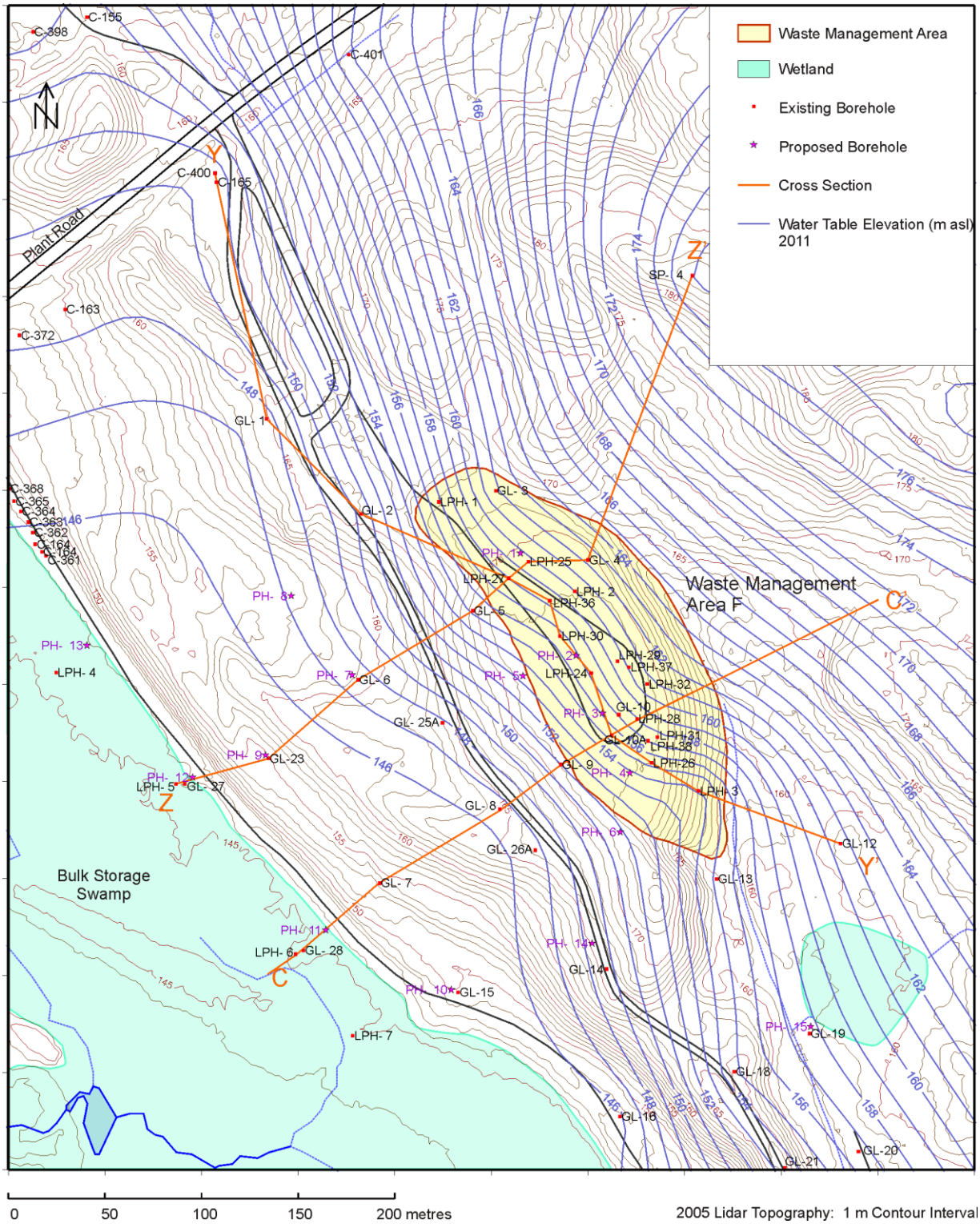

Figure 3.1 – Topographical map of WMAF showing groundwater elevations and cross section locations (Killey, 2013).

The stratigraphy at WMAF is well delineated and typical of a shield depositional setting. Sands are the dominate unconsolidated material in the vicinity of WMAF and overlie discontinuous units of interstratified silt and clay, sand till, and monzonitic to granitic gneiss bedrock (Figure 3.2, Figure 3.3, Figure 3.4) (Killey, 2015). The bedrock is considered highly competent with few microscale fractures. As such, the bedrock is considered to be the local groundwater flow boundary for the site. A gravelly boulder unit has been encountered at many locations overlying the bedrock surface, but is known to be discontinuous and no piezometers have been installed in this unit. Based on past drilling investigations, this unit is assumed to be highly permeable and variable in extent.

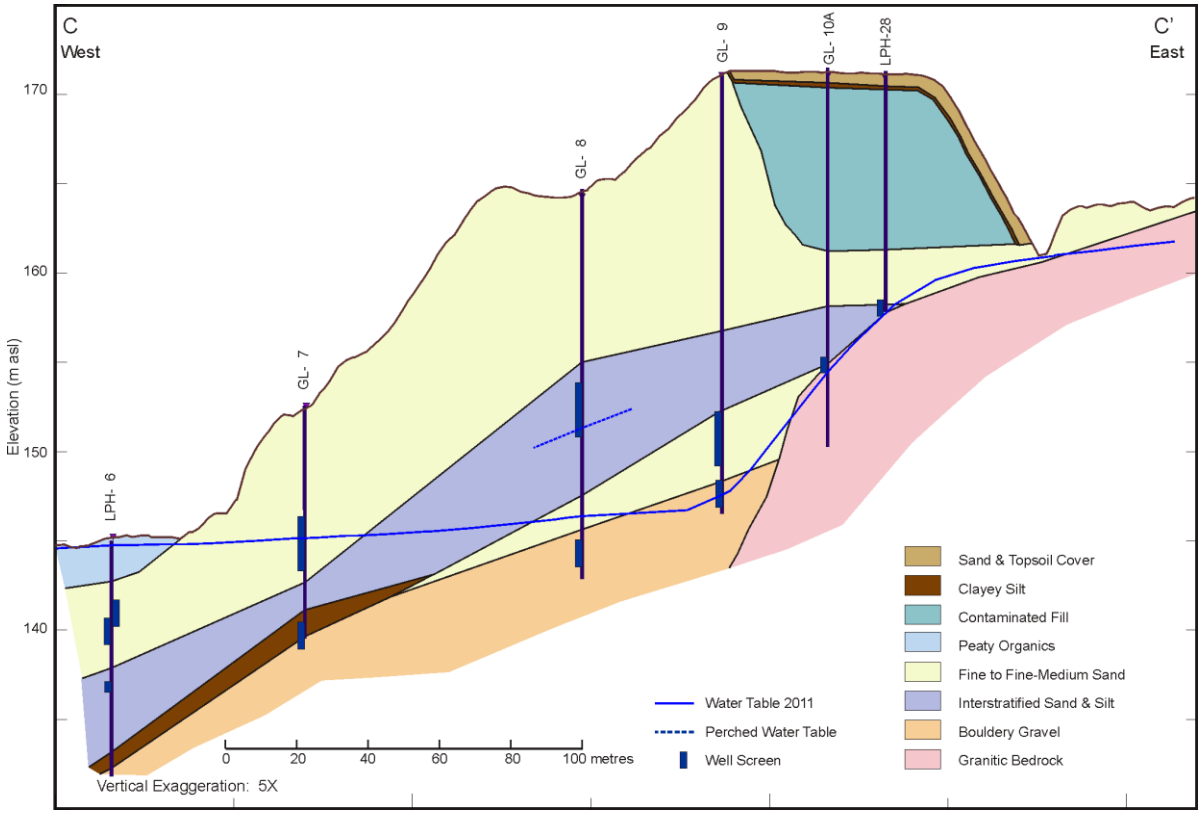

Figure 3.2 – Stratigraphy along cross section C-C' (Killey, 2013).

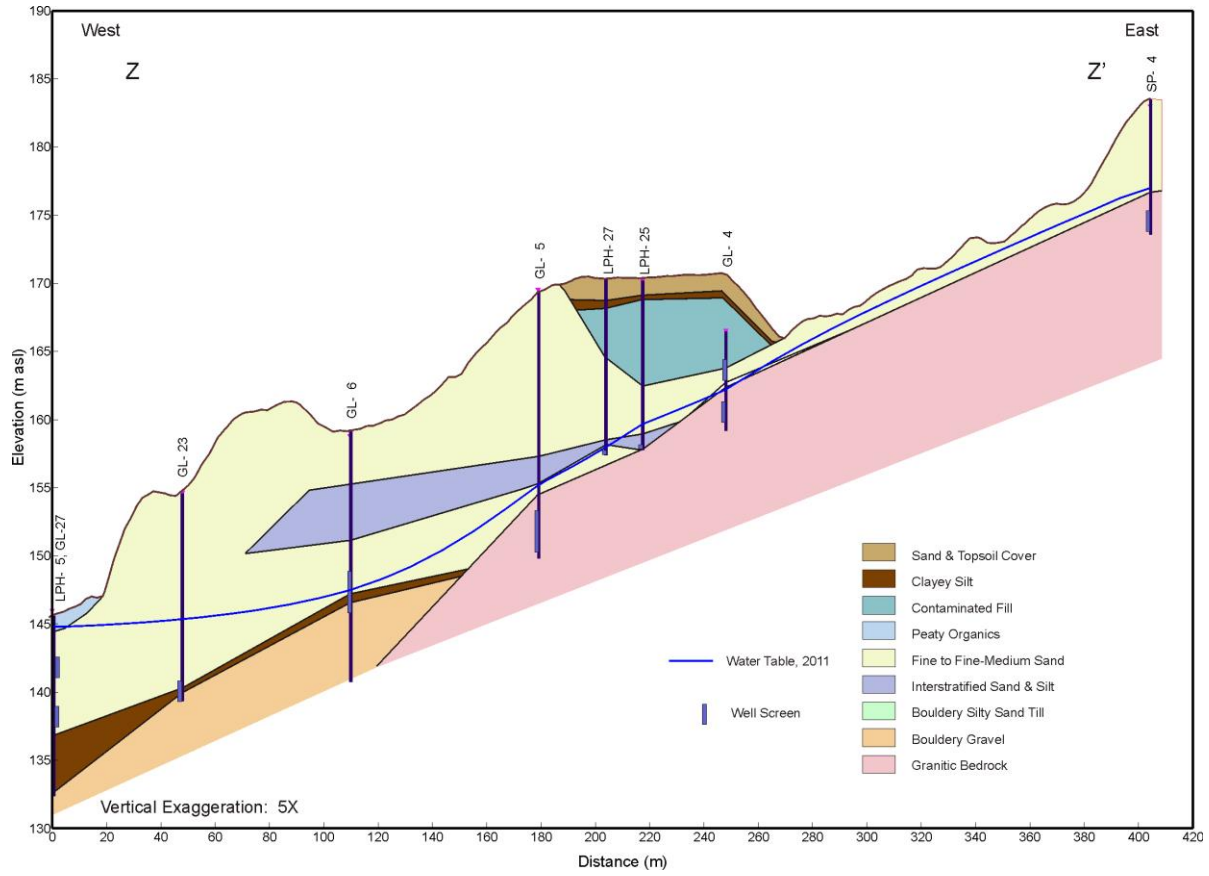

Figure 3.3 – Stratigraphy along cross section Z-Z' (Killey, 2013).

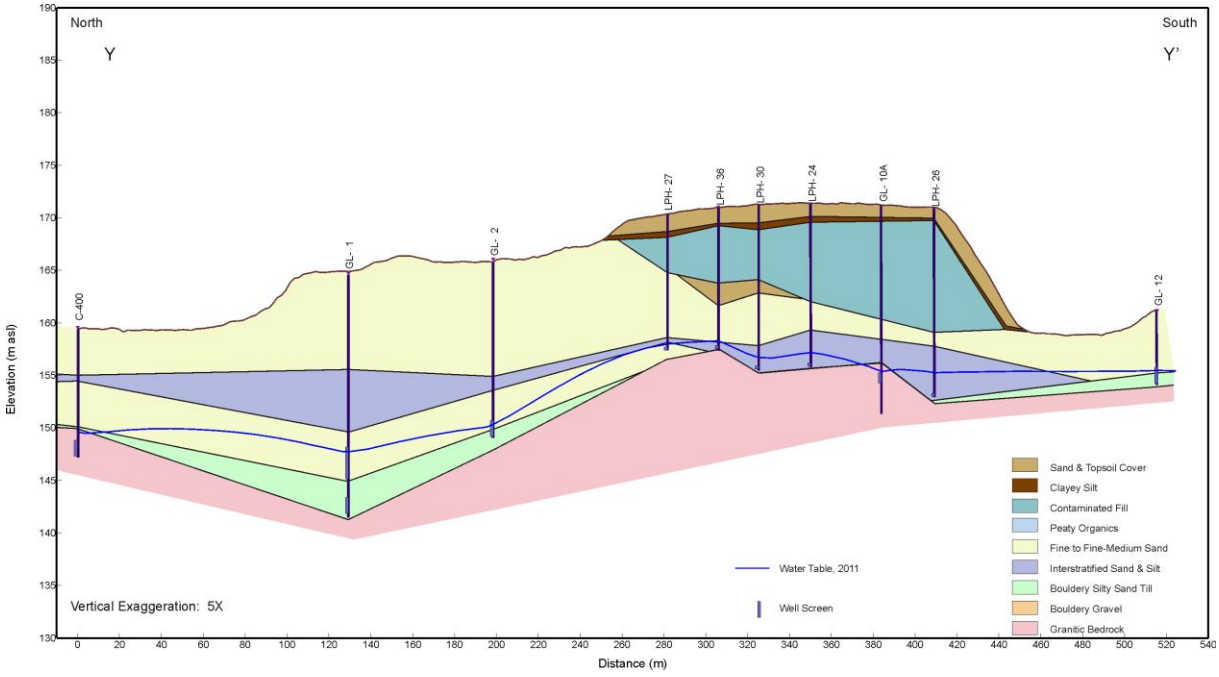

Figure 3.4 – Stratigraphy along cross section Y-Y' (Killey, 2013).

3.3 Data Collection and Analysis

The field component of the thesis was completed in August 2014. Hydraulic response testing and water level measurements were performed using the existing site monitoring wells. The data obtained was used to assess the hydraulic parameters for each of the stratigraphic units and estimate the groundwater flow within the vicinity of the WMAF.

3.4 Water Level Measurements

Water level measurements were taken during the 2014 field program. A water level indicator was used to take manual readings and level loggers were installed in a number of wells to automatically record temporal readings (Figure 3.5). The combination of manual and automated water level measurements ensured that static conditions were achieved and enabled the calculation of vertical and horizontal gradients.

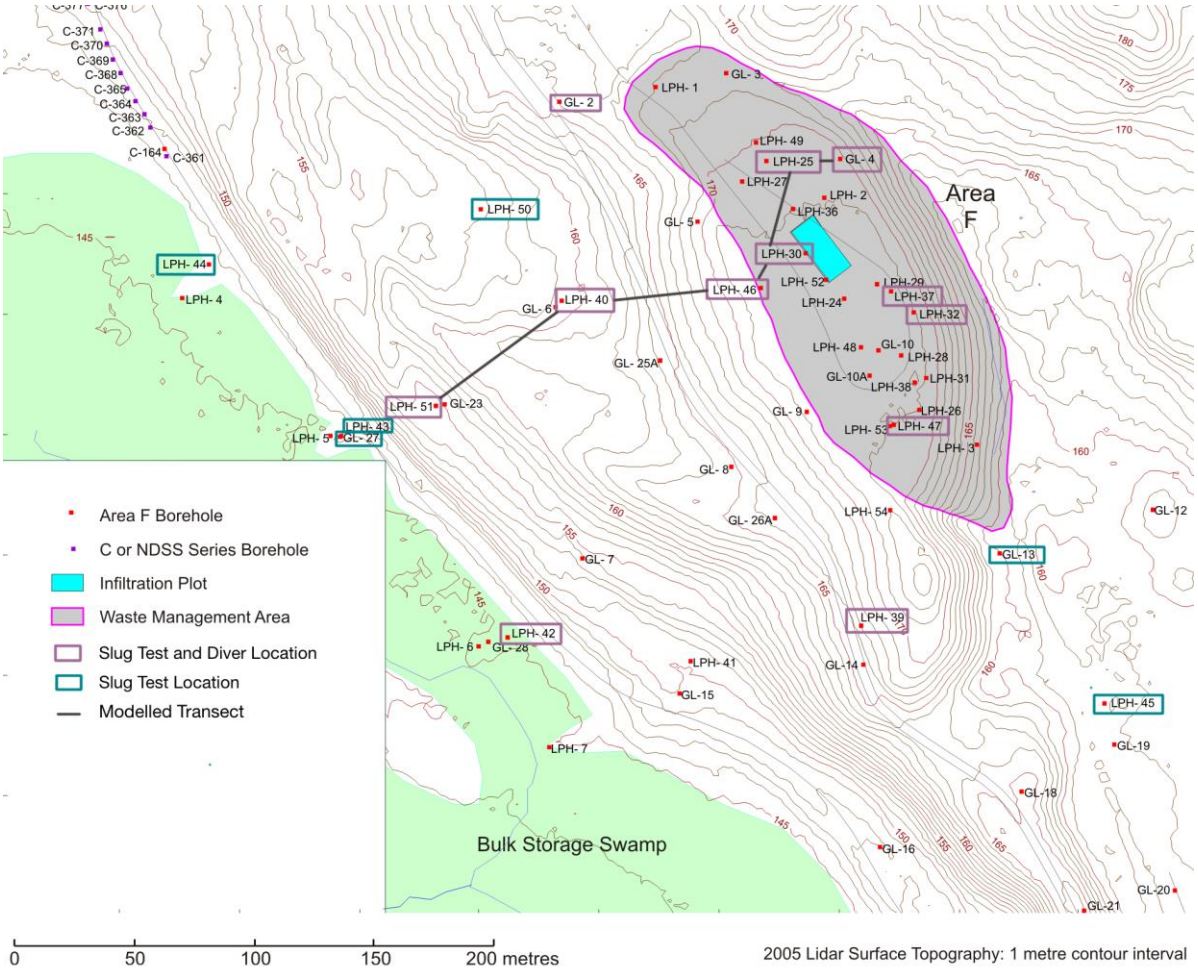

Figure 3.5 – Location of installed pressure transducers and hydraulic response tests

3.5 Hydraulic Response Testing

Hydraulic response testing was completed at 22 locations within WMAF (Figure 3.5). Falling and rising head response tests were completed in wells, where time permitted, through the addition and removal of an aluminum slug, respectively. A manual water level indicator and a logging water level pressure transducer were used to record the aquifer response.

The data obtained from hydraulic response testing was used to estimate the hydraulic conductivity for each formation. These hydraulic parameters were incorporated into numerical models and enabled the estimation of the hydraulic flow regime for the site.

3.6 Groundwater Modelling

The GEO-SLOPE International Ltd. commercial modelling software SEEP/W was used to generate the numerical model. SEEP/W uses Darcy's law to form the fundamental flow equations for modelling. Darcy's law states that the discharge from porous media is proportional to the difference in hydraulic head at the domain end points and inversely proportional to the length of the domain (Fetter, 2001).

Darcy's Law:

$$Q = -kiA \qquad (3.1)$$

where: Q=discharge (m^3/s)

k=hydraulic conductivity (m/s)

i=hydraulic gradient ($\Delta H/\Delta x$)

A=cross sectional area (m^2)

Darcy's law can be written as a specific discharge or Darcian velocity:

$$q = ki \qquad (3.2)$$

where: q=Q/A (m/s)

Darcy's law was originally derived for saturated conditions, but was later shown it could be applied to unsaturated conditions (GEO-SLOPE International Ltd. 2013). In unsaturated conditions, the hydraulic conductivity is no longer assumed to be constant but changes with water content and pressure.

The partial differential equation in unsaturated conditions:

$$\frac{\partial}{\partial x}\left(k_x \frac{\partial H}{\partial x}\right) + \frac{\partial}{\partial y}\left(k_y \frac{\partial H}{\partial y}\right) + Q = \frac{\partial \theta}{\partial t} \quad (3.3)$$

where: k_x=hydraulic conductivity in the x-direction (m/s)

k_y=hydraulic conductivity in the y-direction (m/s)

Q=applied flux (m^3/s)

θ=volumetric water content

t=time (s)

Under steady state conditions, the change in volumetric water content does not change with time and the governing equation reduces to:

$$\frac{\partial}{\partial x}\left(k_x \frac{\partial H}{\partial x}\right) + \frac{\partial}{\partial y}\left(k_y \frac{\partial H}{\partial y}\right) = -Q \quad (3.4)$$

The contaminant transport was modelled using the Geostudios program C-TRAN/W. C-TRAN/W couples with the SEEP/W program to estimate transport based on Darcy's law and hydrodynamic dispersion (Bredehoeft et al., 1973).

Previously, the Darcian velocity was defined as q=Q/A where A is the full cross sectional area. In porous media, the actual cross sectional area available for flow is smaller due to the presence of solids. To account for this reduced area and determine the average linear velocity, the Darcian velocity is divided by the porosity:

$$v = \frac{q}{n} \quad (3.5)$$

where: v=average linear velocity (m/s)

q=Darcian velocity (m/s)

n=porosity ($n=V_v/V_T$)

Under saturated conditions, the volumetric water content is equal to the porosity:

$$v = \frac{q}{\theta} \quad (3.6)$$

The C-TRAN/W program uses the volumetric water content and the Darcian velocity estimated in SEEP/W to determine the average linear velocity for saturated and unsaturated conditions.

The transport equation for advection and dispersion in C-TRAN/W is derived as follows.

Representative elementary volume:

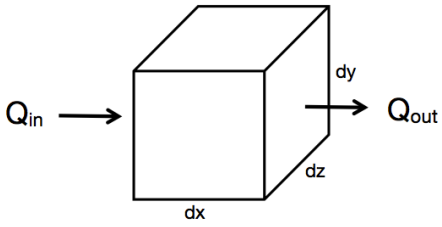

Conservation of Mass:

$$Q_{m\,in} - Q_{m\,out} = \frac{\partial M}{\partial t} \quad (3.7)$$

$$q_m = q_w(C) - \theta(D_h)\left(\frac{\partial M}{\partial t}\right) \quad (3.8)$$

$$M = C(V_T)(\theta) \quad (3.9)$$

where: M=mass (kg)

C=concentration (kg/m^3)

D_h=dispersion coefficient (m^2/s)

q=specified flux

$$Q_{m\,in} - Q_{m\,out} = \frac{\partial M}{\partial t} \quad (3.10)$$

$$q_{m\,in}(dydz) - q_{m\,out}(dydz) = \frac{\partial M}{\partial t} \quad (3.11)$$

$$q_m(dydz) - [(q_m + \frac{\partial q_m}{\partial x}(dx)](dydz) = \frac{\partial M}{\partial t} \quad (3.12)$$

Divergence of mass flux: $$-\frac{\partial q_m}{\partial x}(V_T) = \frac{\partial(\theta V_T C)}{\partial t} \quad (3.13)$$

Assume: $$\frac{\partial \theta}{\partial t} = 0 \text{ and } \frac{\partial V_T}{\partial t} = 0 \quad (3.14)$$

Therefore: $$-\frac{\partial q_m}{\partial x} = \theta \frac{\partial C}{\partial t} \quad (3.15)$$

Sub in (13): $$-\frac{\partial (C q_w - \theta D_h \frac{\partial C}{\partial x})}{\partial x} = n \frac{\partial C}{\partial t} \quad (3.16)$$

Assume: $$\frac{\partial q_w}{\partial x} = 0;\ \frac{\partial \theta}{\partial x} = 0;\ \text{and } \frac{\partial D_h}{\partial x} = 0 \quad (3.17)$$

Therefore: $$-\frac{\partial q_w}{\partial x} + \theta D_h \frac{\partial^2 C}{\partial x^2} = \theta \frac{\partial C}{\partial t} \quad (3.18)$$

Assume: $$\theta_{area} = \theta_{volume} \quad (3.19)$$

Therefore: $$-\frac{q_w}{\theta}\frac{\partial C}{\partial x} + D_h \frac{\partial^2 C}{\partial x^2} = \frac{\partial C}{\partial t} \quad (3.20)$$

Advection-dispersion Equation: $$D_h \frac{\partial^2 C}{\partial x^2} - v \frac{\partial C}{\partial x} = \frac{\partial C}{\partial t} \quad (3.21)$$

A series of outcomes were generated based on the variance in potential spatial and temporal patterns of recharge and range of different hydraulic parameters. In effect, a sensitivity analysis will be performed using the following components:

1. Spatial patterns of recharge,
2. Temporal patterns of recharge,
3. Variance in the hydraulic conductivity for each stratigraphic unit, and
4. Variance in the dispersivity coefficient for each stratigraphic unit.

The sensitivity analysis was used to generate potential outcomes for the site and provide insights into how parameter estimations affect modeling.

3.7 Finite Element Method

A conceptual model of the WMAF site, indicating the boundary conditions used, was developed prior to the creation of the model (Figure 3.6). The local groundwater flow in the vicinity of WMAF is predominantly in the southwest direction with a local groundwater divide located at a

topographic high in the northeast and a surface water discharge location in the southwest. For modelling purposes, it was assumed a no flow boundary exists at the base of the model domain and along the northeast boundary. Average annual recharge at Chalk River is approximately 0.2 m/yr (Robertson et al., 1985; Killey et al., 1985). The vegetation across the modelling domain varies spatially and would impact recharge, but for simplicity recharge was assumed to be a constant flux across the surface. At the southwest extent of the model, the water level within the Bulk Storage Swap was assumed to form the constant head boundary for the model.

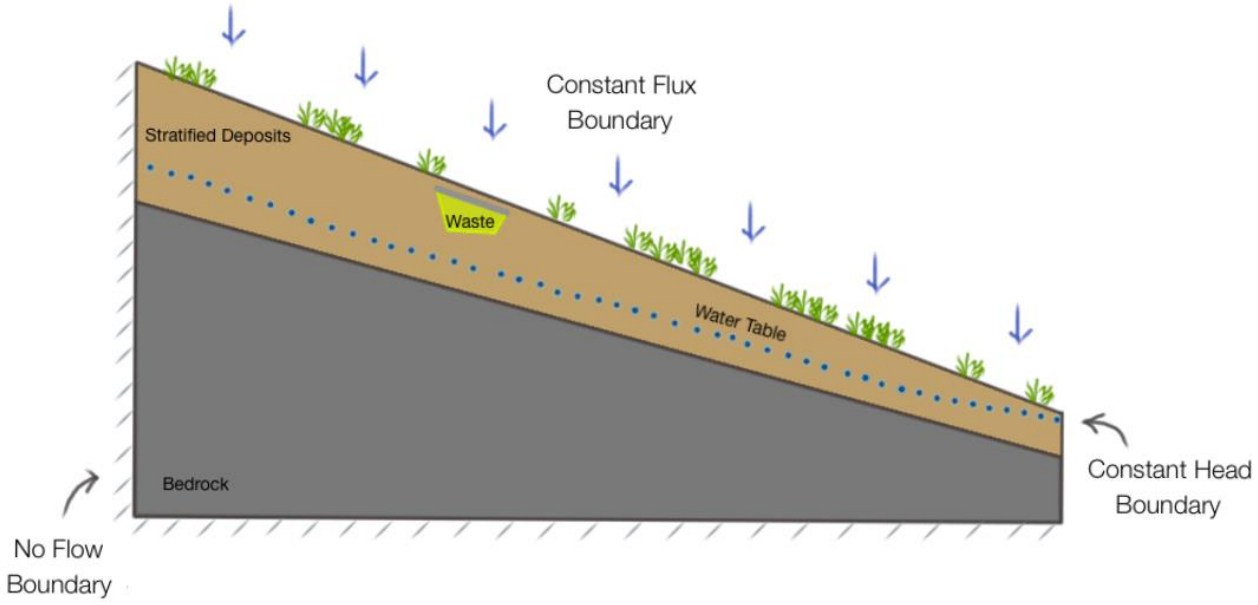

Figure 3.6 – Conceptual model of WMAF.

SEEP/W and C-TRAN/W are finite element modelling programs that use the Galerkin weighted residuals method to commute approximations (GEO-SLOPE International Ltd. 2013). Finite element models (FEM) have an unstructured domain consisting of triangular or irregularly shaped elements (Bear and Cheng 2010). In effect, discretizing the domain into elements allows for local interpolation functions to be defined for each element rather than using a single global function. The approximations for each element are stitched together in a piecewise manner to estimate head levels across the domain.

The Galerkin method is a weighted residual method of integration and is often used in finite element modelling applications. Under steady state conditions, the Galerkin method follows the variation principle philosophy that assumes a physical quantity can be expressed in terms of potential throughout the domain at each of the nodes (Wang and Anderson 1982). In the weighted

residual method, the finite element equation is formulated at each node based on the partial differential equation (Wang and Anderson 1982). The residual error value is calculated based on the degree at which it does not equal the partial governing equation. For example, given the partial differential equation (27), the approximate solution would result in a residual error (Bear and Cheng 2010, Wang and Anderson 1982, GEO-SLOPE International 2013):

$$\frac{\partial}{\partial x}\left(k_x \frac{\partial H}{\partial x}\right) + \frac{\partial}{\partial y}\left(k_y \frac{\partial H}{\partial y}\right) = R(x,y) \neq 0 \qquad (3.22)$$

where: R(x,y)=residual error

The weighted residual method seeks to minimize the error across the model domain through a weighting function (Bear and Cheng 2010):

$$\int R(x,y)dV = 0 \qquad (3.23)$$

where: dV=volume of flow domain

$$\int R(x,y)w_i(x,y)dV = 0; \quad i = 1,2,3 \ldots n \qquad (3.24)$$

where: w_i=the weighting function

The weighting function is defined as some given basis function in the Galerkin method (Bear and Cheng 2010). Unlike other weighted residual methods, the basis function used in the Galerkin method must satisfy the boundary conditions as well as the internal nodes. This method effectively decreases the maximum error across the domain through the integration process. The weighted residual method becomes less accurate when the domain is subdivided into elements because you are integrating over a lower order of polynomials. The Galerkin weight residuals method is an example of an implicit solution and is considered unconditionally stable (Bear and Cheng 2010).

The mesh size and time step used for the steady state and transient problems were estimated based on the Peclet and Courant Criteria (Bear 2012, El-Kadi and Ling 1993, Jousma et al., 1989).

Peclet Criteria: $$\frac{v\Delta x}{D} \leq 2 \qquad (3.25)$$

Courant Criteria: $$\frac{v\Delta t}{\Delta x} \leq 1 \qquad (3.26)$$

where: v=average linear velocity (m/s)

Δx=nodal spacing (m)

D=hydrodynamic dispersion coefficient (m^2/s)

Δt=incremental timestep

3.7.1 Modelling Parameters and Scenarios

The stratigraphy at WMAF was compiled based on borehole logs from past drilling investigations. The simplified stratigraphy within WMAF consists of granitic gneiss overlain with sands, gravels, silts, clays, and till (Table 3.1, Figure 3.7).

Table 3.1 – Monitoring well stratigraphy

Monitoring Well Location	UTM NAD83 (Zone 18N) Easting (m)	UTM NAD83 (Zone 18N) Northing (m)	Cumulative Distance (m)	GL Elevation (masl)	Sand Top Depth (masl)	Clayey Silt Top Depth (masl)	Waste Top Depth (masl)	Sand Top Depth (masl)	Interstratified Sand and Silt Top Depth (masl)	Clayey Silt Top Depth (masl)	Till Top Depth (masl)	Granitic Gneiss Top Depth (masl)	Bottom of Hole (masl)
SP- 4	314235.0	5101379.5	-	182.96	182.96	-	-	-	-	-	-	176.71	172.69
GL- 4	314149.9	5101014.1	375.18	166.51	166.51	-	-	-	-	-	162.7	162.39	159.34
LPH- 25	314119.1	5101013.3	405.99	170.21	170.21	169.12	168.81	162.47	158.96	-	-	157.87	157.81
LPH- 36	314130.2	5100993.3	428.86	171	171	169.41	169.31	163.78	-	-	157.89	-	157.44
LPH- 30	314135.5	5100974.9	448.01	171.18	171.18	169.5	168.89	164.17	157.77	-	-	-	155.48
LPH- 46	314147.8	5101179.2	652.68	171.62	171.62	-	-	-	157.45	-	153.58	-	152.42
LPH- 40	314064.6	5101173.9	736.08	159.24	159.24	-	-	-	152.78	148.06	146.62	145.84	141.81
LPH- 51	314012.0	5101130.1	804.53	154.4	154.4	-	-	-	-	141.45	140.2	-	139.01
LPH- 5	313936.8	5100898.8	1047.72	145.94	145.94	-	-	-	-	136.79	-	-	132.53

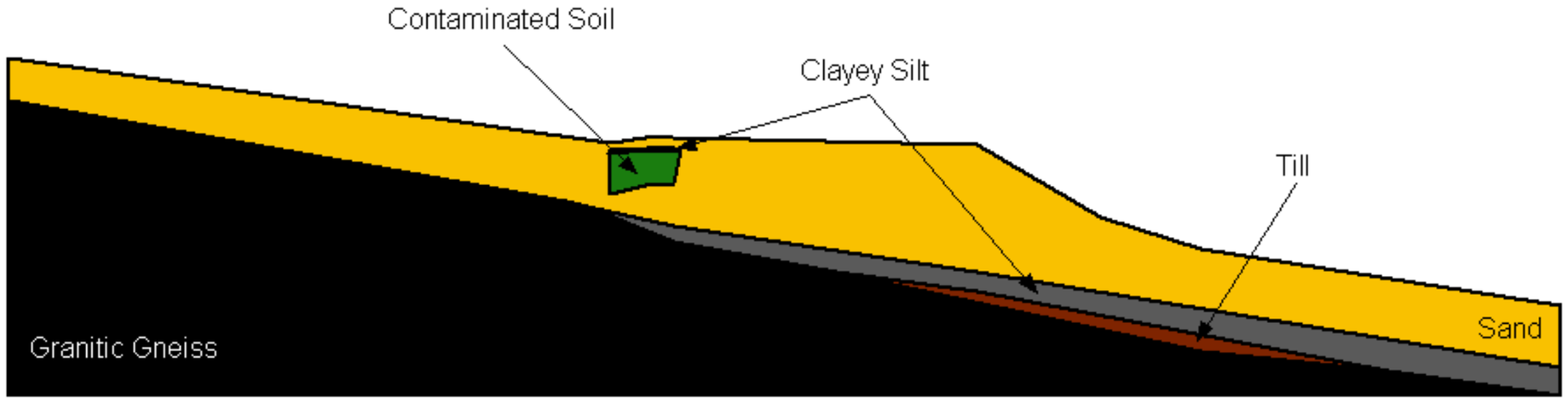

Figure 3.7 – Model domain showing stratigraphic units.

A number of assumptions were made to setup the modelling domain and define the parameters. For the unsaturated zone sediments, the volumetric water content function was estimated based on the average grain size distribution curve. SEEP/W estimates a soil water characteristic curve based on basic material properties using the modified Kovac's method (GEO-SLOPE International Ltd. 2013). The input parameters include saturated volumetric water content, 10% passing grain size, 60% passing grain size, and liquid limit. The grain size distribution was determined from samples taken at site for each of the stratigraphic units. No liquid limit testing was completed; the values for liquid limits were taken from literature for different sediment types.

The saturated hydraulic conductivity values were averaged for each stratigraphic unit based on hydraulic response tests completed at site (Table 3.2). The unsaturated hydraulic conductivity was estimated based on the soil water characteristic curve and the saturated hydraulic conductivity for each unit. All units, excluding the granitic gneiss, were assumed to be unsaturated (Table 3.2). The porosity, anisotropy ratio, and dry density estimates were provided in a number of CNL reports (Table 3.2).

Table 3.2 – Modelling Parameters

Stratigraphic Unit	Saturated Hydraulic Conductivity (m/s)	Estimated Liquid Limit* (%)	Porosity (%)	Kv/Kh	D60 (mm)	D10 (mm)	Dry Density (g/m^3)
Sand	8.00E-05	20	38	3	0.262	0.137	1.70E+06
Clayey Silt	5.00E-07	70	42	0.1	0.046	0.005	1.70E+06
Waste**	1.00E-06	50	38	1	0.2	0.08	1.70E+06
Sand	8.00E-05	20	38	3	0.262	0.137	1.70E+06
Interstratified Sand and Silt	8.40E-05	30	42	0.1	0.125	0.023	1.70E+06
Clayey Silt	5.00E-07	70	42	0.1	0.046	0.005	1.70E+06
Till	5.00E-06	50	26	1	0.225	0.021	1.70E+06
Granitic Gneiss	1.00E-08	-	1	1	-	-	2.70E+06

* Typical liquid limit values from: ftp://ftp.fao.org/fi/cdrom/fao_training/FAO_Training/General/x6706e/x6706e08.htm

** No lab testing completed, all values estimated based on material properties

A number of scenarios were run to determine the effect of different parameters on the results. The parameters were used to generate approximately 375 scenarios (Table 3.3).

Table 3.3 – Modelling Parameters for Scenarios

Spatial Distribution of Recharge	Hydraulic Conductivity	Dispersivity Coefficient
1x (entire profile)	Average	Average
0.5x (entire profile)	0.1x	0.1x
2x (entire profile)	0.5x	0.5x
1x (up/down slope), 1.5x (waste)	2x	2x
0.5x (up/down slope), 2x (waste)	10x	10x

CHAPTER 4. RESULTS

This chapter summarizes the results of the data collection and analysis completed at WMAF.

4.1 Water Level Measurements

Groundwater flow within the vicinity of WMAF generally follows local topography and flows from the northeast to the southwest towards the Bulk Storage Swamp. The potentiometric elevations were obtained November 2014 by staff at CNL (Figure 4.1).

During the 2014 field season, point groundwater level measurements were collected at select monitoring wells within the vicinity of WMAF (Table 4.1). Pressure transducers were installed in 15 wells to automatically collect groundwater level data on a half hour basis. These wells were selected to observe seasonal trends along the topographic profile from the waste storage location towards the bulk storage swamp. The groundwater levels were collected from August 2014 to October 2016 (Figure 4.2, Appendix A). No data was recorded between 9 September 2015 and January 2016 due to lack of CNL staff availability. Subtle seasonal trends were observed with potentiometric highs occurring, as anticipated, during spring and early summer (April to July) on an annual basis. At most piezometer locations, groundwater elevations vary by approximately 1 m on annual basis.

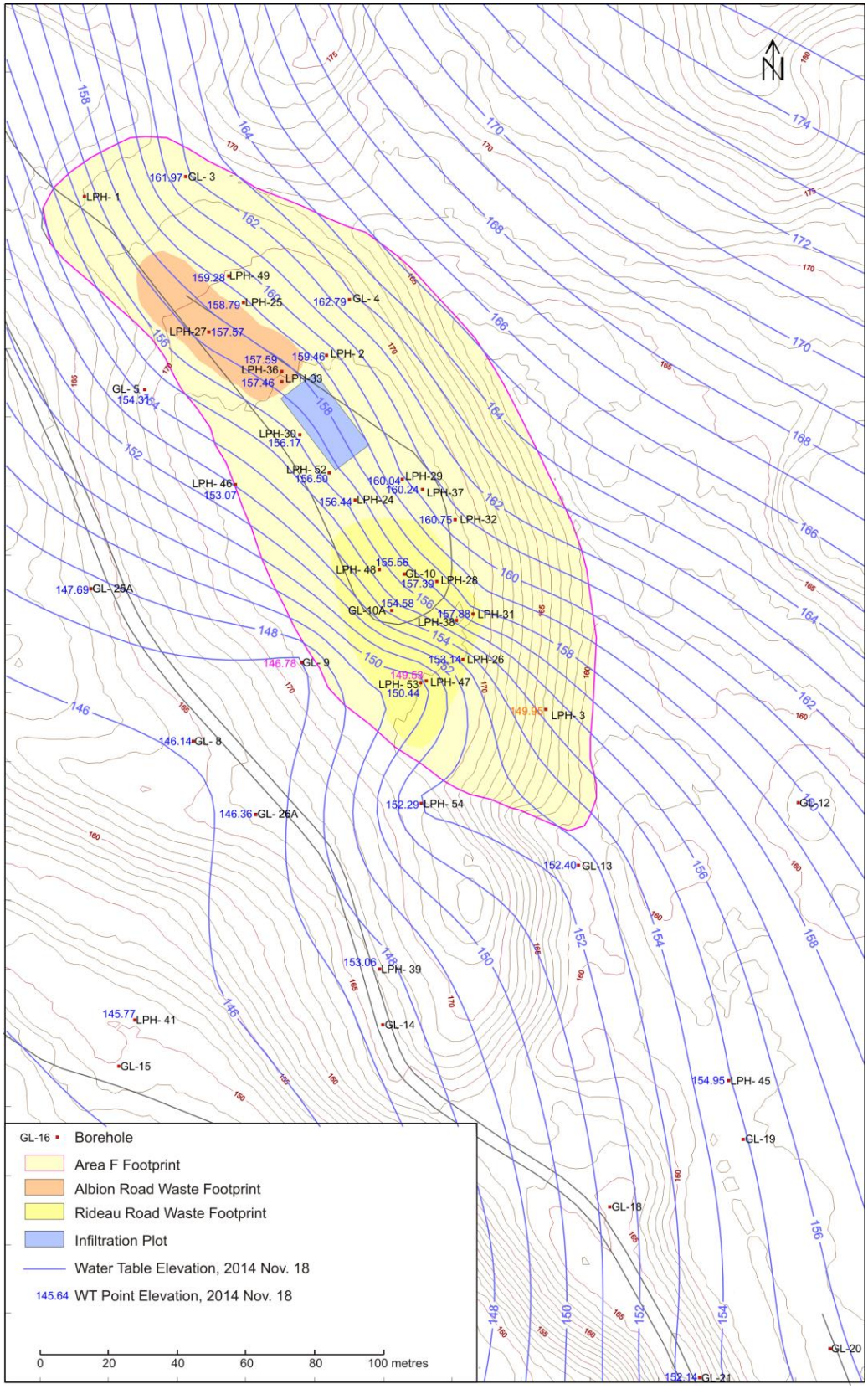

Figure 4.1 – Groundwater levels within the vicinity of WMAF (Killey, 2015).

Table 4.1 – Manual groundwater measurement taken August 2014.

Borehole	Number	UTM Coordinates				Total Depth	Ground Elev.	TOC Elev.	Stick-up	Diameter	Screen Length	Top of Screen	Bottom of Screen	TOS Elev.	BOS Elev.	Static WL	Static WL Elev.	Date WL Obtained
		NAD27		NAD83														
		Easting	Northing	Easting	Northing	(m)	(m)	(m)	(m)	(mm)	(m)	(m)	(m)	(m)	(m)	(mbTOC)	(m)	
GL- 2	I	314032.5	5101038.0	314063.6	5101256.8	16.86	166.02	166.67	0.65	32.00	1.52	15.33	16.86	150.69	149.16	17.02	149.64	14-Aug
GL- 4	II	314149.9	5101014.1	314181.0	5101232.9	3.63	166.51	172.45	5.94	25.40	1.52	2.10	3.63	164.40	162.88	10.33	162.12	14-Aug
LPH- 25	I	314119.1	5101013.3	314150.2	5101232.1	12.34	170.21	171.45	1.24	25.40	0.30	12.04	12.34	158.17	157.87	12.57	158.89	14-Aug
LPH- 30	I	314135.5	5100974.9	314166.6	5101193.7	15.55	171.18	172.10	0.92	32.00	0.30	15.25	15.55	155.93	155.63	15.86	156.24	14-Aug
LPH- 32	I	314180.7	5100950.2	314211.8	5101169.0	12.65	170.95	171.64	0.69	32.00	0.30	12.34	12.65	158.61	158.30	10.95	160.70	14-Aug
LPH- 37	I	314171.2	5100959.0	314202.3	5101177.8	12.56	171.16	172.00	0.84	32.00	0.30	12.26	12.56	158.90	158.60	11.78	160.21	14-Aug
LPH- 39	I	314158.7	5100819.7	314189.8	5101038.5	22.83	166.70	167.61	0.91	50.00	3.05	19.78	22.83	146.92	143.87	19.83	147.78	14-Aug
LPH- 39	II	314158.2	5100821.4	314189.3	5101040.2	16.73	166.73	167.63	0.90	50.00	1.52	15.21	16.73	151.52	150.00	14.33	153.30	14-Aug
LPH- 40	II	314033.5	5100955.1	314064.6	5101173.9	17.39	159.24	160.22	0.97	32.00	3.05	14.34	17.39	144.90	141.85	12.52	147.70	14-Aug
LPH- 41	I	314087.4	5100804.9	314118.5	5101023.7	14.31	150.27	151.02	0.75	50.00	3.05	11.26	14.31	139.01	135.96	5.34	145.68	14-Aug
LPH- 41	II	314090.3	5100803.7	314121.4	5101022.5	6.77	150.25	151.17	0.92	50.00	1.52	5.25	6.77	145.00	143.48	5.32	145.85	14-Aug
LPH- 42	I	314010.9	5100814.8	314042.0	5101033.6	11.12	145.66	146.64	0.98	50.00	3.05	8.07	11.12	137.59	134.54	1.51	145.13	14-Aug
LPH- 42	II	314011.7	5100815.6	314042.8	5101034.4	1.80	145.74	146.66	0.92	50.00	1.52	0.28	1.80	145.46	143.94	1.61	145.04	14-Aug
LPH- 43	I	313940.8	5100898.4	313971.9	5101117.2	19.76	146.22	147.18	0.96	50.00	1.52	18.24	19.76	127.98	126.46	2.13	145.05	14-Aug
LPH- 43	II	313941.3	5100897.7	313972.4	5101116.5	3.36	146.23	147.29	1.06	50.00	1.52	1.84	3.36	144.39	142.87	2.22	145.07	14-Aug
LPH- 45	I	314260.4	5100787.3	314291.5	5101006.1	9.67	159.03	159.92	0.89	50.00	3.05	6.62	9.67	152.41	149.36	5.21	154.71	14-Aug
LPH- 45	II	314260.3	5100787.4	314291.4	5101006.2	5.74	159.09	160.02	0.93	50.00	1.52	4.22	5.74	154.87	153.35	5.17	154.86	14-Aug
LPH- 46	II	314116.7	5100960.4	314147.8	5101179.2	19.34	171.62	172.54	0.92	50.00	3.05	16.29	19.34	155.33	152.28	19.95	152.59	14-Aug
LPH- 47	II	314172.3	5100903.4	314203.4	5101122.2	21.54	171.03	172.00	0.97	50.00	1.52	20.02	21.54	151.01	149.49	22.45	149.55	14-Aug
LPH- 50	I	313999.7	5100993.2	314030.8	5101212.0	10.83	156.70	157.64	0.94	50.00	1.52	9.31	10.83	147.39	145.87	10.59	147.05	14-Aug
LPH- 51	I	313980.9	5100911.3	314012.0	5101130.1	15.05	154.40	155.36	0.96	50.00	1.52	13.53	15.05	140.87	139.35	9.75	145.61	14-Aug

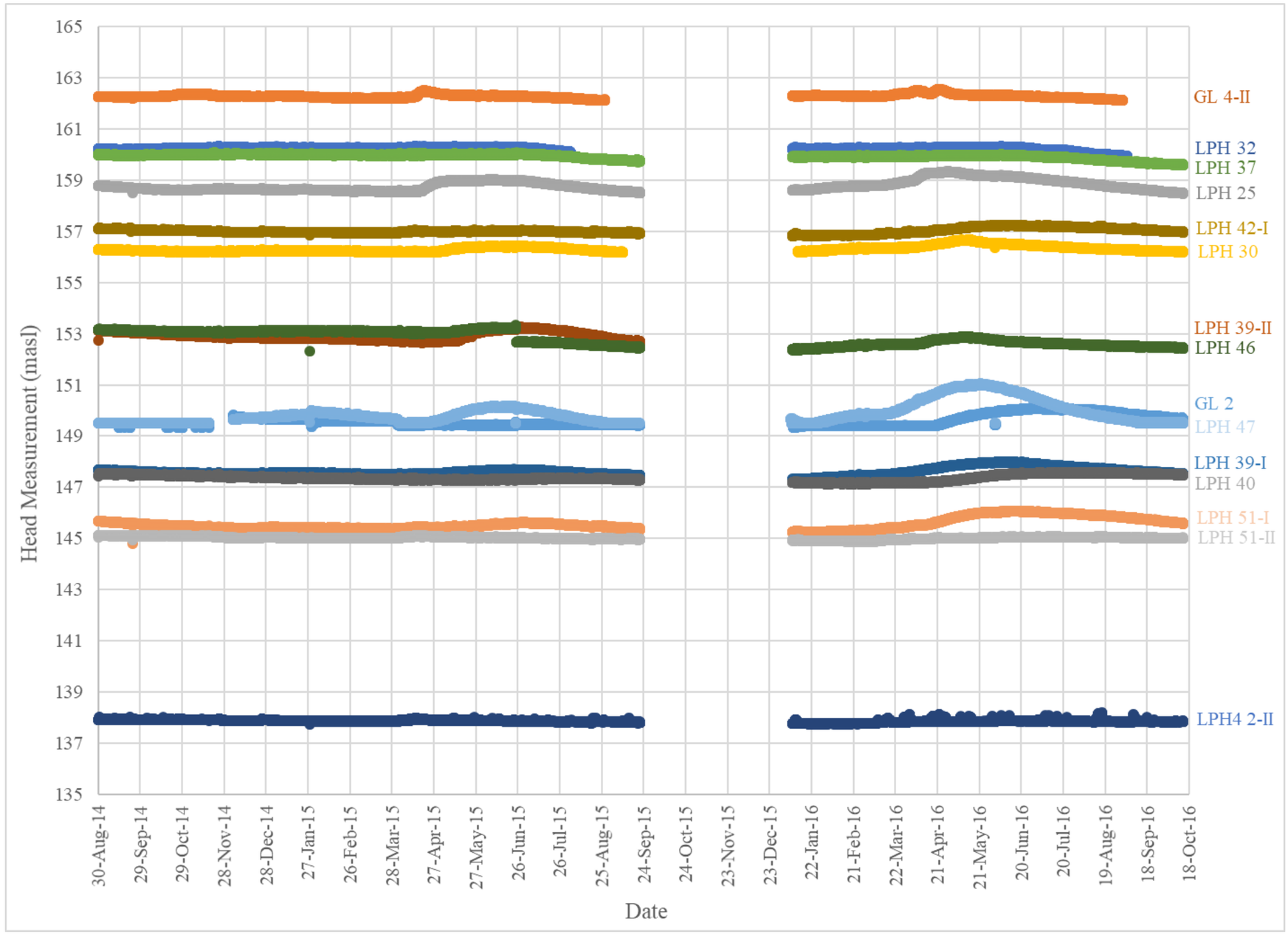

Figure 4.2 – Groundwater level measurement from August 2014 to October 2015.

4.2 Hydraulic Response Testing

Falling and rising head tests were completed at all piezometer locations with the exception of LPH-25, LPH 30, LPH 43, and LPH 47. Only falling head tests were completed at these locations due to insufficient water column height measured from the base of the piezometer to the top of the water table.

The response test data was analyzed using AQTESOLV software (**Error! Reference source not found.**). The Hvorslev method was used for estimating hydraulic conductivities for each stratigraphic unit (Table 4.2).

Table 4.2 -- Hydraulic response testing results

Borehole	Number	Stratigraphy	Hydraulic Conductivity (m/s)		
			Min	Max	Mean
GL- 2	I	Till	7.77E-07	1.51E-06	1.08E-06
LPH- 25	I	Silt	1.40E-06		
LPH- 30	I	Silt	3.56E-06		
LPH- 32	I	Sand	4.74E-06	6.12E-06	5.38E-06
LPH- 37	I	Till	2.57E-04	1.73E-06	2.11E-05
LPH- 39	II	Sand (perched)	1.18E-05	1.88E-05	1.49E-05
LPH- 40	II	Bedrock	1.24E-07		
LPH- 41	II	Sand	1.57E-04	2.22E-04	1.87E-04
LPH- 42	I	Sand	2.12E-06	1.56E-05	5.74E-06
LPH- 42	II	Sand	8.07E-05	9.56E-05	8.79E-05
LPH- 43	I	Till	6.92E-07		
LPH- 43	II	Sand	1.32E-04	1.76E-04	1.53E-04
LPH- 45	I	Till	1.68E-06	1.67E-06	1.68E-06
LPH- 45	II	Sand	1.09E-06	4.06E-06	2.11E-06
LPH- 46	II	Silt	1.04E-06	5.33E-04	2.35E-05
LPH- 47	II	Till	2.28E-06		
LPH- 50	I	Silt	1.27E-06	6.79E-07	9.28E-07
LPH- 51	I	Till	5.66E-07	6.41E-07	6.02E-07

4.3 Groundwater Modelling and Contaminant Transport

Three hundred and seventy five scenarios were considered to estimate the potential groundwater contaminant transport to the bulk storage swamp. These scenarios were based on the manipulation

of three parameters: hydraulic conductivity, dispersivity coefficient, and spatial distribution of recharge (Table 4.3, Appendix B). The hydraulic conductivity and the dispersivity coefficient were varied by two orders of magnitude. Recharge was considered in two ways. The first was to vary the recharge applied to the entire profile and the second was to vary the ratio of recharge occurring on the vegetated slopes to the largely exposed waste area.

Table 4.3 – Hydraulic Parameters for Scenarios

Spatial Distribution of Recharge	Hydraulic Conductivity	Dispersivity Coefficient
1x (entire profile)	Average	Average
0.5x (entire profile)	0.1x	0.1x
2x (entire profile)	0.5x	0.5x
1x (up/down slope), 1.5x (waste)	2x	2x
0.5x (up/down slope), 2x (waste)	10x	10x

The contaminant transport scenarios were constrained by the following assumptions:

1. Simulations were evaluated using a conservative tracer (chloride) at a concentration of 1000g/m^3.
2. Simulations were run for a 100 year period assuming a constant contaminant source.
3. Steady-state flow was assumed for each scenario and the elevation of the bulk storage swamp remained constant.

The contaminant transport modelling was limited to the saturated zone below WMAF. As such, a constant contaminant source was applied to water table below the waste. A mass flux free exit boundary was applied to the discharge face of the modelling domain.

4.4 Calibration

Five different potentiometric elevations were simulated under different recharge conditions and used to assess the effect spatial distribution of recharge has on the modelled results (Table 4.4).

Table 4.4 – Recharge conditions.

Base Case		R1		R2		R3		R4	
1x (entire profile)		0.5x (entire profile)		2x (entire profile)		1x (up/down slope), 1.5x (waste)		0.5x (up/down slope), 2x (waste)	
Recharge		Recharge		Recharge		Recharge		Recharge	
Slope	Waste	Slope	Waste	Slope	Waste	Slope	Waste	Slope	Waste
(mm/yr)	(mm/yr)	(mm/yr)	(mm/yr)	(mm/yr)	(mm/yr)	(mm/yr)	(mm/yr)	(mm/yr)	(mm/yr)
0.22	0.22	0.11	0.11	0.44	0.44	0.22	0.33	0.11	0.44

For calibration purposes, the potentiometric elevations simulated in SEEPW were compared to the field measurements taken at WMAF (Figure 4.3).

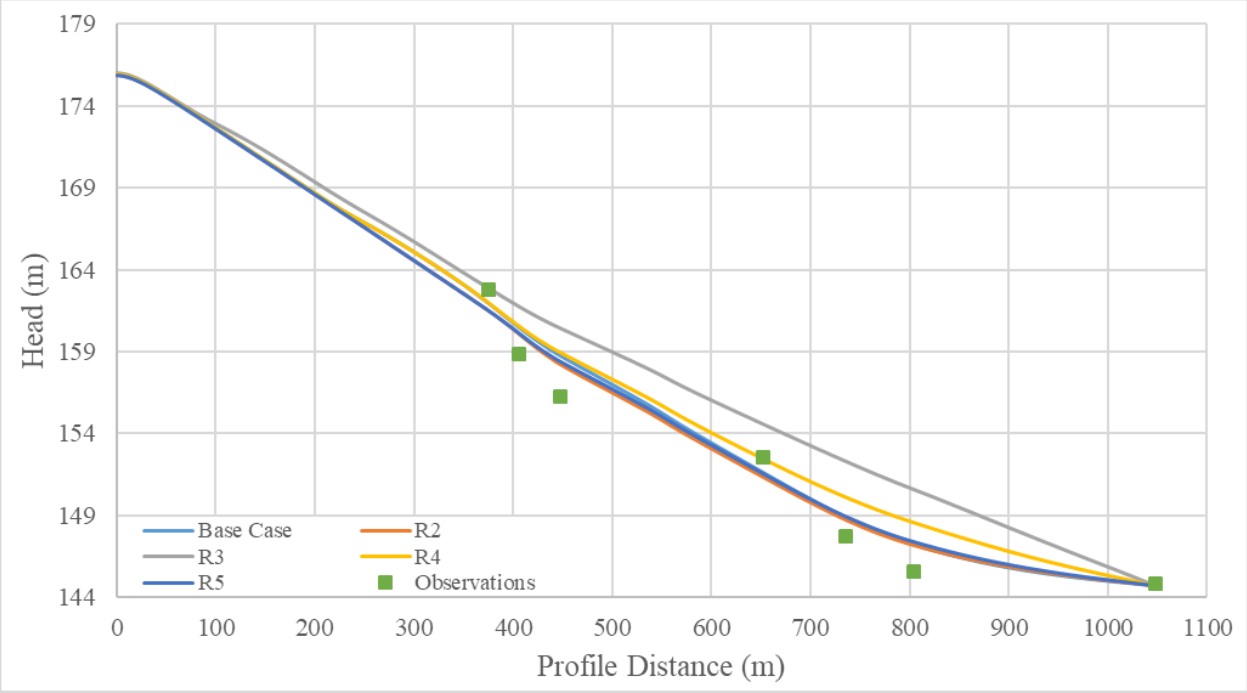

Figure 4.3 – Comparison of the simulated and observed potentiometric elevations across the modelled profile.

The simulated heads for each of the different recharge conditions follow the general trend of the field observations. The misfit can be attributed to recharge inputs within the model and the misalignment between piezometer locations and the modelled transect. Where recharge was doubled across the profile (R2), the potentiometric head is approximately 1.0-5.0 m greater than the field observations. Scenario R4, where the vegetated slope recharge is decreased by half and

the waste area recharge is doubled, the simulated potentiometric head elevation increases downslope from 500 m to the end of the profile due to the increased recharge applied to the waste area. The base case, R1, and R3 scenarios result in similar head simulations that closely align with field observations. Scenarios R1 and R3 both show slightly lower head elevations near the waste area (~500 m) despite having more (R3) or less (R1) recharge applied the waste area. This indicates that increasing the portion of recharge applied to a small area may not greatly affect the modelled results. A statistical comparison of observed and predicted head elevations from each modelled scenario was completed using RMSE and R^2 with P Value. Based on the statistical analysis, the head elevations predicted by the R1 scenario most closely matched that of the measured elevations, whereas the R2 scenario predictions most poorly fit the observed data.

Table 4.5 – Statistical analysis of predicted and observed head elevations.

Method	BC	R1	R2	R3	R4
RMSE	1.343	1.227	3.075	1.775	1.298
R Squared	0.985	0.986	0.962	0.981	0.985
P Value	0.21	0.422	0.018	0.081	0.328

Typically, modelling results are calibrated to select field observations to ensure the model can accurately represent a groundwater system. The purpose of the groundwater contaminant transport modelling for WMAF is to estimate future state of the groundwater. This is a predictive exercise and there are no site specific observations that can be used to evaluate or compare with the contaminant transport modelling results.

4.5 Base Case Results

The base case scenario was based on the average hydrostratigraphy in the vicinity of WMAF, an average potentiometric surface, and average hydraulic parameters (Table 4.6). The steady state groundwater flow model was generated in SEEPW. The steady-state groundwater flow model was used to simulate the base case potentiometric surface at WMAF (Figure 4.4).

Table 4.6 – Base case modelling parameters.

Saturated Hydraulic Conductivity						Longitudinal Dispersivity	Transverse Dispersivity	Recharge
Sand	Clayey Silt	Waste	Interstratified Sand and Silt	Till	Granitic Gneiss			
(m/s)	(m/s)	(m/s)	(m/s)	(m/s)	(m/s)	(m)	(m)	(mm/yr)
8.0E-05	5.0E-07	1.0E-06	8.40E-05	5.0E-06	1.0E-08	1.0E+00	1.0E-03	0.22

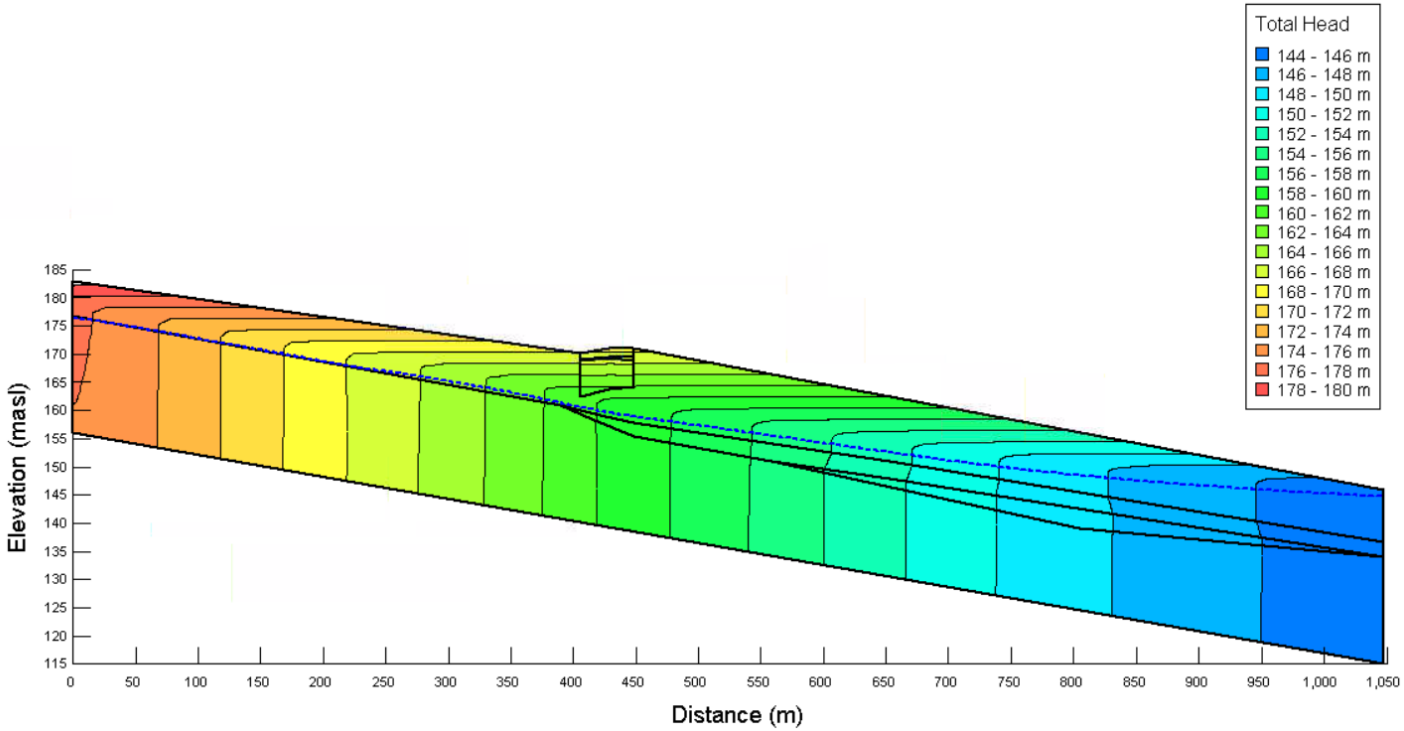

Figure 4.4 – Simulated potentiometric elevation for the base case scenario.

The base case contaminant transport was simulated at 5, 10, 25, 50 and 100 years (Figure 4.5 to Figure 4.9). The potential contaminant plume reaches the bulk storage swamp at a concentration of 500 g/m^3 within 25 years and after 100 years, the advancing front has reached a vertical distance of approximately 10 m below the groundwater table.

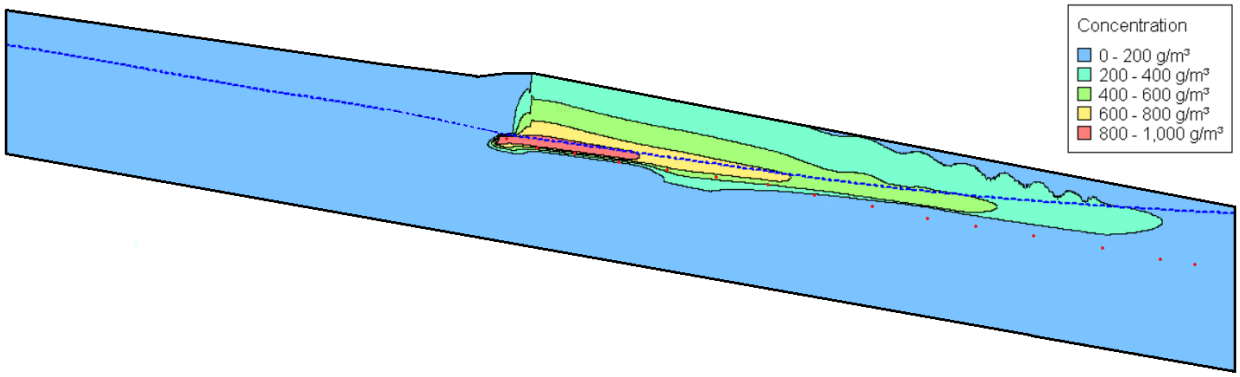

Figure 4.5 – Base case simulated concentration at 5 years.

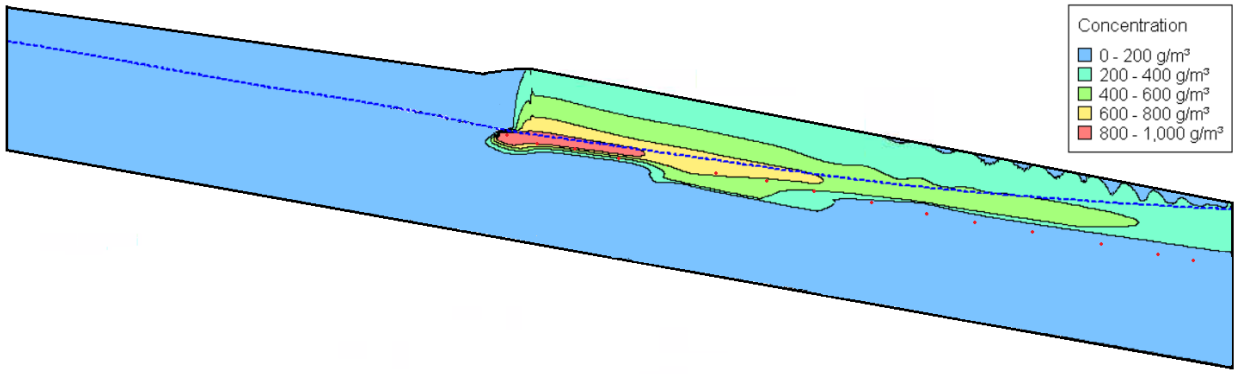

Figure 4.6 – Base case simulated concentration at 10 years.

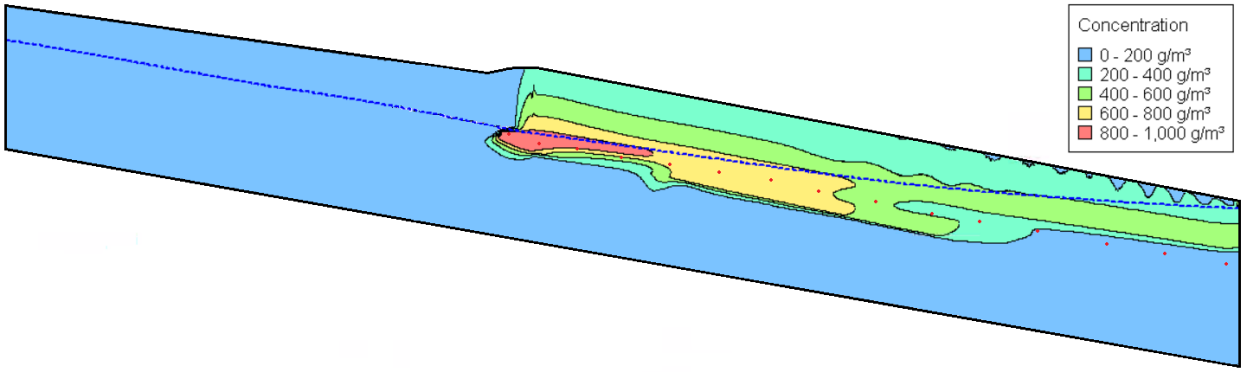

Figure 4.7 – Base case simulated concentration at 25 years.

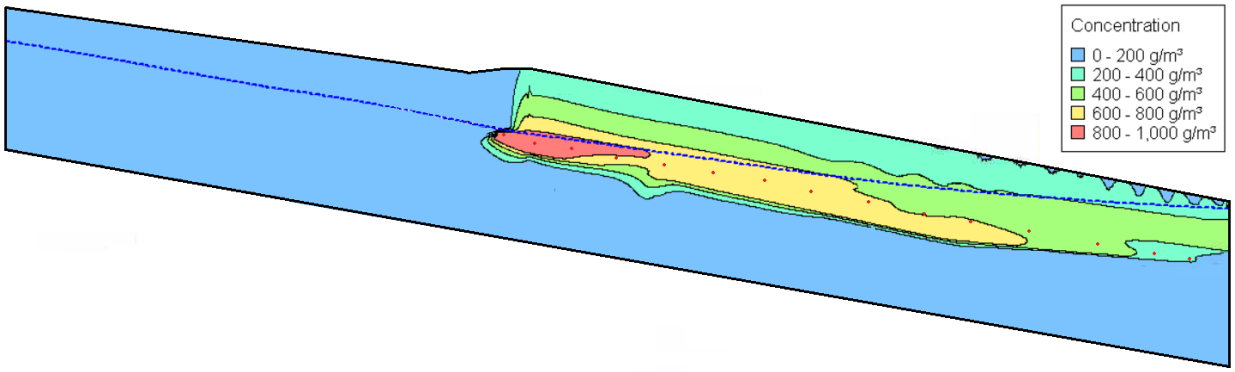

Figure 4.8 – Base case simulated concentration at 50 years.

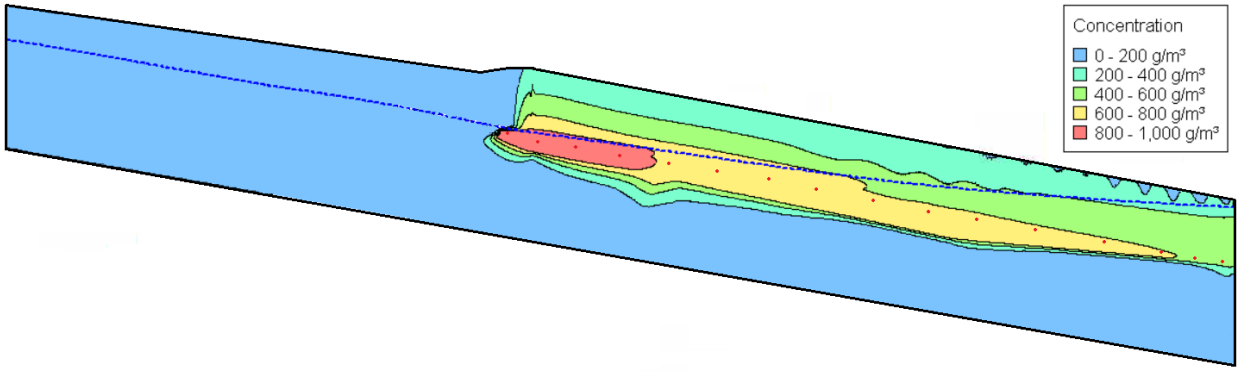

Figure 4.9 – Base case simulated concentration at 100 years.

The modelled advance of the contaminant plume appears to be controlled primarily by the stratigraphy at site. The advance of the contaminant plume toward the bulk storage swamp corresponds with the slope of the granitic bedrock surface. The presence of the low hydraulic conductivity silt unit initially confines contaminant transport to the higher conductivity sand unit, but at 25 years, we see diffusion controlled advance into the lower conductivity unit. The upward contaminant advancement into unsaturated soils and the apparent oscillations at the front of the contaminant plume can be attributed to the anisotropy ratio and dispersivity estimates applied to the sand unit and numerical noise.

Breakthrough time is defined as the point in time where the concentration is at 50% of the maximum concentration at a specific location. The resulting breakthrough time for the base case

modelling scenario was summarized at 16 nodes within the modelled mesh (Figure 4.10). The breakthrough times were estimated at each of the node locations (Figure 4.11). The base case modelling results indicate that once the tracer reaches the groundwater table below WMAF, it will take approximately 100 years for breakthrough into the bulk storage swamp.

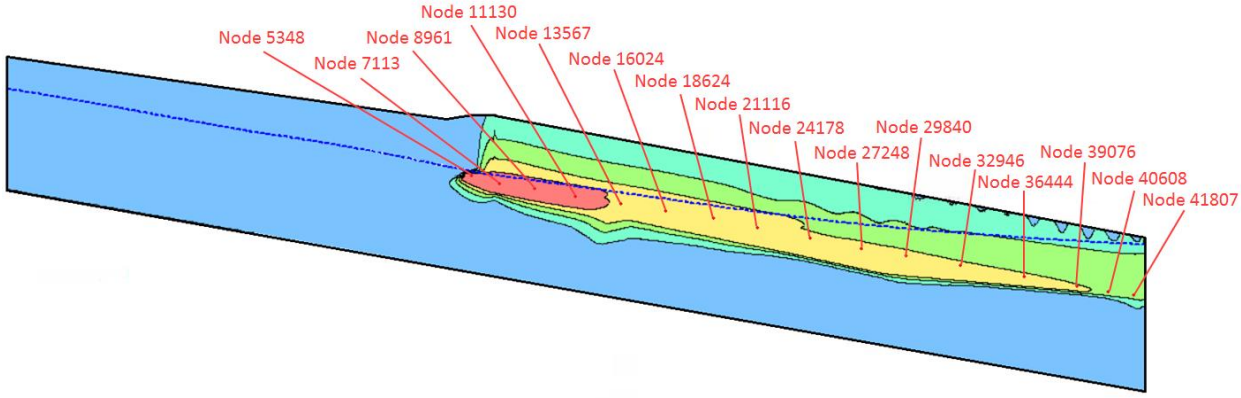

Figure 4.10 – Node locations within the modelling mesh used for analysis.

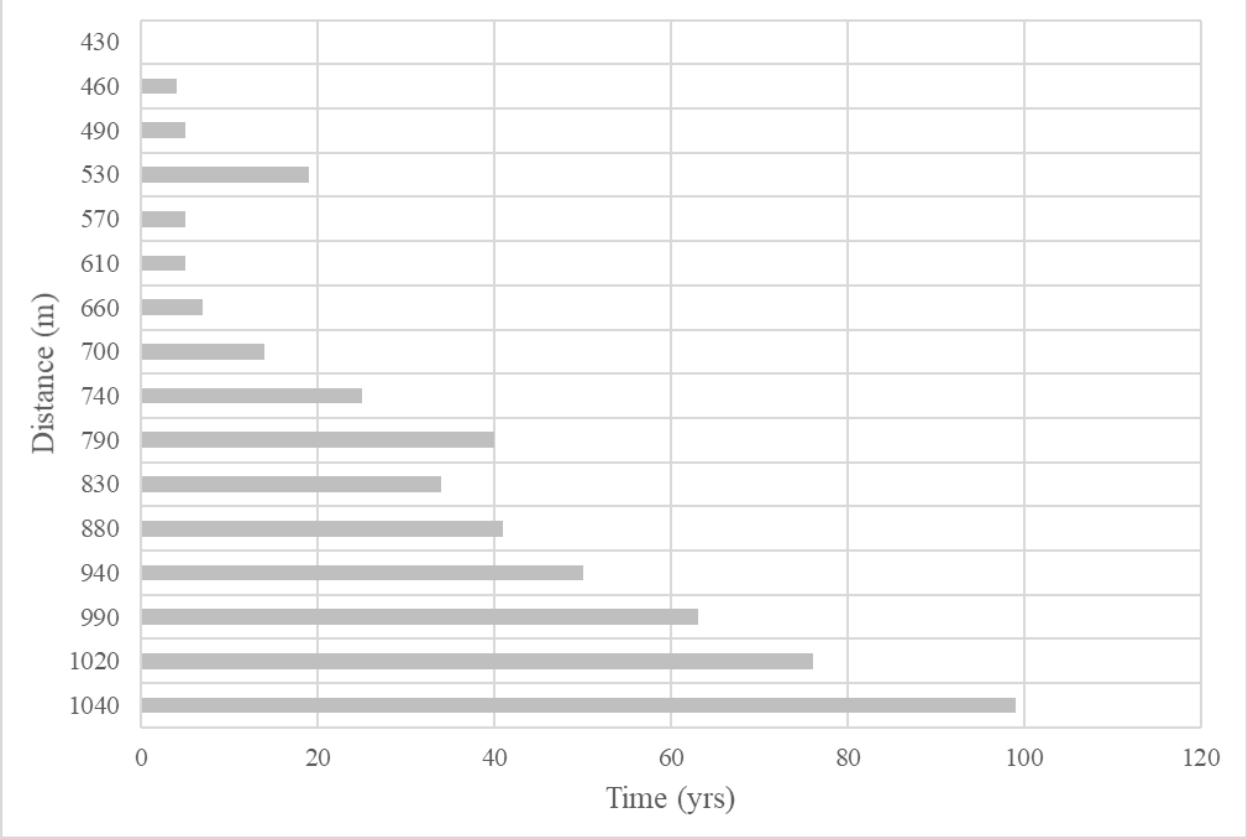

Figure 4.11 – Base case breakthrough time at 16 locations along the contaminant pathway.

The influence of hydraulic conductivity, dispersivity, and recharge on the base case scenario was analyzed to determine which parameter had the greatest impact on breakthrough estimates. The data resulting from the 375 modelled scenarios was tabulated based on the five different manipulations of each parameter. A range of breakthrough times was estimated for each parameter scenario and the standard deviation was compared to the base case results.

The standard deviation of breakthrough times estimated by varying hydraulic conductivity, ranged from 10 to 53 years (Figure 4.12). For the range of dispersivity and recharge considered, the standard deviation of breakthrough times ranged from 1 to 51 years and 1 to 24 years, respectively (Figure 4.13 and Figure 4.14).

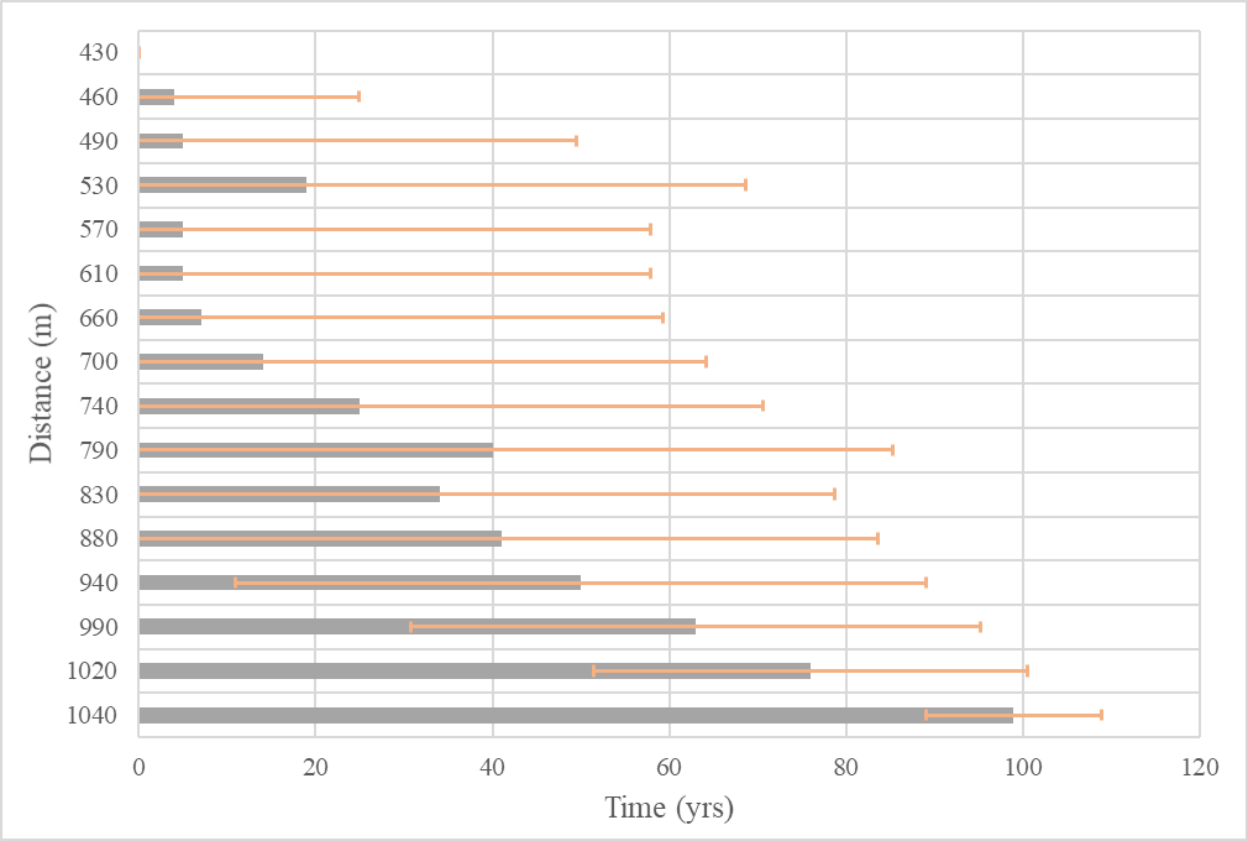

Figure 4.12 – Breakthrough times along the contaminant pathway showing the influence of hydraulic conductivity.

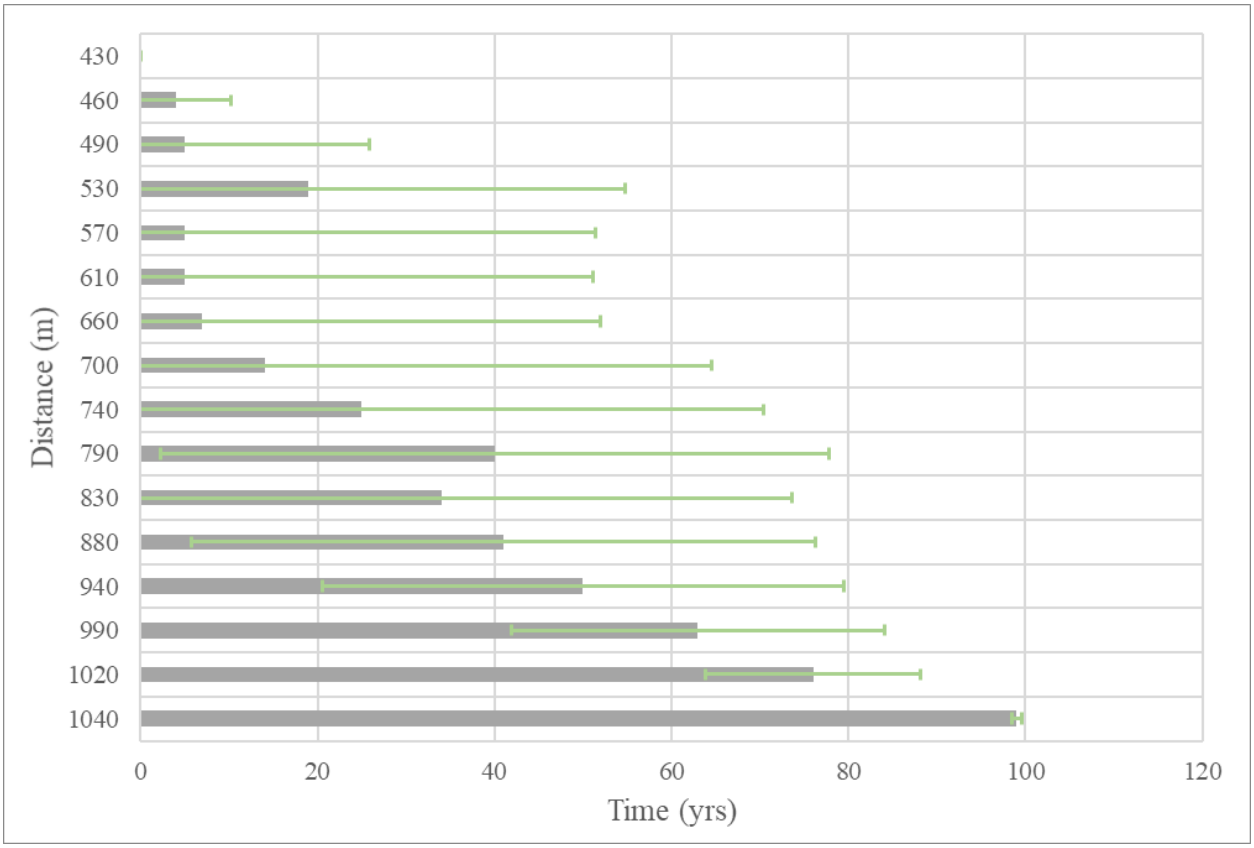

Figure 4.13 – Breakthrough times along the contaminant pathway showing the influence of dispersivity.

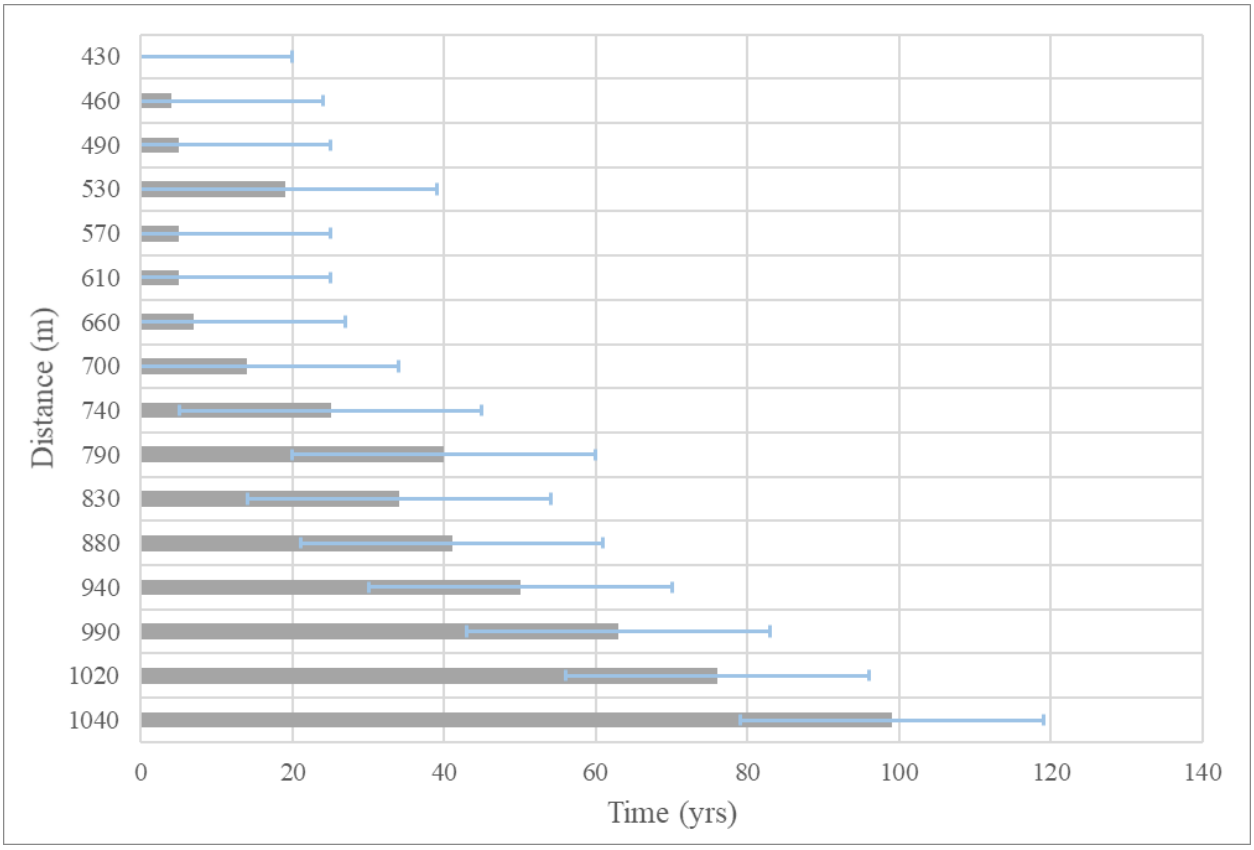

Figure 4.14 – Breakthrough times along the contaminant pathway showing the influence of the recharge.

The modelled breakthrough estimates for each parameter range widely and analysis indicates the modelling results under and overestimate breakthrough times. Killey (2015) estimated groundwater transit times from the water table below WMAF to the bulk storage swamp ranged from 4 to 14 years. Based on this estimate, unrealistic breakthrough estimates were observed in the modelled results and are defined as exceeding 40 years for a conservative tracer to travel 30 m and less than 5 years to travel 550 m.

Excluding the unrealistically fast (< 5 yrs to travel 30 m) and slow (> 40 yrs to travel 550 m) estimates based on the transit estimates from Killey (2015), the range of breakthrough estimates narrows. For the hydraulic conductivity examined, the standard deviation of breakthrough times ranges from 1.5 to 18 years and exceeds 10 years at most node locations (Figure 4.15). The standard deviation of breakthrough times for the dispersivity values examined, excluding the unrealistic estimates, ranges from 1.5 to 31 years and is less than 10 years at most node locations (Figure

4.16). Over the range of recharge rates considered, the standard deviation of breakthrough estimates ranges from 1 to 20 years and is less than 10 years at the majority of node locations (Figure 4.17).

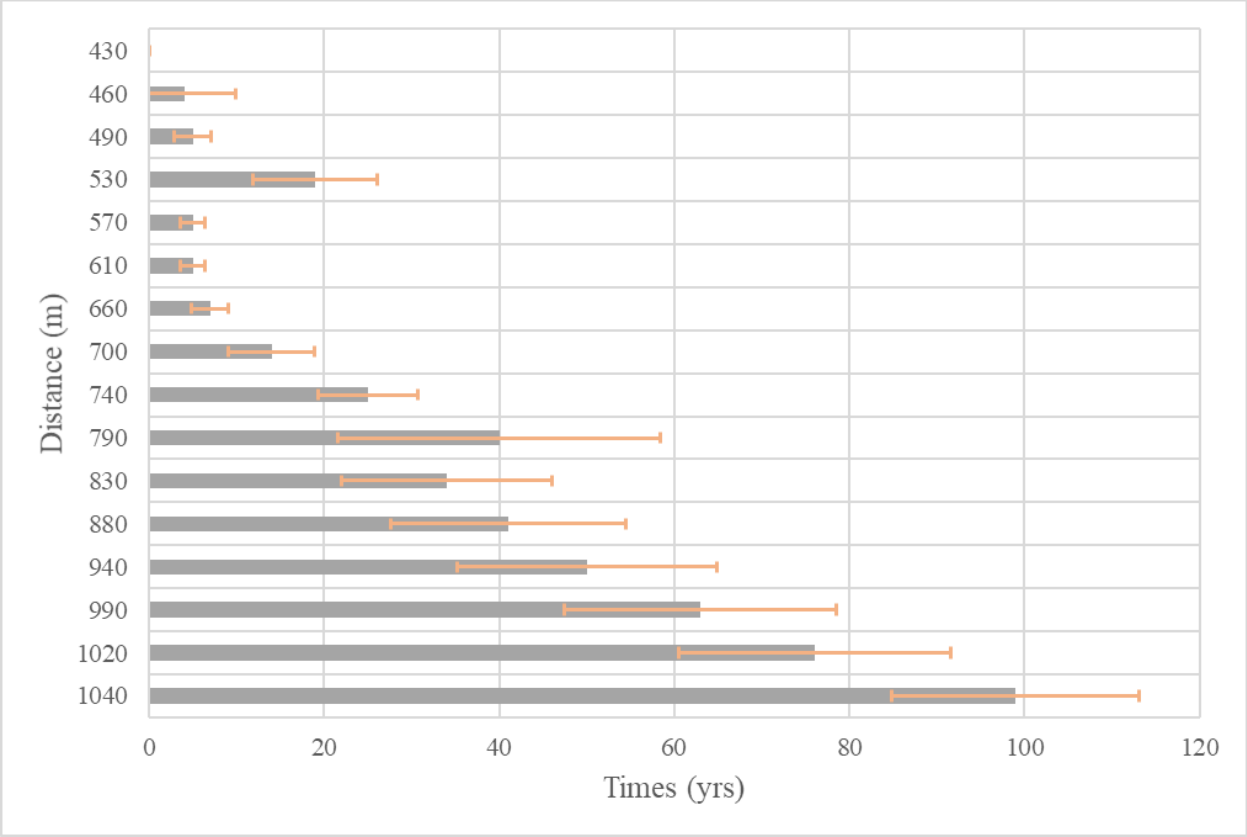

Figure 4.15 – Breakthrough times along the contaminant pathway showing the influence of hydraulic conductivity excluding unrealistic breakthrough times.

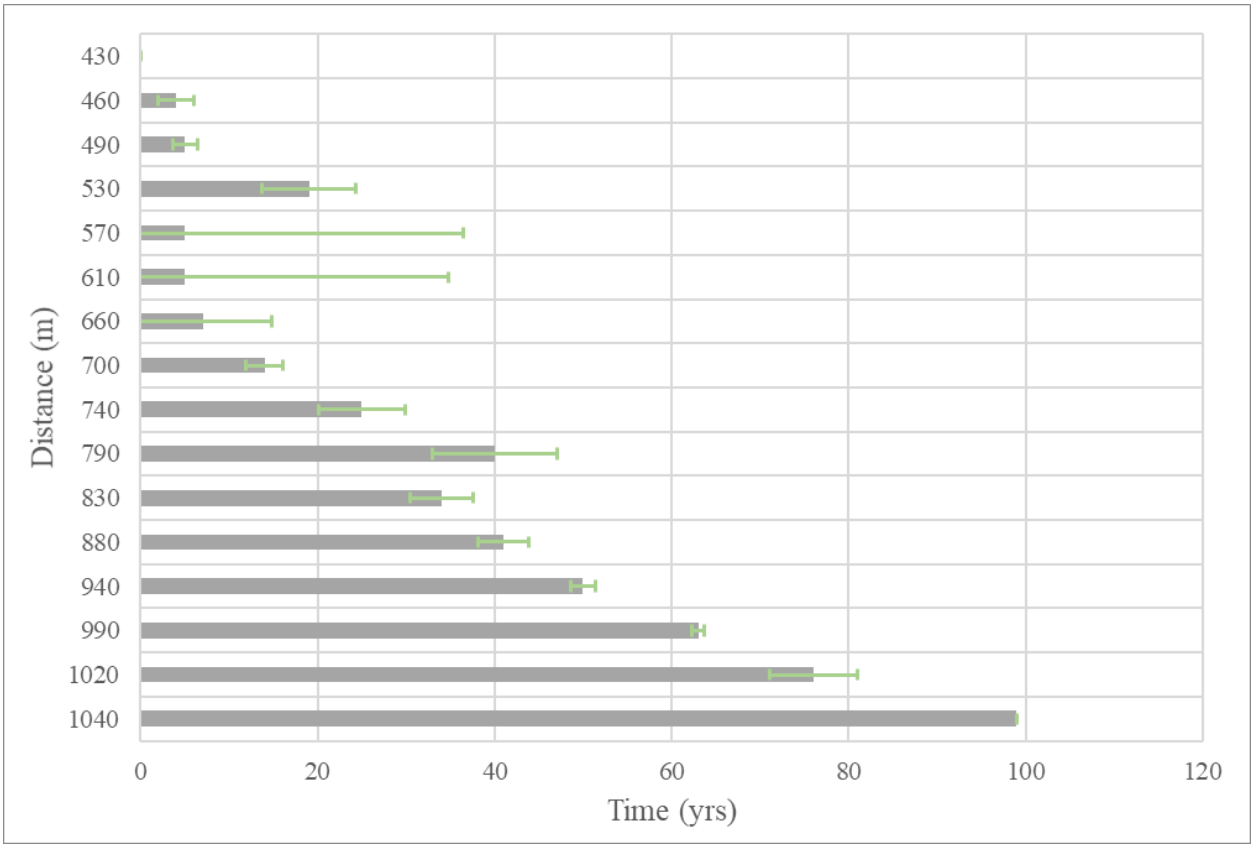

Figure 4.16 – Breakthrough times along the contaminant pathway showing the influence of dispersivity excluding unrealistic breakthrough times.

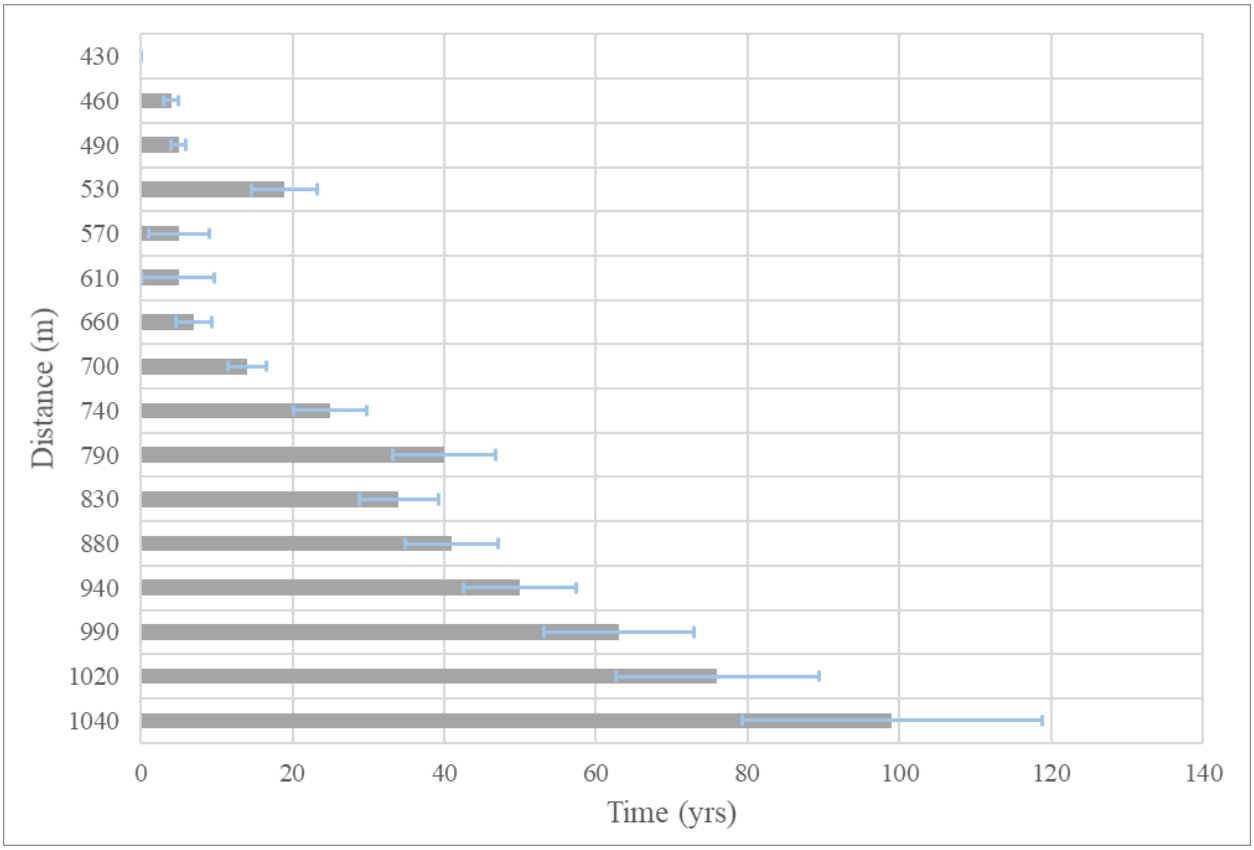

Figure 4.17 – Breakthrough times along the contaminant pathway showing the influence of the recharge excluding unrealistic breakthrough times.

CHAPTER 5. DISCUSSION

5.1 Field Data Collection

Field observation and data collection is fundamental to understanding hydrogeology and aids in interpretation (Brassington, 2017). The field program carried out at WMAF provided an opportunity for a visual assessment of the location, topography, and vegetation. It also allowed for the collection of site specific hydrogeological data. Groundwater level measurements were collected and hydraulic response testing was completed to better understand the hydrogeology in the vicinity of WMAF.

Continuous groundwater measurement were recorded over a two year period to assess the seasonal variability of groundwater levels. The results indicated groundwater levels fluctuate by approximately 1 m throughout the year and a number of the piezometers are hydraulically connected. Point measurements were collected in August 2014, when groundwater levels are typically at their peak, and used to create the steady-state groundwater flow model. Assuming steady-state groundwater conditions simplified modelling efforts, but ignores the observed daily and seasonal fluctuations.

The hydraulic response testing and analysis found hydraulic conductivity estimates for each stratigraphic unit ranged from 2-3 orders of magnitude. The range of hydraulic conductivity estimates can be attributed to the testing method and the heterogeneity of porous media. Slug tests are an effective method for estimating hydraulic conductivity, but like all testing methods, they are scale dependent and can be impacted by the piezometer installation technique (Dafflon et al., 2011, Schulze-Makuch et al., 1997). The data collected from slug testing may only be representative of the aquifer material in the near vicinity of the piezometer screen and the accuracy may be impacted by the piezometer filter pack, poor well development, and skin effects (Cunningham et al., 2011).

5.2 Groundwater and Contaminant Transport Modelling

Groundwater and contaminant transport modelling can be useful policy tools, but they need to be simplified and constrained to provide any sort of value. The primary purpose of the modelling completed for the WMAF was to provide a preliminary model of the physical hydrogeology and understand how the public understands/perceives modelling results. The model, in its current state, cannot provide an accurate estimate of the contaminant transport occurring onsite because it did not consider the sorption processes of the primary constituents of concern (arsenic, uranium, and

radium). The model does provide insight into how the stratigraphy impacts contaminant transport at WMAF and how uncertainty with the hydrogeological parameters impact contaminant transport.

Models are only ever tools and as such are ubiquitously flawed (Konikow et al., 1992, Oreskes et al., 1994). The physical world is complex and there is not a simple tool to effectively replicate the intricacies of the physical environment, nor should there be. Groundwater models are tools that can be used to evaluate hypotheses and aid in technical judgement in regards to future risk and consequences (Konikow et al., 1992; Beven, 2012). The observed hydrogeological data collected from WMAF provides evidence of the wide range of measured hydraulic conductivity, dispersivity, and recharge. The measured hydraulic conductivity was found to range from 2-3 orders of magnitude in similar stratigraphic units across the site.

Based on the results of the modelling at WMAF, hydrogeological parameters have an effect on the breakthrough time, with hydraulic conductivity having the greatest impact. Hydraulic conductivity estimates can range by two to three orders of magnitude and the effect of this uncertainty resulted in a wide range of modelled breakthrough estimates that differed by as much as 50 years. The greater impact of hydraulic conductivity on the contaminant transport at WMAF in comparison to dispersivity and recharge is reasonable given the relatively sandy subsurface. In high hydraulic conductivity soils, like at WMAF, advection typically controls contaminant transport with diffusion being less significant factor (Fetter, 2001, Barbour et al., 2011, Gilham et al., 1982). In comparison to hydraulic conductivity and recharge, dispersivity had the least impact on breakthrough time and distance. A larger recharge rate increases the head elevations and hydraulic gradient across the sites. Varying the recharge rate spatially across the site did not have a significant impact to the saturated contaminant transport at the site. It is likely the spatial component of recharge would have a greater impact on contaminant transport within the unsaturated zones. With all three parameters examined, unrealistic breakthrough times were observed when applying the low and high end of the ranges. This speaks to the importance of evaluating a model under real world conditions and understanding what is likely based on physical data.

While input parameters have a significant impact on the contaminant transport rate and distance, stratigraphy appears to have the greatest impact on contaminant transport at WMAF. The modelling results indicate contaminants travel largely in the high hydraulic conductivity soils that lie above the bedrock. It appears the low hydraulic head and relatively low permeability of the subsurface

slow contaminant transport. The impact of heterogeneity, anisotropy, and fracturing will be greater determinants of contaminant transport at this site in comparison to physical hydrogeological parameters. Unfortunately, models are limited in their capacity to recreate the complexity of the physical world (Konikow et al., 2012, Beven, 2012). Effectively modelling the heterogeneity at WMAF would require additional physical data and the development of a more complex model. Given the slow contaminant transport rate indicated by monitoring data obtained to date and the modelling results, building a more complex model is not practical or worthwhile.

5.3 Communicating Uncertainty

Environmental decision making is a difficult task not only because of complex natural system but also because of the interconnection between the environment, society, and economy. In the context of policy and future planning, it is not enough to consider the scientific facts or estimates; stakeholders must be incorporated into the decision making process (Antunes 2006). Water is inherently important in almost everything we do as humans and managing our water resources is an example of a wicked problem; a problem riddled with complexity that lacks an agreed upon definition and there are no clear solutions (Head 2010). Essentially, there is a level of uncertainty that is present in every environmental investigation and was observed in the WMAF modelling results. Scientists are often comfortable with uncertainty and recognize that scientific hypotheses cannot be validated, only invalidated (Bredehoeft et al., 1993). There is an appreciation that with every modelled result, there may be numerous alternative approaches and solutions that exist. Unfortunately, it is difficult to create public buy in for policy that is based on uncertain science (Quay 2010, Gober et al., 2010, Linstone, 2004).

Research into people's willingness to accept uncertainty and trust data has shown a positive correlation between increased knowledge and increased acceptance of results despite uncertainty (Visscher 2018). There is a need for presenting complex information in their complexity and ensuring the public has the necessary knowledge to understand an issue (Visscher, 2018). Too often the public is presented with simplistic, partial information. Dismissing complexity assumes the public is not intelligent enough to comprehend it. This is not to suggest policy decisions must wait on an unending collection of knowledge, but that collection and communication of knowledge behind a decision can aid in public buy-in (Knaggard, 2014). As such, communicating the results of the study at WMAF is not sufficient; considered effort should be made to share the background

knowledge, site specific complexities, what assumptions were made and why, and how this effects possible outcomes.

A problematic area in assessing public perception is how information is communicated. There is evidence of the need for stakeholder engagement to be integrated into scientific studies in order to determine groups of people to target with specific communication strategies and detailed information (Fischer et al., 2013, Broomell, 2017). Too often scientific research is presented in a discourse that limits the audience and alienates the general public. People deal with complexity in all parts of their lives and are capable of making decisions regardless of the murkiness. If the results of the WMAF study are to be shared with the public, a strategic communication approach should be taken to consider who the audience is, what background information they may need, and what language should be used. There is a need for honest, open communication with an emphasis on timely discussions to ensure people understand.

Another area of concern in the communication of scientific uncertainty, is implicit biases. People's individual values can affect their understanding of scientific results and uncertainty (Broomell, 2017; Leiserowitz, 2013; Budescu et al., 2012; Lewandowsky, 2013). If an individual has strong opinions on nuclear waste storage, scientific data from WMAF may have little effect in altering their opinion on the matter. Despite the implications of individual values on their perception of scientific results, there is evidence that the communication of scientific uncertainty is affected by expert agreement on a subject and the quality of evidence provided and can change individual's perceptions and belief in scientists (Broomell, 2017; Leiserowitz, 2013).

CHAPTER 6. CONCLUSION

The purpose of the thesis at Canadian National Laboratories' (CNL) Chalk River, Waste Management Area F (WMAF) was to characterize the hydrogeology and gain insight into how people respond to scientific uncertainty. Groundwater monitoring and hydraulic response testing was completed in the fall of 2014 and data was used in the creation of a 2D groundwater flow model. The groundwater model was used to evaluate the effect of parameter uncertainty and how people engage with scientific models.

The groundwater modelling results indicate hydraulic conductivity, dispersivity, and recharge all effect contaminant breakthrough times, but hydraulic conductivity had the greatest impact. In addition, stratigraphy was found to control the groundwater movement and contaminant transport at the site. The groundwater model provided insight into how groundwater and contaminants travel within the subsurface of WMAF, but it cannot definitively predict future contaminant distribution. The model ignores the geochemical processes that would influence the rate and distance contaminants travel. The model does offer one line of evidence that advective transport of contaminants below WMAF would be slow. The model would be improved by coupling with geochemical processes and further investigation into the heterogeneity present at the site, but the monitoring data and modelling results indicate there is no immediate risk to receptors.

The research at WMAF supports the conclusions made by Konikow (1992), Beven et al. (2012), and Oreskes (1994). Groundwater models are only ever tools for analysis, not predictions of future states. Models can aid in estimating potential risks and consequences, but will never relieve the need for technical judgement. Rather than emphasizing the elimination of uncertainty, more attention should be given to the communication of how technical judgements are made despite the potential uncertainty.

Further work recommended at WMAF includes research into the geochemical processes affecting contaminant transport, stratigraphic and hydrogeological characterization, and scale dependency. A better understanding of the geochemical processes at WMAF would allow for the coupling of a hydrogeological and geochemical model and refine contaminant transport estimations. The sorption and desorption of contaminants of interest at the site is of particular interest in determining contaminant breakthrough times. A strategic stratigraphic and hydrogeological drilling program, that included bedrock characterization and the installation of piezometers into the bedrock surface,

would aid numerical estimations of contaminant transport and provide further evidence that contaminants are not being transported through bedrock fractures. Additional hydraulic tests, such as pumping or tracer tests, would aid in narrowing the hydraulic parameter estimations and improve model estimates. Diffusion likely plays an important role in contaminant transport at WMAF, particularly within the near vicinity of the buried waste. Bench scale column tests using core samples from WMAF would provide a means of estimating diffusion coefficients for each of the stratigraphic unit. There is also a need to assess the scale dependency at WMAF. Further modeling work should focus on the immediate buried waste area to better understand what is currently impeding contaminant transport.

There is a need for the ongoing research into the communication of scientific estimations and depoliticizing scientific results. Questions into how trust effects public buy-in and how to educate without overwhelming the public remain unanswered from the study at WMAF. Further research into how to effectively communicate scientific results and the inherent uncertainty is needed.

REFERENCES

Abbotts, J., & Weems, C. (2008). Remediation and review: Developing groundwater strategy at the Hanford site. Remediation, 18, 163-178. doi:10.1002/rem.20166

Antunes, P., Santos, R., & Videira, N. (2006). Participatory decision making for sustainable development - The use of mediated modelling techniques. Land Use Policy, 23(1), 44–52. doi:10.1016/j.landusepol.2004.08.014

Ahmed, Bulbul & Cao, Bin & Mishra, Bhoopesh & Boyanov, Maxim & Kemner, K. & Fredrickson, Jim & Beyenal, Haluk. (2012). Immobilization of U(VI) from oxic groundwater by Hanford 300 Area sediments and effects of Columbia River water. Water research. 46. 3989-98. 10.1016/j.watres.2012.05.027.

Bachu, S., & Michael, K. (2002). Flow of variable-density formation water in deep sloping aquifers: minimizing the error in representation and analysis when using hydraulic-head distributions. Journal of Hydrology, 259(1-4), 49–65. doi:10.1016/S0022-1694(01)00585-6

Bakker, K. (2012). Water Security: Research Challenges and Opportunities. Science, 337, 914–915. doi:10.1126/science.1226337

Barbour, S., & Krahn, J. (2004). Numerical modelling–Prediction or process. Geotechnical News, (December), 44–52. Retrieved from http://www.geo-slope.com/res/numerical modelling - prediction or process.pdf

Barbour, S.L., Hendry, M.J., & Wassenaar, L.I. (2012). In situ experiment to determine advective-diffusive controls on solute transport in a clay-rich aquitard. Journal of contaminant hydrology, 131 1-4, 79-88 .

Barnett, Mark & Jardine, Phil & Brooks, Scott. (2002). U(VI) Adsorption to Heterogeneous Subsurface Media: Application of a Surface Complexation Model. Environmental science & technology. 36. 937-42. 10.1021/es010846i.

Bear, J., & Cheng, A. (2010). Modeling groundwater flow and contaminant transport. doi:10.1007/978-1-4020-6682-5

Bear, J., Haimes, Y.,Walter, F. (1979). Hydraulics of groundwater. New York: McGraw-Hill Inc.

Behrends, Thilo & Van Cappellen, Philippe. (2005). Competition between enzymatic and abiotic reduction of Uranium(VI) under iron reducing conditions. Chemical Geology. 220. 315-327. 10.1016/j.chemgeo.2005.04.007.

Beven, Keith. (2012). Causal models as multiple working hypotheses about environmental processes. Comptes Rendus Geoscience. 344. 77-88. 10.1016/j.crte.2012.01.005.

Bots, Pieter & Behrends, Thilo. (2008). Uranium mobility in subsurface aqueous systems: The influence of redox conditions. Mineralogical Magazine. 72. 10.1180/minmag.2008.072.1.381.

Brassington, Rick. (2017). Field Hydrogeology – 4th Edition. John Wiley & Sons.

Bredenhoeft, J.D., & Konikow, L.F. (1993). Ground-water models: validate or invalidate?. Ground Water, 31(2), 178-179.

Broomell, Stephen & Kane, Patrick. (2017). Public perception and communication of scientific uncertainty. Journal of Experimental Psychology: General. 146. 286-304. 10.1037/xge0000260.

Brunner, R. D. (2010). Adaptive governance as a reform strategy. Policy Sciences, 43(May), 301–341. doi:10.1007/s11077-010-9117-z

Budescu, D.V., Por, H. & Broomell, S.B. (2012). Effective communication of uncertainty in the IPCC reports. Climatic Change 113, 181–200. doi:10.1007/s10584-011-0330-3

Camacho, A. E. (2009). Adapting Governance to Climate Change: Managing Uncertainty through a Learning Infrastructure. Emory Law Journal, 59, 4–77. doi:10.2139/ssrn.1352693

Cao, Zuohao & Cai, Huaqing. (2011). Detection of Tornado Frequency Trend Over Ontario, Canada. The Open Atmospheric Science Journal. 511. 27-31. doi:10.2174/1874282301105010027.

Cary, Annette. (2019). Hanford cleanup costs triple. And that's the 'best case scenario' in a new report. TriCity Herald. 1 Feb 2019. Retrieved from https://www.tri-cityherald.com/news/local/hanford/article225386510.html

Catalano, Jeffrey & Brown, Gordon. (2006). Uranyl Adsorption Onto Montmorillonite: Evaluation of Binding Sites And Carbonate Complexation. Geochimica et Cosmochimica Acta. 69. 2995-3005. 10.1016/j.gca.2005.01.025.

Catto, N. R., Patterson, R. J., Gorman, W. A., & Sea, C. (1982). The late Quaternary geology of the Chalk River region, Ontario and Quebec.

Charlet, Laurent & Liger, E. & Gerasimo, P.. (1998). Decontamination of TCE- and U-rich waters by granular iron: Role of sorbed FE(II). Journal of Environmental Engineering. 124. 25-30. 10.1061/(ASCE)0733-9372(1998)124:1(25).

Cherry, J. A., Gilham, R. W., & Pickens, J. F. (1975). Contaminant Hydrogeology - Part 1: Physical Processes. Geoscience Canada, 2(2). Retrieved from https://journals.lib.unb.ca/index.php/GC/article/view/2909

Crane, Richard & Dickinson, M & Popescu, Ioana-Carmen & Scott, Thomas. (2011). Magnetite and zero-valent iron nanoparticles for the remediation of Uranium contaminated environmental water. Water research. 45. 2931-42. 10.1016/j.watres.2011.03.012.

Crowley, KD & Ahearne, JF. (2003). Managing the environmental legacy of US nuclear-weapons production - Although the waste from America's arms buildup will never be "cleaned up," human and environmental risks can be reduced and managed. American Scientist. 91. 5-5. 10.1511/2002.39.792.

Cunningham, W.L., and Schalk, C.W., comps., 2011, Groundwater technical procedures of the U.S. Geological Survey: U.S. Geological Survey Techniques and Methods 1-A1, 151 p.

Dafflon, B., W. Barrash, M. Cardiff, and T. C. Johnson (2011), Hydrological parameter estimations from a conservative tracer test with variable-density effects at the Boise Hydrogeophysical Research Site,WaterResour.Res.,47 , W12513, doi:10.1029/ 2011WR010789.

De Barros, F. P. J., Ezzedine, S., & Rubin, Y. (2012). Impact of hydrogeological data on measures of uncertainty, site characterization and environmental performance metrics. Advances in Water Resources, 36, 51–63. doi:10.1016/j.advwatres.2011.05.004

Deregel C., Peres J.M., Cessac B., Francois P. (2008) Issues in Decommissioning and Remediation of Nuclear Legacy Sites. In: Sneve M.K., Kiselev M.F. (eds) Challenges in Radiation Protection and Nuclear Safety Regulation of the Nuclear Legacy. NATO Science for Peace and Security Series C: Environmental Security. Springer, Dordrecht

Dixit, Suvasis & Hering, Janet. (2003). Comparison of Arsenic(V) and Arsenic(III) Sorption onto Iron Oxide Minerals. Environmental science & technology. 37. 4182-9. 10.1021/es030309t.

Dogrul, E. C., & Kadir, T. N. (2006). Flow computation and mass balance in Galerkin finite-element groundwater models. Journal of Hydraulic Engineering, 132(11), 1206–1214. doi:10.1061/(ASCE)0733-9429(2006)132:11(1206)

Dong, Wenming & Ball, William & Liu, Chongxuan & Wang, Zheming & Stone, Alan & Bai, Jing & Zachara, John. (2005). Influence of Calcite and Dissolved Calcium on Uranium(VI) Sorption to a Hanford Subsurface Sediment. Environmental science & technology. 39. 7949-55. 10.1021/es0505088.

Dougherty, D., & Bagtzoglou, C. (1993). A caution on the regulatory use of numerical solute transport models. Ground Water, 31(6), 1007–1010.

Easley, Megan. (2012). Standing in Nuclear Waste: Challenging the Disposal of Yucca Mountain Cornell L. Rev. 97 (659). Retrieved from https://scholarship.law.cornell.edu/clr/vol97/iss3/6

El-Kadi, A. I., & Ling, G. (1993). The Courant and Peclet Number criteria for the numerical solution of the Richards Equation. Water Resources Research, 29(10), 3485–3494. doi:10.1029/93WR00929

Ewing, Rodney C;Macfarlane, Allison. (2002) “Yucca Mountain” Science. 296(5568).

Fein, J., & Powell, B. (2013). Uranium Adsorption: Speciation at mineral-water and bacterial cell-water interface. Uranium- Cradle to Grave, Ed. Peter Burns and Ginger Sigmon. Winnipeg: Mineralogical Association of Canada, 2013. 165-192. Print.

Fernandes, Maria & Baeyens, Bart & Dähn, Rainer & Scheinost, Andreas & Bradbury, M.H.. (2012). U(VI) sorption on montmorillonite in the absence and presence of carbonate: A macroscopic and microscopic study. Geochimica et Cosmochimica Acta. 93. 262–277. 10.1016/j.gca.2012.04.017.

Fetter, C., (2001). Applied hydrogeology. New Jersey: Prentice-Hall Inc.

Fetter, C.W. & Boving, Thomas & Kreamer, David. (2017). Contaminant Hydrogeology – 3rd Edition. Waveland Press.

N. I. Fisher, A. J. Lee & J. H.J. Cribb (2013) A Scientific Approach to Monitoring Public Perceptions of Scientific Issues, International Journal of Science Education, Part B, 3:1, 25-51, DOI: 10.1080/09500693.2011.652364

Fried, J., & Eyles, J. (2011). Welcome waste- interpreting narratives of radioactive waste disposal in two small towns in Ontario, Canada. Journal of Risk Research, 14(9), 1017-1037.

Gartner Lee Associates Ltd., (1977). Hydrogeological Study of Waste Management Area “F” Port Hope Disposal Site.

GEO-SLOPE International Ltd. (2013). Seepage Modeling with SEEP/W, (July), 197.

Gillham, Robert & Cherry, John. (1982). Contaminant Migration in Saturated Unconsolidated Geologic Deposits. Geological Society of America Special Paper. 189. 10.1130/SPE189-p31.

Gillogly, Mari, Sneve, Malgorzata, & Smith, Graham (2017). Legacy management: An old challenge with a new focus. NEA News, (35-1), 4-7.

Gober, P. (2013). Getting Outside the Water Box: The Need for New Approaches to Water Planning and Policy. Water Resources Management, 27, 955–957. doi:10.1007/s11269-012-0222-y

Gober, P., Kirkwood, C. W., Balling, R. C., Ellis, A. W., & Deitrick, S. (2010). Water Planning Under Climatic Uncertainty in Phoenix: Why We Need a New Paradigm. Annals of the

Association of American Geographers, 100(February 2015), 356–372. doi:10.1080/00045601003595420

Gorelick, S. M., & Geological, U. S. (1983). A Review of Distributed Parameter Groundwater Management Modeling Methods, 19(2), 305–319.

He, X., Sonnenborg, T. O., Jørgensen, F., Høyer, a.-S., Møller, R. R., & Jensen, K. H. (2013). Analyzing the effects of geological and parameter uncertainty on prediction of groundwater head and travel time. Hydrology and Earth System Sciences, 17(8), 3245–3260. doi:10.5194/hess-17-3245-2013

Hvorslev, M.. (1951). Time Lag and Soil Permeability in Ground Water Obsevations. U.S. Army Corps of Engrs, Waterways Experiment Station, Vicksburg, MI. Bull.. 36.

Hossain, M. A., & Yonge, D. R. (1999). On Galerkin models for transport in groundwater. Applied Mathematics and Computation, 100(2-3), 249–263. doi:10.1016/S0096-3003(98)00025-3

Huitema, D. & Meijerink, S. (2010). Realizing water transitions: the role of policy entrepreneurs in water policy change. Water, 15(2), 25.

Hsi, Ching-Kuo & Langmuir, Donald. (1985). Adsorption of uranyl onto ferric oxyhydroxides: Application of the surface complexation site-binding model. Geochimica et Cosmochimica Acta. 49. 1931-1941. 10.1016/0016-7037(85)90088-2.

Johnson, G. (2007). The discourse of democracy in Canadian nuclear waste management policy. Policy Sciences, 40(2), 79-99. doi:10.1007/s11077-007-9032-0.

Jousma, G., Bear, J., Haimes, Y., Walter, F. (1989). Groundwater contamination: use of models in decision making. Springer Science & Business Media.

Jurgens, Bryant & Fram, Miranda & Belitz, Kenneth & Burow, Karen & Landon, Matthew. (2009). Effects of Groundwater Development on Uranium: Central Valley, California, USA. Ground water. 48. 913-28. 10.1111/j.1745-6584.2009.00635.x.

Karl, T. R., Meehl, G. a., Miller, C. D., Hassol, S. J., Waple, A. M., & Murray, W. L. (2008). Weather and Climate Extremes in a Changing Climate Regions of Focus :, (June). Retrieved from http://www.agci.org/dB/PDFs/Publications/07S1_USCCSP.pdf

Kasperson, R. E., & Kasperson, J. X. (1996). The Social Amplification and Attenuation of Risk. The ANNALS of the American Academy of Political and Social Science, 545, 95–105. doi:10.1177/0002716296545001010

Killey, D. (2015). Hydrogeological and Contaminant Update at Waste Management Area F.

Killey, D. (2013). Assessment of Contaminant Movement at Waste Management Area F,

Killey, D. (2009). Technical Note: Limited Geological & Hydrogeological Investigation of the Proposed NDSS Site 4A.

Killey, D., Young, J., Welch, S., Dal Bianco, R., King, K. (1993). Waste Management Area F: Arsenic, Radium, and Uranium Distributions 14 years after Emplacement.

Killey, D., Myrand, D. (1985). The movement of water, Arsenic, and radium at a Chalk River waste management area 1979-1983.

Knaggård, Åsa (2014) What do policy-makers do with scientific uncertainty? The incremental character of Swedish climate change policy-making, Policy Studies, 35:1, 22-39, DOI: 10.1080/01442872.2013.804175

Konikow, L. F. (2011). The Secret to Successful Solute-Transport Modeling. Ground Water, 49(2), 144–159. doi:10.1111/j.1745-6584.2010.00764.x

Konikow, L. F. and Bredehoeft. J.D. (1992) Ground-water models cannot be validated. Advances in Water Resources, 15(1), pp. 75-83. https://doi.org/10.1016/0309-1708(92)90033-X

Lachapelle, E., & Borick, C. P. (2011). Public attitudes toward climate science and climate policy in federal systems: Canada and the U.S. compared, 1–28.

Leiserowitz, A. A., Maibach, E. W., Roser-Renouf, C., Smith, N., & Dawson, E. (2013). Climategate, Public Opinion, and the Loss of Trust. American Behavioral Scientist, 57(6), 818–837. https://doi.org/10.1177/0002764212458272

Lewandowsky, S., Gignac, G. E., & Oberauer, K. (2013). The role of conspiracist ideation and worldviews in predicting rejection of science. PLoS One, 8(10) doi:http://dx.doi.org/10.1371/journal.pone.0075637

Lichtenstein, ND. (2004). The Hanford Nuclear Waste Site: A Legacy of Risk, Cost, and Inefficiency. Natural resources journal. 44. 809-839.

Liger, Emmanuelle & Charlet, Laurent & Van Cappellen, Philippe. (1999). Surface Catalysis of Uranium(VI) Reduction by Iron(II). Geochimica et Cosmochimica Acta. 63. 2939-2955. 10.1016/S0016-7037(99)00265-3.

Linstone, H. A. (2004). Shaping the Next One Hundred Years: New Methods for Quantitative, Long-Term Policy Analysis. Technological Forecasting and Social Change (Vol. 71). doi:10.1016/j.techfore.2003.09.006

MacPherson, Alex. “'There is life after remediation': Gunnar mine reclamation forging ahead despite legal battle.” Saskatoon Star Phoenix, 9 Jun 2019.

Milly, P. C. D., Betancourt, J., Falkenmark, M., Hirsch, R. M., Kundzewicz, Z. W., Lettenmaier, D. P., & Stouffer, R. J. (2008). Climate change. Stationarity is dead: whither water

management? Science (New York, N.Y.), 319(February), 573–574. doi:10.1126/science.1151915

Muldoon, Joe and Schramm, Laurier. (2009). Gunnar Uranium Mine Environmental Remediation: Northern Saskatchewan. 10.1115/ICEM2009-16102.

O'Kane Consultants Inc. (2015). Gunnar Site Remediation Project – Tailings Remediation Plan (Public Distribution). (Report No. 963/1-01). Retrieved from https://www.src.sk.ca/sites/default/files/resources/gunnar%2520tailings%2520remediation%2520plan%2520report%2520%28aug%252017%25202015%29.pdf

Oreskes, N. (2010). Evaluation (Not Validation) of Quantitative Model. Environmental Health, 106(May), 1453–1460.

Oreskes, N., Shrader-Frechette, K., & Belitz, K. (1994). Verification, validation, and confirmation of numerical models in the Earth sciences. Science (New York, N.Y.), 263(5147), 641–646. doi:10.1126/science.263.5147.641

Norman, E. S., Bakker, K., & Dunn, G. (2011). Recent Developments in Canadian Water Policy: An Emerging Water Security Paradigm. Canadian Water Resources Journal, 36(February 2015), 53–66. doi:10.4296/cwrj3601053

Nimmo, J. R. (2007). Simple predictions of maximum transport rate in unsaturated soil and rock. Water Resources Research, 43(May), 139–141. doi:10.1029/2006WR005372

Patchen, M. (2006). Public attitudes and behaviour about climate change: what shapes them and how to influence them, (October).

Phuong, N.M., Kang, Y., Sakurai, K. et al. Environ Monit Assess (2012) 184: 4501. https://doi.org/10.1007/s10661-011-2281-6

Quay, R. (2010). Anticipatory Governance. Journal of the American Planning Association, 76(February 2015), 496–511. doi:10.1080/01944363.2010.508428

Ramana, M.V. (2013). Shifting strategies and precarious progress: Nuclear waste management in Canada. Energy Policy, 61. 196-206.

Schneider, S. H. (2006). Climate change: Do we know enough for policy action? Science and Engineering Ethics, 12(4), 607–636. doi:10.1007/s11948-006-0061-4

Schindler, D. W., & Donahue, W. F. (2006). An impending water crisis in Canada's western prairie provinces. Proceedings of the National Academy of Sciences of the United States of America, 103, 7210–7216. doi:10.1073/pnas.0601568103

Schindler, M., & Ilton, E. Uranium mineralogy and geochemistry on the nano- to micrometer scale: redox, dissolution, and precipitation processes at the mineral-water interface.

Uranium- Cradle to Grave, Ed. Peter Burns and Ginger Sigmon. Winnipeg: Mineralogical Association of Canada, 2013. 203-240. Print.

Schulze-Makuch, D. & Cherkauer, D. Variations in hydraulic conductivity with scale of measurement during aquifer tests in heterogeneous, porous carbonate rocks. Hydrogeology Journal (1998) 6: 204. https://doi.org/10.1007/s100400050145

Schramm, L.L., Gunnar Uranium Mine: Canada's Cold War Ghost Town, Saskatchewan Research Council, Saskatoon, and Amazon.com Inc., 2016.

Schwartz, F.W., & Zhang, H. (2003). Fundamentals of Groundwater. New York: John Wiley and Sons Inc.

Scietific America. (2020). What does the U.S. do with nuclear waste? 24 Jun 2008. Retrieved from https://www.scientificamerican.com/article/what-does-the-us-do-with-nuclear-waste/

Sharp, Jonathan & Lezama Pacheco, Juan & Schofield, Eleanor & Junier, Pilar & Ulrich, Kai-Uwe & Chinni, Satya & Veeramani, Harish & Margot-Roquier, Camille & Webb, Samuel & Tebo, Bradley & Giammar, Daniel & Bargar, John & Bernier-Latmani, Rizlan. (2011). Uranium speciation and stability after reductive immobilization in aquifer sediments. Geochimica et Cosmochimica Acta. 75. 6497–6510. 10.1016/j.gca.2011.08.022.

Slovic, P., Flynn, J., & Layman, M. (1991). Perceived Risk, Trust, and the Politics of Nuclear Waste. Science, 254(5038), 1603-1607.

Smedley, P.L. & Kinniburgh, D.. (2001). A Review of the Source, Behaviour and Distribution of Arsenic in Natural Waters. Applied Geochemistry. 17. 517-568. 10.1016/S0883-2927(02)00018-5.

Sorensen, Eric. (2019). "Canada's nuclear waste to be buried in deep underground repository." Global News. 29 May 2019. Retrieved from https://globalnews.ca/news/5329835/canadas-nuclear-waste-to-be-buried-in-deep-underground-repository/

SRC. (2019). Gunnar mine and mill site. Retrieved from https://www.src.sk.ca/project-cleans/gunnar-mine-and-mill-site

Stewart, Brandy & Amos, Richard & Fendorf, Scott. (2011). Effect of Uranium(VI) Speciation on Simultaneous Microbial Reduction of Uranium(VI) and Iron(III). Journal of environmental quality. 40. 90-7. 10.2134/jeq2010.0304.

Survey, U. S. G., & Commission, U. S. N. R. (n.d.). Consideration of Geochemical Issues in Groundwater Restoration at Uranium In-Situ Leach Mining Facilities.

Tollefson, J. Battle of Yucca Mountain rages on. Nature 473, 266–267 (2011) doi:10.1038/473266a

Trenberth, K. (2010). More knowledge, less certainty. Nature Reports, 4(February 2010), 20–21. doi:10.1038/nature08281

Turner, Geoff. (2017). "Nuclear waste disposal in Canada is 'an accident waiting to happen' says Indigenous leader." CBC Radio: The Current. 23 Apr 2017. Retrieved from https://www.cbc.ca/radio/thecurrent/the-current-for-april-23-2018-1.4628764/nuclear-waste-disposal-in-canada-is-an-accident-waiting-to-happen-says-indigenous-leader-1.4629258

Um, W., Icenhower, J., Brown, C., Serne, R., Wang, Z., Dodge, C., & Francis, A. (2010). Characterization of uranium-contaminated sediments from beneath a nuclear waste storage tank from Hanford, Washington: Implications for contaminant transport and fate. Geochimica et Cosmochimica Acta.

Waite, T. & Davis, Jenny & Payne, Timothy & Waychunas, Glenn & Xu, Naili. (1994). Uranium(VI) adsorption to ferrihydrite: Application of a surface complexation model. Geochimica et Cosmochimica Acta. 58. 5465-5478. 10.1016/0016-7037(94)90243-7.

Wang, H., Anderson, M. (1982). Introduction to groundwater modeling: Finite difference and finite element modeling. San Francisco: W.H. Freeman and Company.

Wilding, E. (2012). Framing Ethical Acceptability: A Problem with Nuclear Waste in Canada. Science and Engineering Ethics, 18(2), 301-313. dio:10.1007/s11948-011-9262-6.

van der, Kamp, G., Luba, L.D., Cherry, J.A. and Maathuis, H. (1994), Field Study of a Long and Very Narrow Contaminant Plume. Groundwater, 32: 1008-1016. doi:10.1111/j.1745-6584.1994.tb00940.x

Visschers, V.H.M. (2018), Public Perception of Uncertainties Within Climate Change Science. Risk Analysis, 38: 43-55. doi:10.1111/risa.12818

Zachara, J., Ilton, E., & Liu, Chongxuan. "Reactive transport of the uranyl ion in soils, sediments, and groundwater systems." Uranium- Cradle to Grave, Ed. Peter Burns and Ginger Sigmon. Winnipeg: Mineralogical Association of Canada, 2013. 255-289. Print.

Zinn, B. (2003). When good statistical models of aquifer heterogeneity go bad: A comparison of flow, dispersion, and mass transfer in connected and multivariate Gaussian hydraulic conductivity fields. Water Resources Research, 39(3), 1–19. doi:10.1029/2001WR001146

APPENDIX A

Hydraulic Response Test Analyses

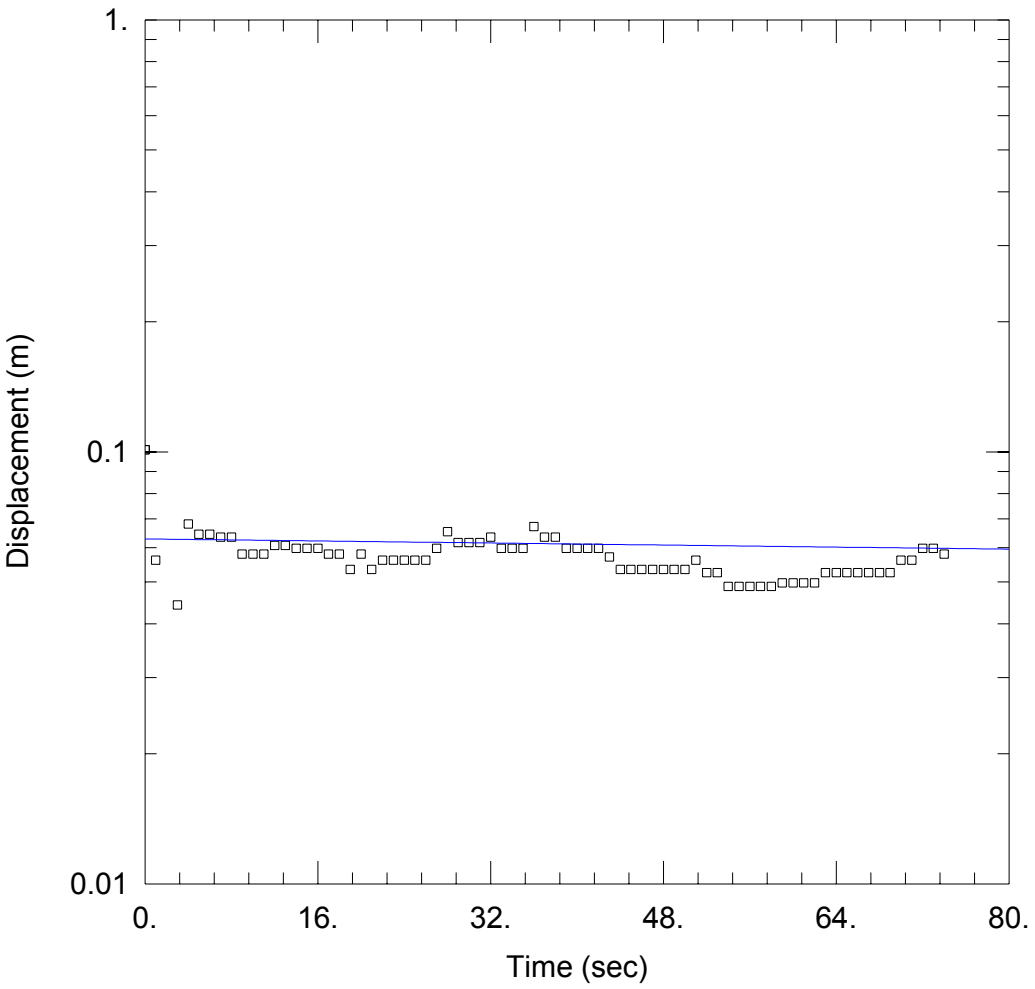

WELL TEST ANALYSIS

Data Set: W:\Grad Studies\Chalk River Field Work\AqteSOLV\Response Testing\GL2-I_FH.aqt
Date: 12/08/14 Time: 13:50:39

PROJECT INFORMATION

Location: Chalk River: WMAF
Test Well: GL2-I
Test Date: 25-Aug-14

AQUIFER DATA

Saturated Thickness: 0.48 m Anisotropy Ratio (Kz/Kr): 1.

WELL DATA (GL2-I)

Initial Displacement: 0.1011 m
Total Well Penetration Depth: 16.85 m
Casing Radius: 0.02 m
Static Water Column Height: 16.37 m
Screen Length: 1.52 m
Well Radius: 0.02 m

SOLUTION

Aquifer Model: Unconfined
Solution Method: Hvorslev
K = 1.506E-6 m/sec
y0 = 0.06287 m

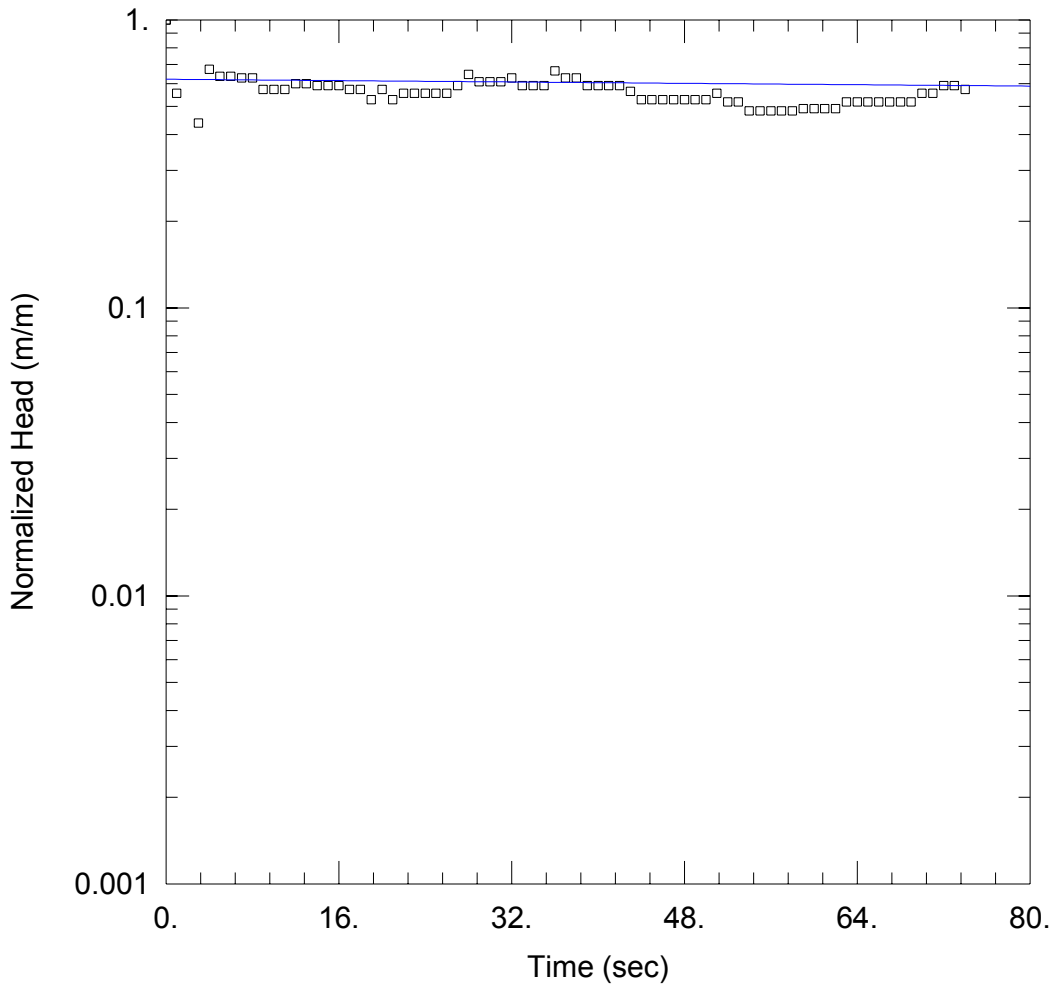

WELL TEST ANALYSIS

Data Set: W:\Grad Studies\Chalk River Field Work\AqteSOLV\Response Testing\GL2-I_FH.aqt
Date: 12/08/14 Time: 13:59:30

PROJECT INFORMATION

Location: Chalk River: WMAF
Test Well: GL2-I
Test Date: 25-Aug-14

AQUIFER DATA

Saturated Thickness: 0.48 m Anisotropy Ratio (Kz/Kr): 1.

WELL DATA (GL2-I)

Initial Displacement: 0.1011 m
Total Well Penetration Depth: 16.85 m
Casing Radius: 0.02 m
Static Water Column Height: 16.37 m
Screen Length: 1.52 m
Well Radius: 0.02 m

SOLUTION

Aquifer Model: Unconfined
Solution Method: Hvorslev
K = 1.506E-6 m/sec
y0 = 0.06287 m

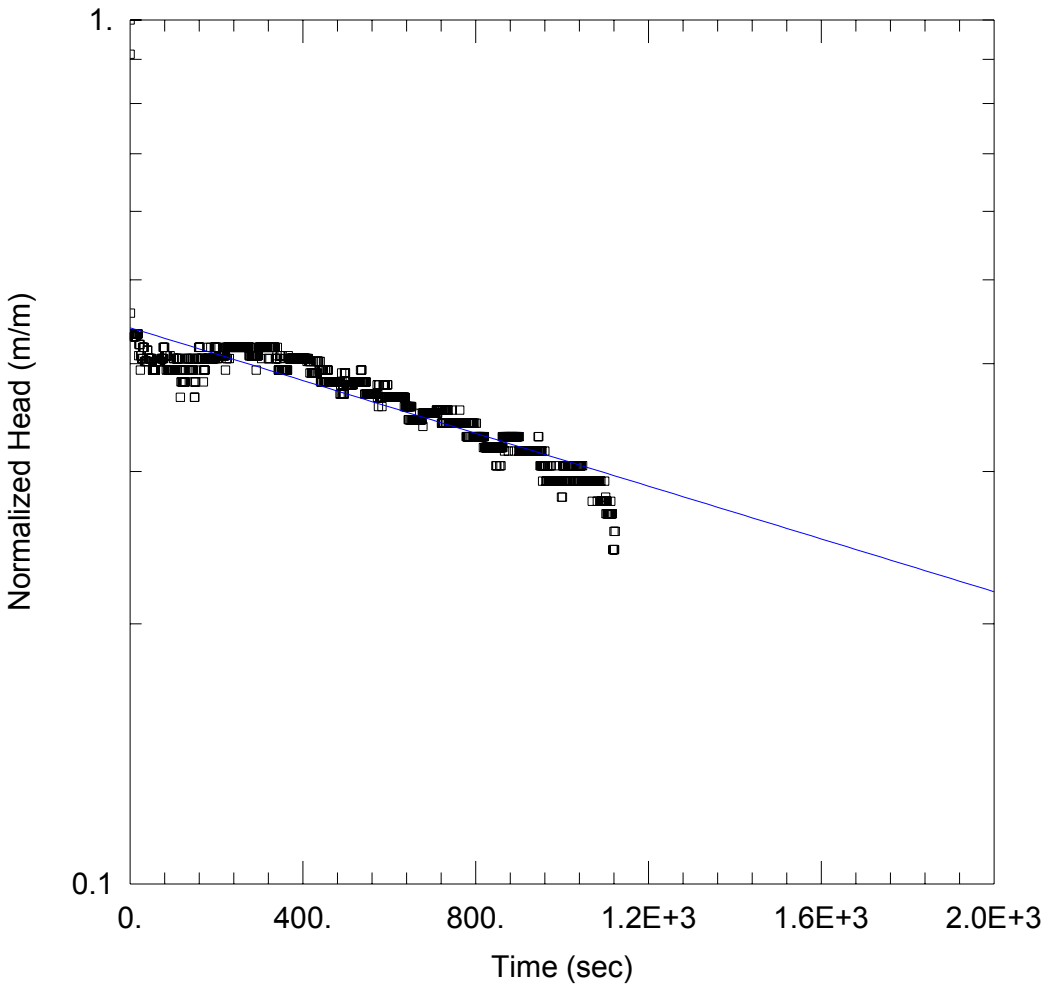

WELL TEST ANALYSIS

Data Set: W:\Grad Studies\Chalk River Field Work\AqteSOLV\Response Testing\GL2-I_RH.aqt
Date: 12/08/14 Time: 14:00:54

PROJECT INFORMATION

Location: Chalk River: WMAF
Test Well: GL2-I
Test Date: 25-Aug-14

AQUIFER DATA

Saturated Thickness: 0.48 m Anisotropy Ratio (Kz/Kr): 1.

WELL DATA (New Well)

Initial Displacement: 0.3 m
Total Well Penetration Depth: 16.85 m
Casing Radius: 0.02 m
Static Water Column Height: 16.37 m
Screen Length: 1.52 m
Well Radius: 0.02 m

SOLUTION

Aquifer Model: Unconfined
Solution Method: Hvorslev
K = 7.766E-7 m/sec
y0 = 0.1321 m

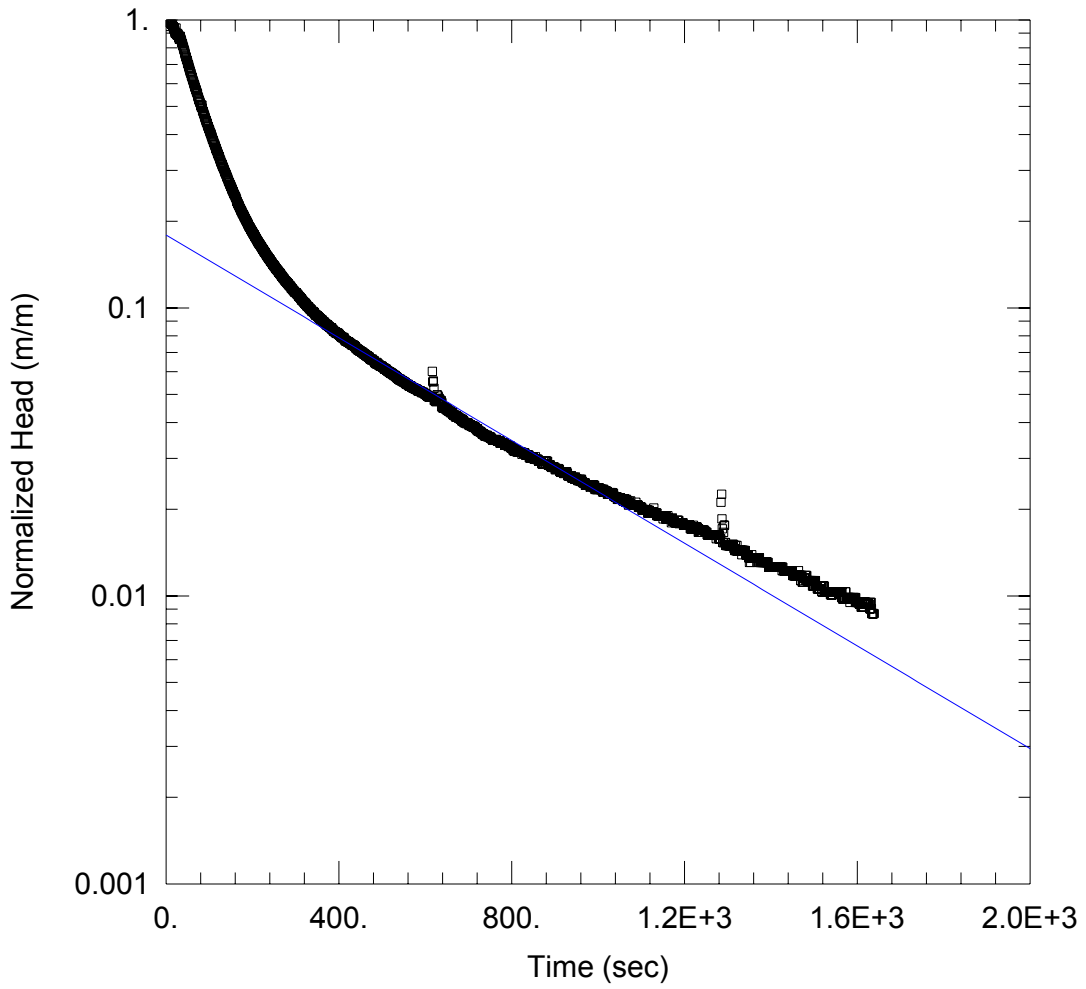

WELL TEST ANALYSIS

Data Set: W:\Grad Studies\Chalk River Field Work\AqteSOLV\Response Testing\LPH25_FH.aqt
Date: 12/08/14 Time: 14:03:19

PROJECT INFORMATION

Location: Chalk River: WMAF
Test Well: LPH25-I
Test Date: 27-Aug-14

AQUIFER DATA

Saturated Thickness: 1.02 m Anisotropy Ratio (Kz/Kr): 1.

WELL DATA (LPH25_FH)

Initial Displacement: 8.423 m Static Water Column Height: 1.02 m
Total Well Penetration Depth: 12.34 m Screen Length: 0.3 m
Casing Radius: 0.01 m Well Radius: 0.01 m

SOLUTION

Aquifer Model: Unconfined Solution Method: Hvorslev
K = 1.402E-6 m/sec y0 = 1.509 m

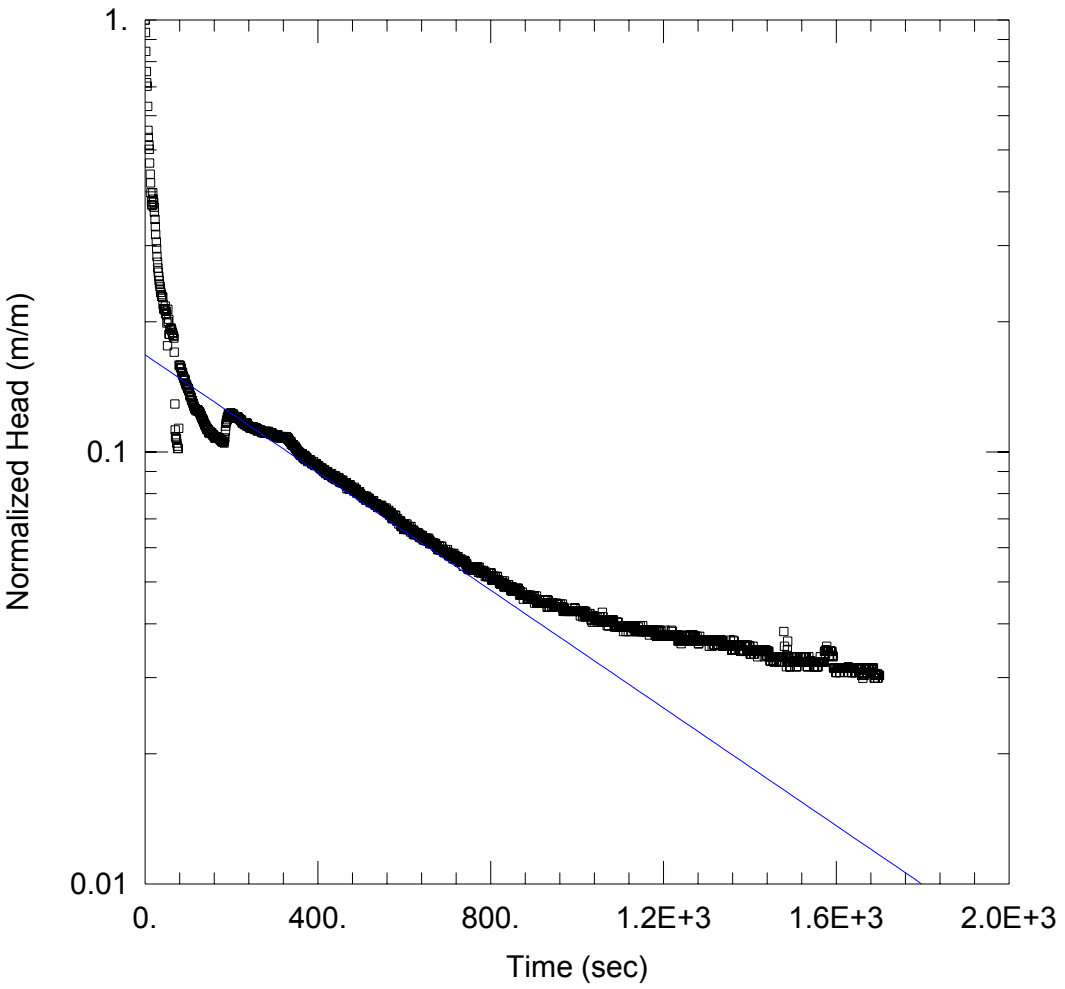

WELL TEST ANALYSIS

Data Set: W:\Grad Studies\Chalk River Field Work\AqteSOLV\Response Testing\LPH30_FH.aqt
Date: 12/08/14 Time: 14:03:54

PROJECT INFORMATION

Location: Chalk River: WMAF
Test Well: LPH25-I
Test Date: 27-Aug-14

AQUIFER DATA

Saturated Thickness: 15.55 m Anisotropy Ratio (Kz/Kr): 1.

WELL DATA (LPH30_FH)

Initial Displacement: 3.79 m
Total Well Penetration Depth: 15.55 m
Casing Radius: 0.02 m
Static Water Column Height: 0.61 m
Screen Length: 0.3 m
Well Radius: 0.02 m

SOLUTION

Aquifer Model: Unconfined
Solution Method: Hvorslev
K = 3.558E-6 m/sec
y0 = 0.6358 m

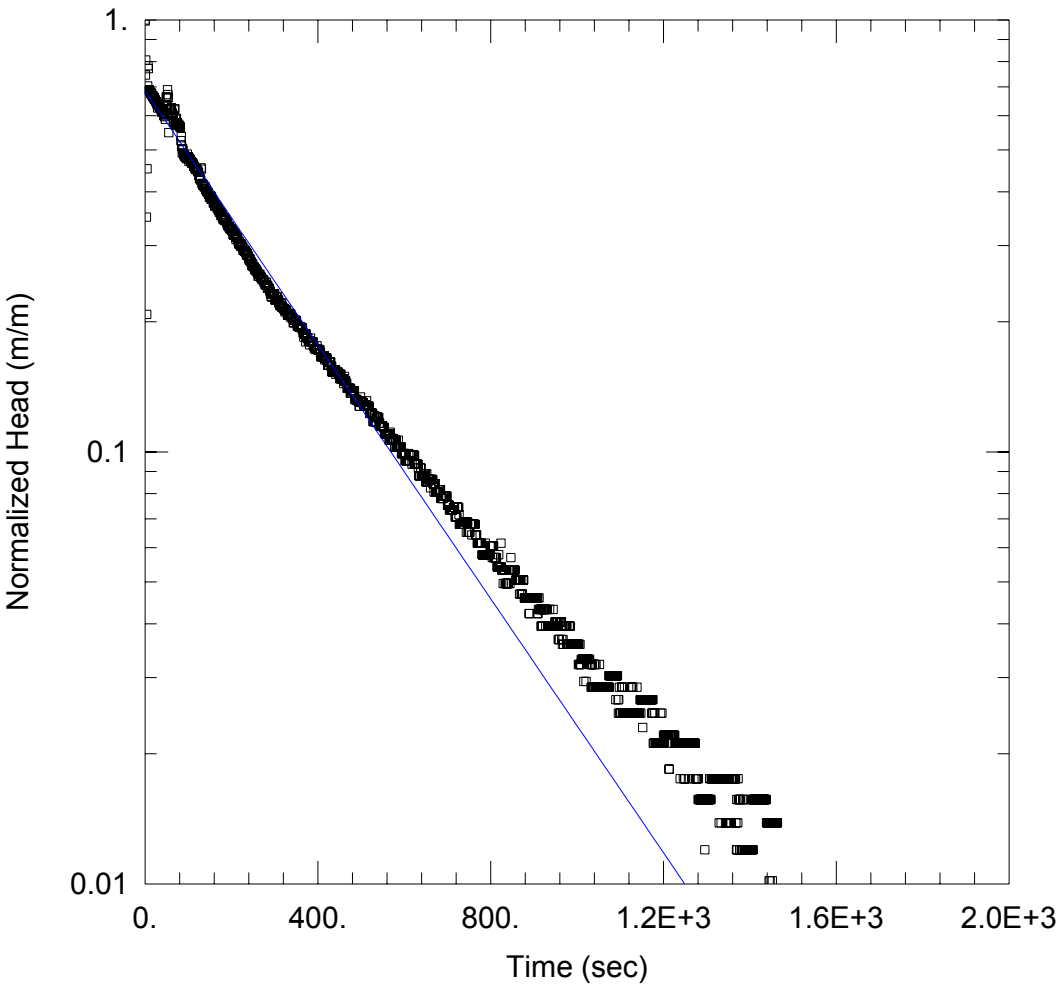

WELL TEST ANALYSIS

Data Set: W:\Grad Studies\Chalk River Field Work\AqteSOLV\Response Testing\LPH32_FH.aqt
Date: 12/08/14 Time: 14:04:56

PROJECT INFORMATION

Location: Chalk River: WMAF
Test Well: LPH25-I
Test Date: 27-Aug-14

AQUIFER DATA

Saturated Thickness: 12.65 m Anisotropy Ratio (Kz/Kr): 1.

WELL DATA (LPH32_FH)

Initial Displacement: 1. m
Total Well Penetration Depth: 12.64 m
Casing Radius: 0.02 m
Static Water Column Height: 2.39 m
Screen Length: 0.3 m
Well Radius: 0.02 m

SOLUTION

Aquifer Model: Unconfined Solution Method: Hvorslev

K = 6.12E-6 m/sec y0 = 0.6851 m

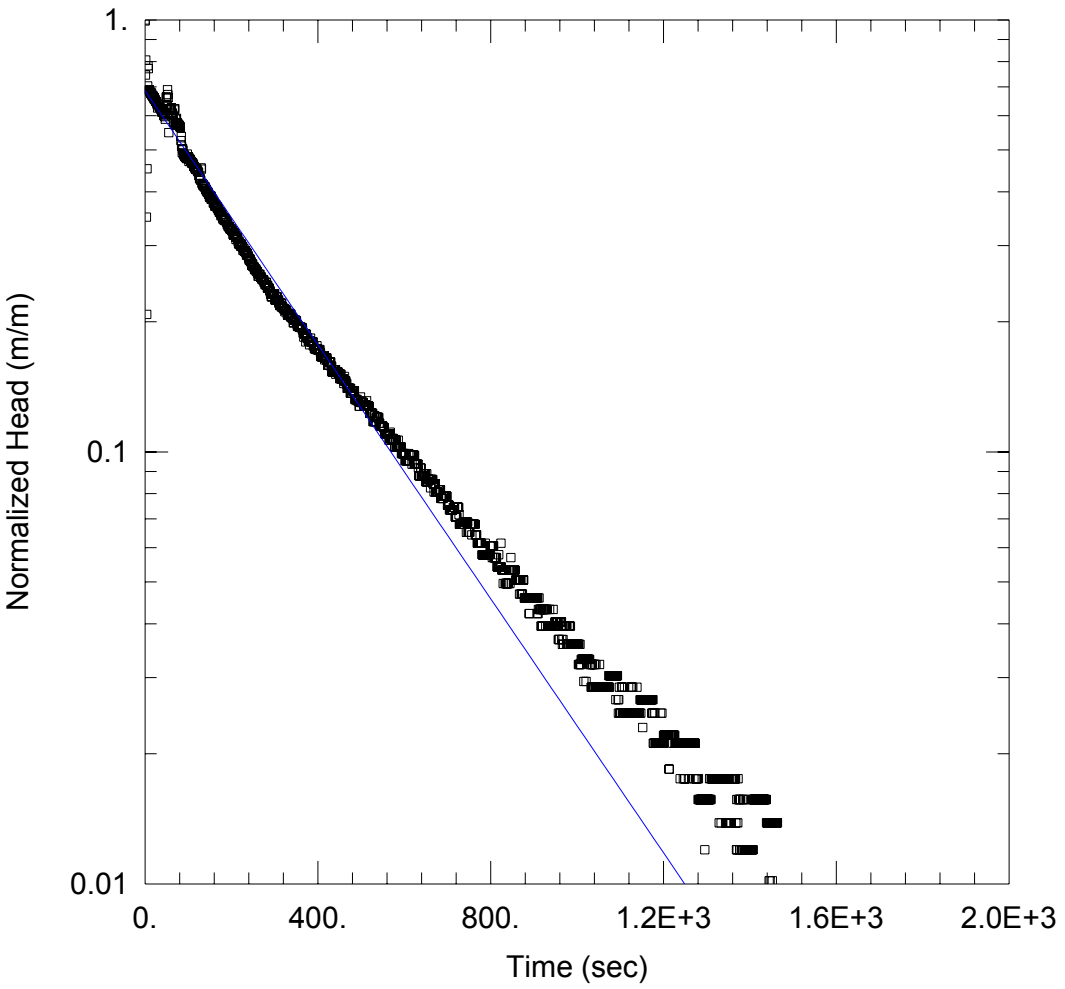

WELL TEST ANALYSIS

Data Set: W:\Grad Studies\Chalk River Field Work\AqteSOLV\Response Testing\LPH32_FH.aqt
Date: 12/08/14 Time: 14:04:27

PROJECT INFORMATION

Location: Chalk River: WMAF
Test Well: LPH25-I
Test Date: 27-Aug-14

AQUIFER DATA

Saturated Thickness: 12.65 m Anisotropy Ratio (Kz/Kr): 1.

WELL DATA (LPH32_FH)

Initial Displacement: 1. m
Total Well Penetration Depth: 12.64 m
Casing Radius: 0.02 m
Static Water Column Height: 2.39 m
Screen Length: 0.3 m
Well Radius: 0.02 m

SOLUTION

Aquifer Model: Unconfined Solution Method: Hvorslev

K = 6.12E-6 m/sec y0 = 0.6851 m

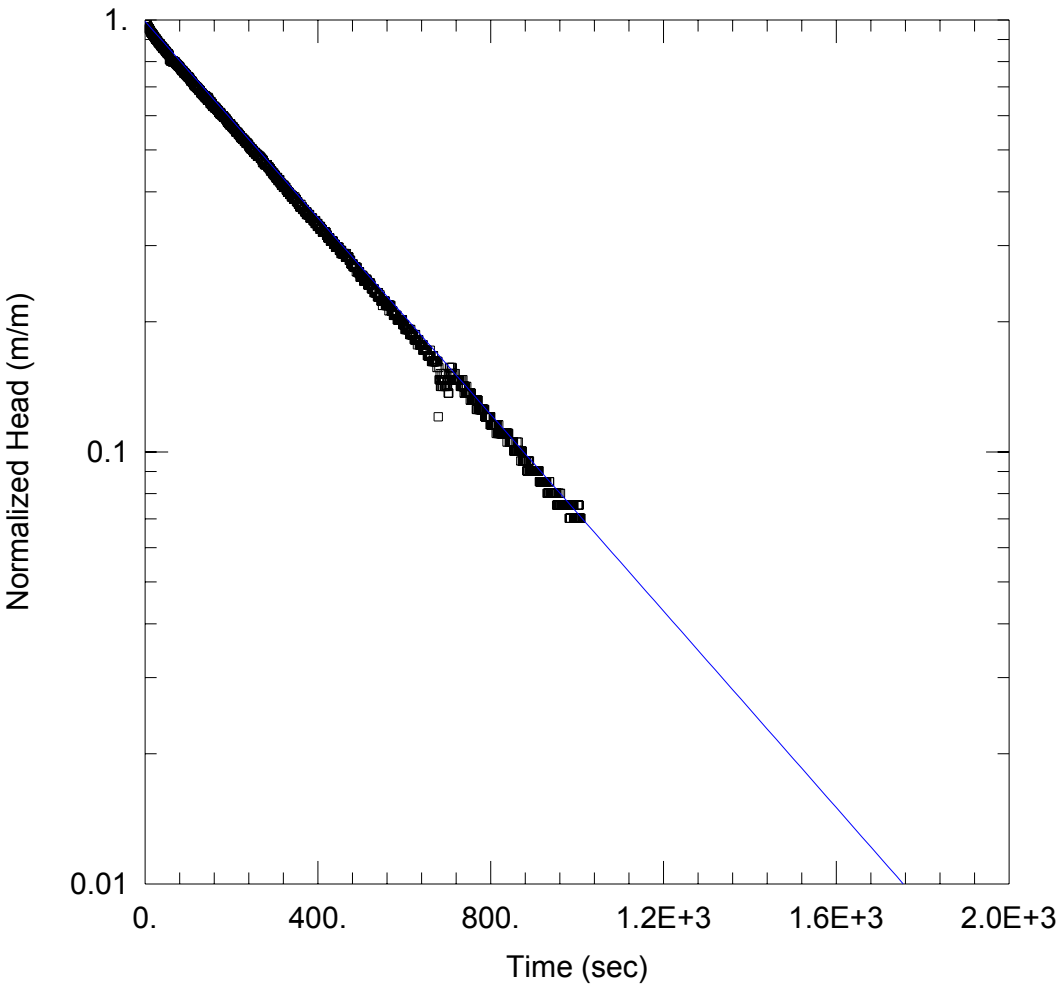

WELL TEST ANALYSIS

Data Set: W:\Grad Studies\Chalk River Field Work\AqteSOLV\Response Testing\LPH32_RH.aqt
Date: 12/08/14 Time: 14:05:20

PROJECT INFORMATION

Location: Chalk River: WMAF
Test Well: LPH25-I
Test Date: 27-Aug-14

AQUIFER DATA

Saturated Thickness: 12.65 m Anisotropy Ratio (Kz/Kr): 1.

WELL DATA (LPH32_RH)

Initial Displacement: 0.73 m
Total Well Penetration Depth: 12.64 m
Casing Radius: 0.02 m
Static Water Column Height: 2.39 m
Screen Length: 0.3 m
Well Radius: 0.02 m

SOLUTION

Aquifer Model: Unconfined
Solution Method: Hvorslev
K = 4.737E-6 m/sec
y0 = 0.7245 m

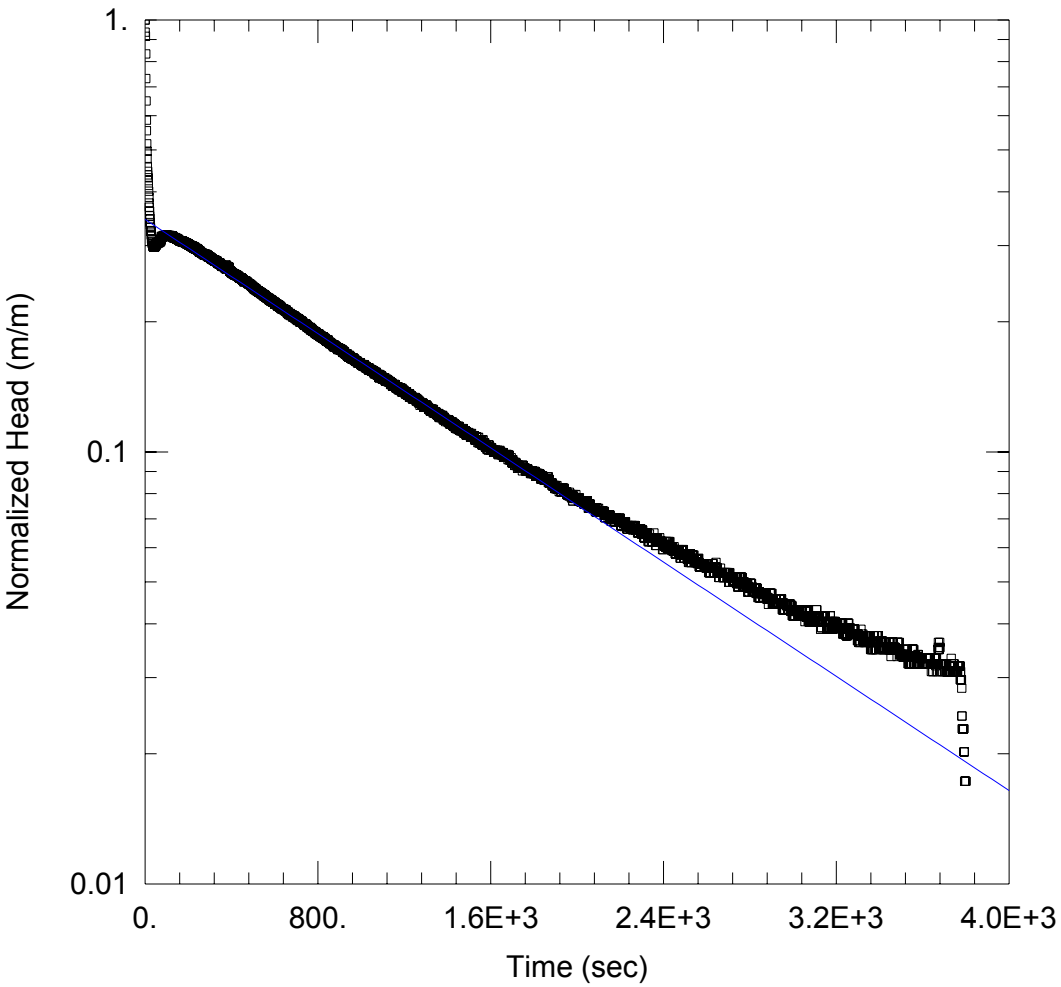

WELL TEST ANALYSIS

Data Set: W:\Grad Studies\Chalk River Field Work\AqteSOLV\Response Testing\LPH37_FH.aqt
Date: 12/08/14 Time: 14:05:52

PROJECT INFORMATION

Location: Chalk River: WMAF
Test Well: LPH25-I
Test Date: 27-Aug-14

AQUIFER DATA

Saturated Thickness: 12.56 m Anisotropy Ratio (Kz/Kr): 1.

WELL DATA (LPH37_FH)

Initial Displacement: 2.81 m Static Water Column Height: 1.62 m
Total Well Penetration Depth: 12.56 m Screen Length: 0.3 m
Casing Radius: 0.02 m Well Radius: 0.02 m

SOLUTION

Aquifer Model: Unconfined Solution Method: Hvorslev
K = 1.726E-6 m/sec y0 = 0.97 m

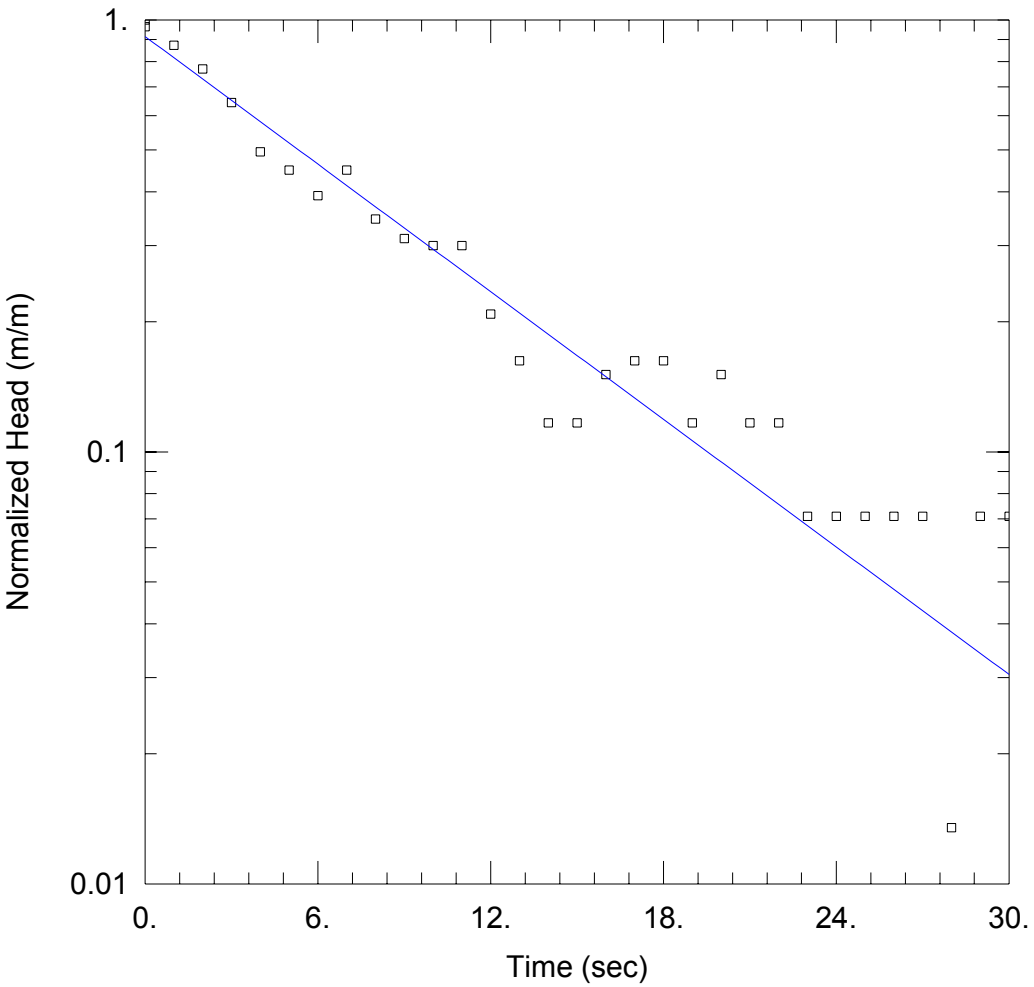

WELL TEST ANALYSIS

Data Set: W:\Grad Studies\Chalk River Field Work\AqteSOLV\Response Testing\LPH37_RH.aqt
Date: 12/08/14 Time: 14:06:22

PROJECT INFORMATION

Location: Chalk River: WMAF
Test Well: LPH25-I
Test Date: 27-Aug-14

AQUIFER DATA

Saturated Thickness: 12.56 m Anisotropy Ratio (Kz/Kr): 1.

WELL DATA (LPH37_RH)

Initial Displacement: 0.08 m
Total Well Penetration Depth: 12.56 m
Casing Radius: 0.02 m
Static Water Column Height: 1.62 m
Screen Length: 0.3 m
Well Radius: 0.02 m

SOLUTION

Aquifer Model: Unconfined
Solution Method: Hvorslev
K = 0.0002571 m/sec
y0 = 0.0732 m

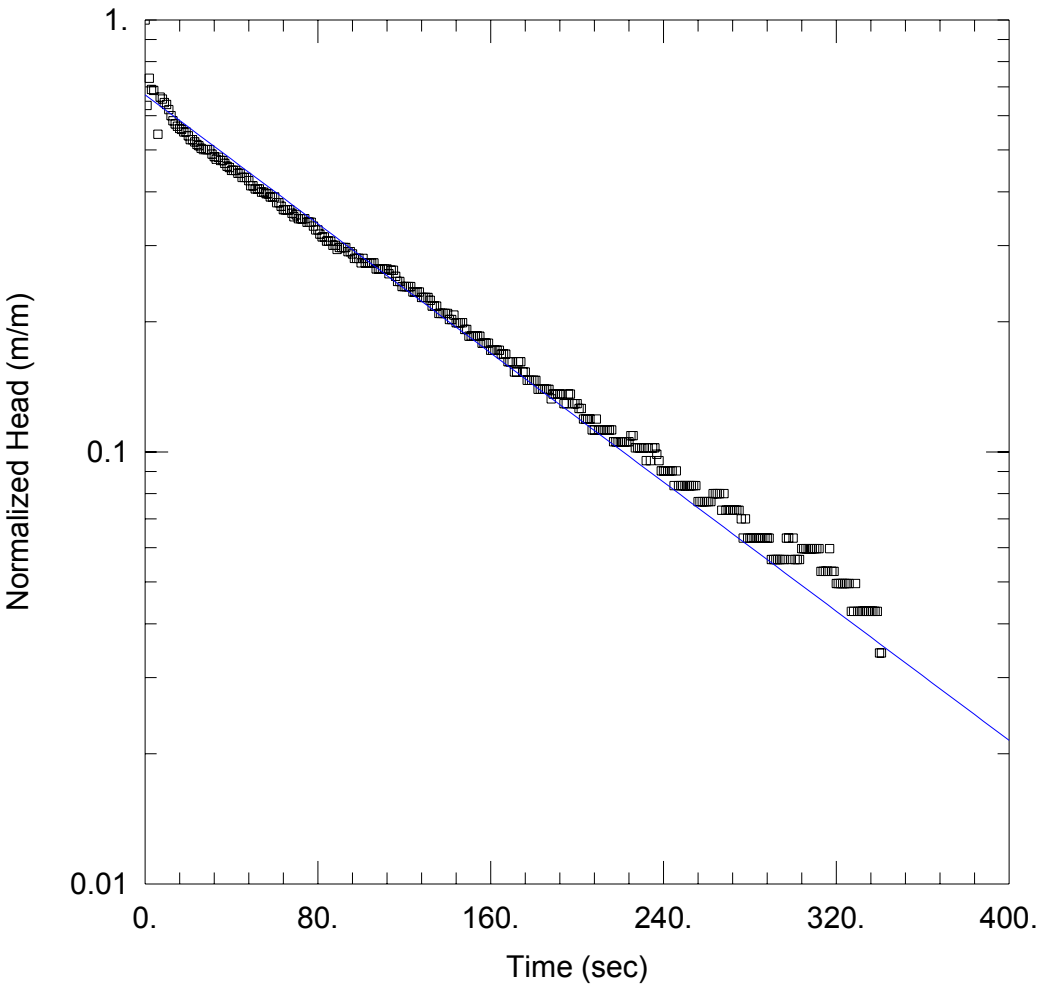

WELL TEST ANALYSIS

Data Set: W:\Grad Studies\Chalk River Field Work\AqteSOLV\Response Testing\LPH39-II_FH.aqt
Date: 12/08/14 Time: 14:06:53

PROJECT INFORMATION

Location: Chalk River: WMAF
Test Well: LPH25-I
Test Date: 27-Aug-14

AQUIFER DATA

Saturated Thickness: 16.73 m Anisotropy Ratio (Kz/Kr): 1.

WELL DATA (LPH39-II_FH)

Initial Displacement: 0.54 m
Total Well Penetration Depth: 16.73 m
Casing Radius: 0.03 m
Static Water Column Height: 13.43 m
Screen Length: 1.52 m
Well Radius: 0.03 m

SOLUTION

Aquifer Model: Unconfined
Solution Method: Hvorslev
K = 1.176E-5 m/sec
y0 = 0.3622 m

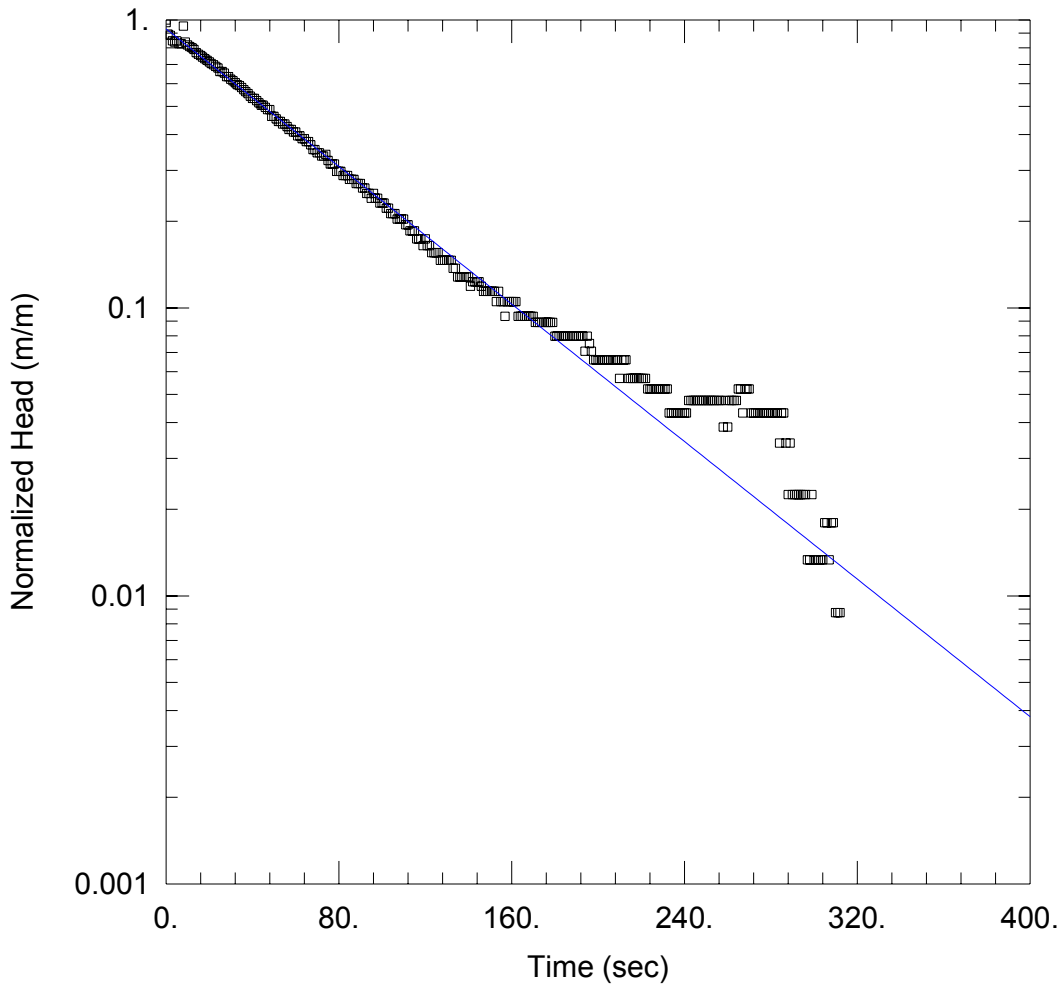

WELL TEST ANALYSIS

Data Set: W:\Grad Studies\Chalk River Field Work\AqteSOLV\Response Testing\LPH39-II_RH.aqt
Date: 12/08/14 Time: 14:07:27

PROJECT INFORMATION

Location: Chalk River: WMAF
Test Well: LPH25-I
Test Date: 27-Aug-14

AQUIFER DATA

Saturated Thickness: 16.73 m Anisotropy Ratio (Kz/Kr): 1.

WELL DATA (LPH39-II_RH)

Initial Displacement: 0.4 m
Total Well Penetration Depth: 16.73 m
Casing Radius: 0.03 m
Static Water Column Height: 13.43 m
Screen Length: 1.52 m
Well Radius: 0.03 m

SOLUTION

Aquifer Model: Unconfined
Solution Method: Hvorslev
K = 1.88E-5 m/sec
y0 = 0.372 m

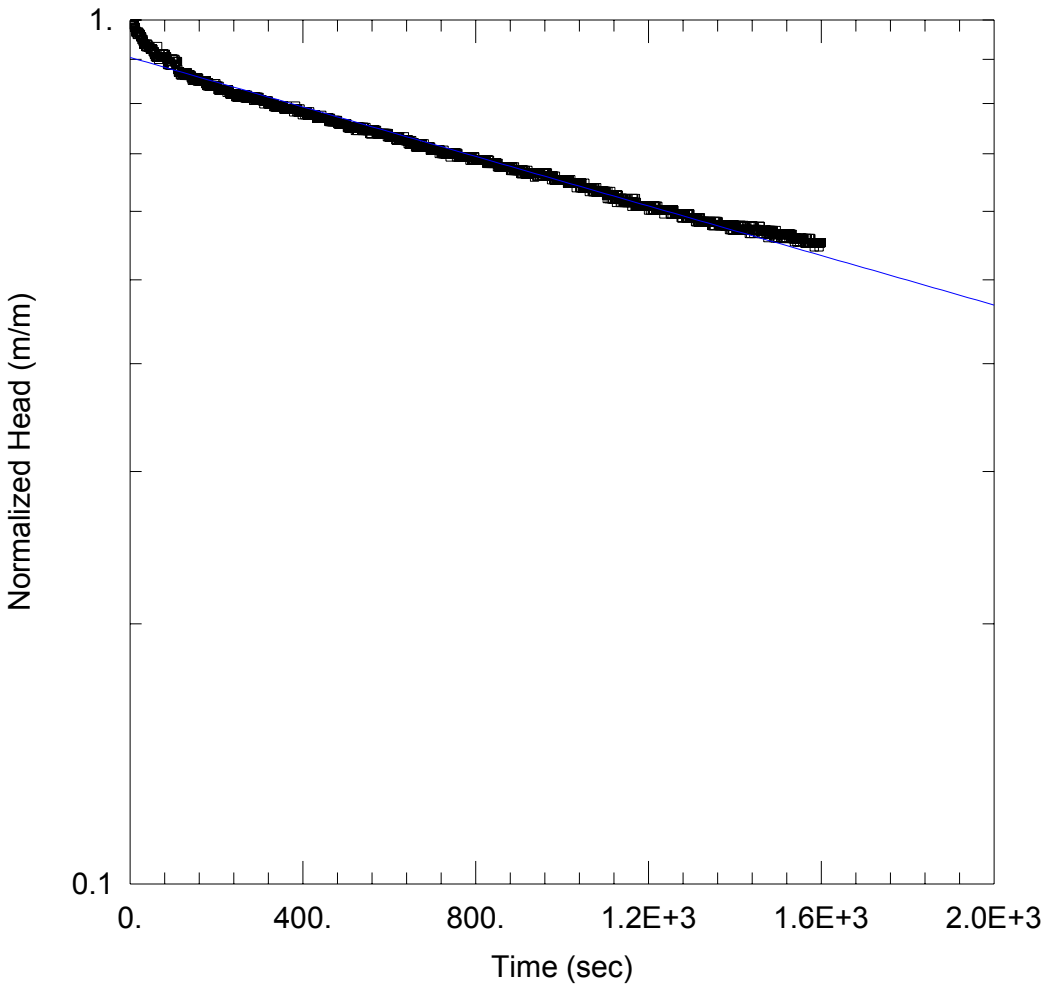

WELL TEST ANALYSIS

Data Set: W:\Grad Studies\Chalk River Field Work\AqteSOLV\Response Testing\LPH40_FH.aqt
Date: 12/08/14 Time: 14:07:53

PROJECT INFORMATION

Location: Chalk River: WMAF
Test Well: LPH25-I
Test Date: 27-Aug-14

AQUIFER DATA

Saturated Thickness: 4.03 m Anisotropy Ratio (Kz/Kr): 1.

WELL DATA (LPH40_FH)

Initial Displacement: 0.6 m
Total Well Penetration Depth: 17.39 m
Casing Radius: 0.02 m
Static Water Column Height: 5.89 m
Screen Length: 3.05 m
Well Radius: 0.02 m

SOLUTION

Aquifer Model: Unconfined
Solution Method: Hvorslev
K = 1.238E-7 m/sec
y0 = 0.5429 m

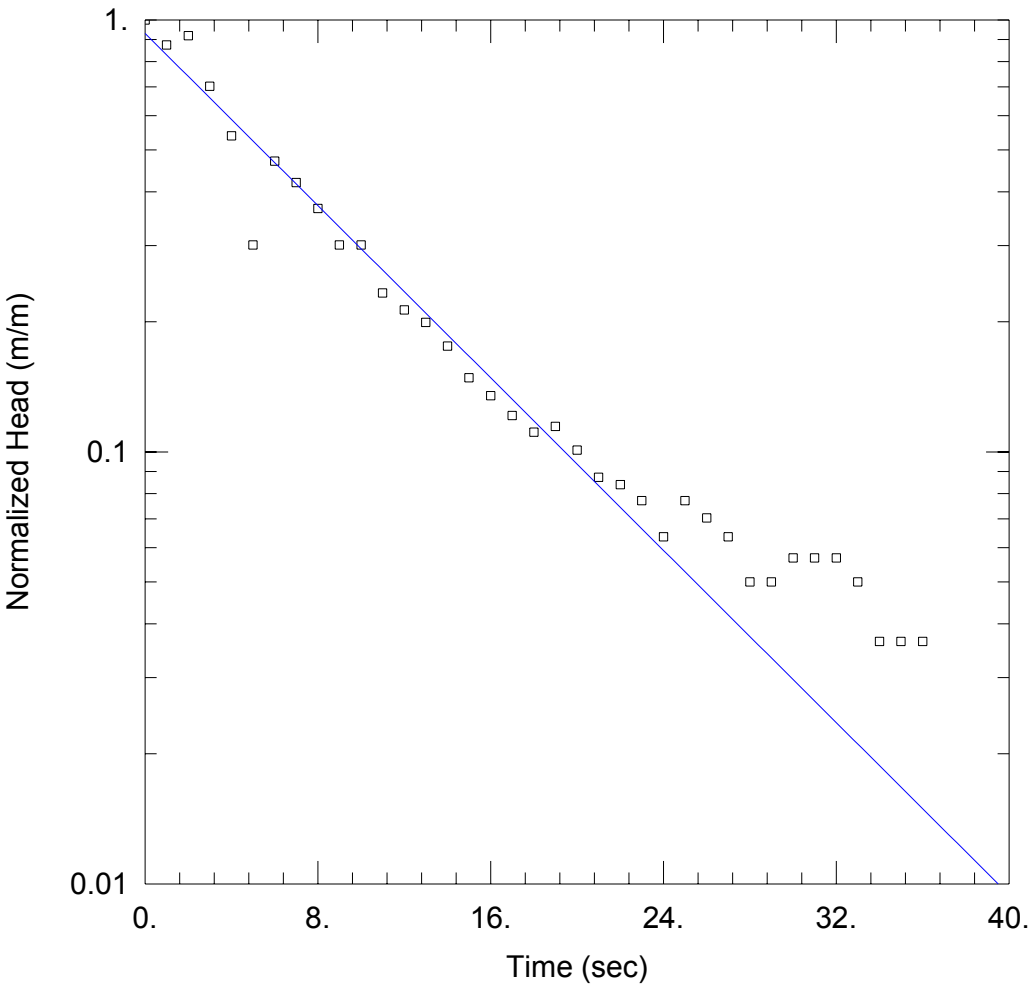

WELL TEST ANALYSIS

Data Set: W:\Grad Studies\Chalk River Field Work\AqteSOLV\Response Testing\LPH41-II_FH.aqt
Date: 12/08/14 Time: 14:08:19

PROJECT INFORMATION

Location: Chalk River: WMAF
Test Well: LPH25-I
Test Date: 27-Aug-14

AQUIFER DATA

Saturated Thickness: 6.77 m Anisotropy Ratio (Kz/Kr): 1.

WELL DATA (LPH41-II_FH)

Initial Displacement: 0.27 m Static Water Column Height: 2.37 m
Total Well Penetration Depth: 6.77 m Screen Length: 1.52 m
Casing Radius: 0.03 m Well Radius: 0.03 m

SOLUTION

Aquifer Model: Unconfined Solution Method: Hvorslev
K = 0.0001569 m/sec y0 = 0.2512 m

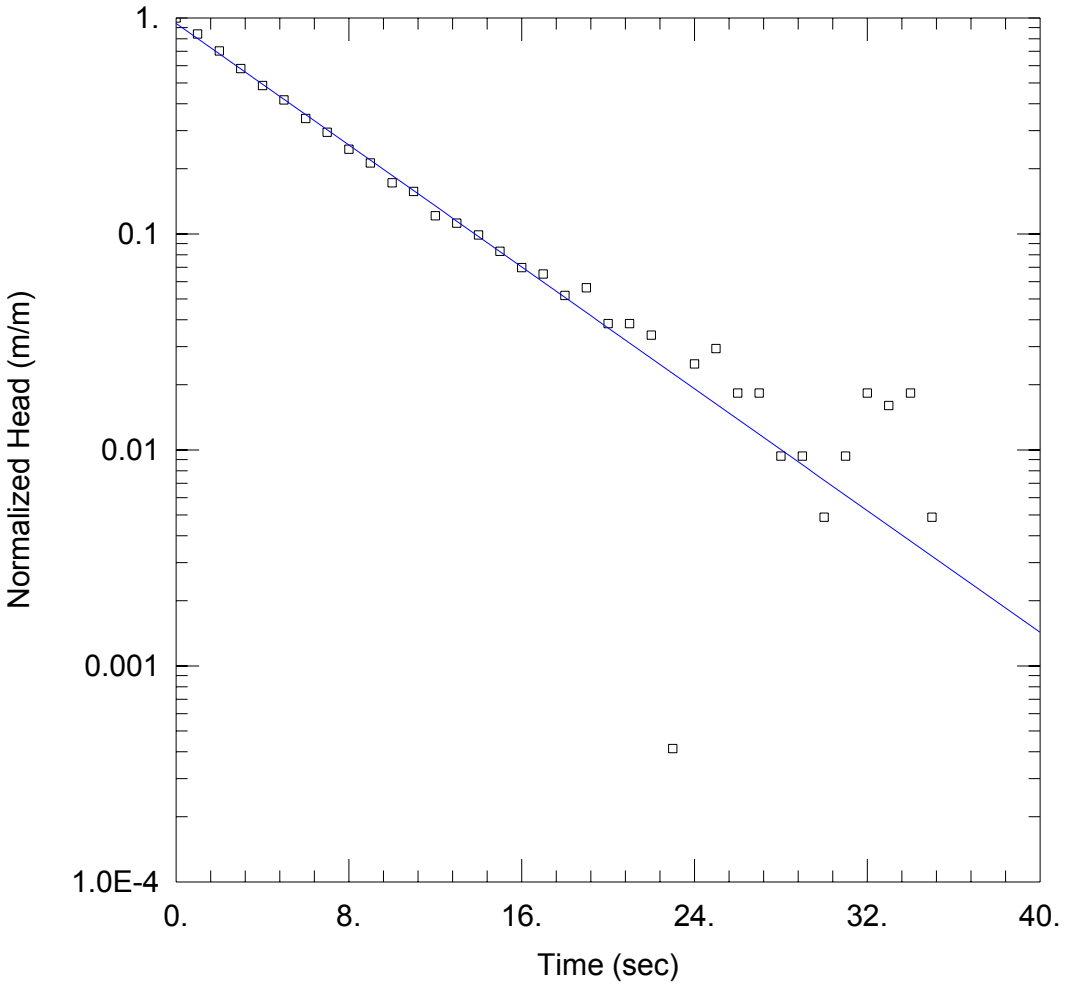

WELL TEST ANALYSIS

Data Set: W:\Grad Studies\Chalk River Field Work\AqteSOLV\Response Testing\LPH41-II_RH.aqt
Date: 12/08/14 Time: 14:09:01

PROJECT INFORMATION

Location: Chalk River: WMAF
Test Well: LPH25-I
Test Date: 27-Aug-14

AQUIFER DATA

Saturated Thickness: 6.77 m Anisotropy Ratio (Kz/Kr): 1.

WELL DATA (LPH41-II_RH)

Initial Displacement: 0.41 m Static Water Column Height: 2.37 m
Total Well Penetration Depth: 6.77 m Screen Length: 1.52 m
Casing Radius: 0.03 m Well Radius: 0.03 m

SOLUTION

Aquifer Model: Unconfined Solution Method: Hvorslev
K = 0.0002218 m/sec y0 = 0.3866 m

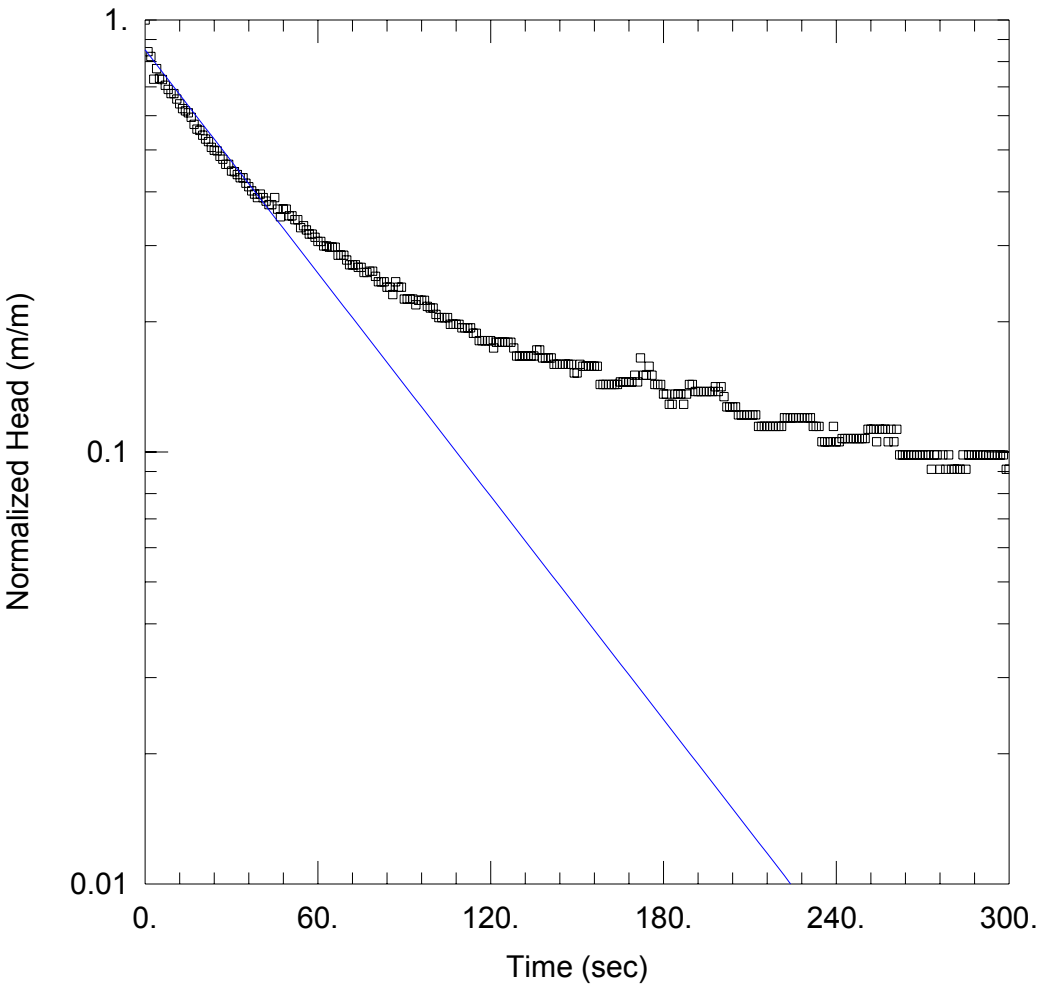

WELL TEST ANALYSIS

Data Set: W:\Grad Studies\Chalk River Field Work\AqteSOLV\Response Testing\LPH42-I_FH.aqt
Date: 12/08/14 Time: 14:10:11

PROJECT INFORMATION

Location: Chalk River: WMAF
Test Well: LPH25-I
Test Date: 27-Aug-14

AQUIFER DATA

Saturated Thickness: 11.12 m Anisotropy Ratio (Kz/Kr): 1.

WELL DATA (LPH42-I_FH)

Initial Displacement: 0.51 m
Total Well Penetration Depth: 11.12 m
Casing Radius: 0.03 m
Static Water Column Height: 10.59 m
Screen Length: 3.05 m
Well Radius: 0.03 m

SOLUTION

Aquifer Model: Unconfined
Solution Method: Hvorslev
K = 1.555E-5 m/sec
y0 = 0.4345 m

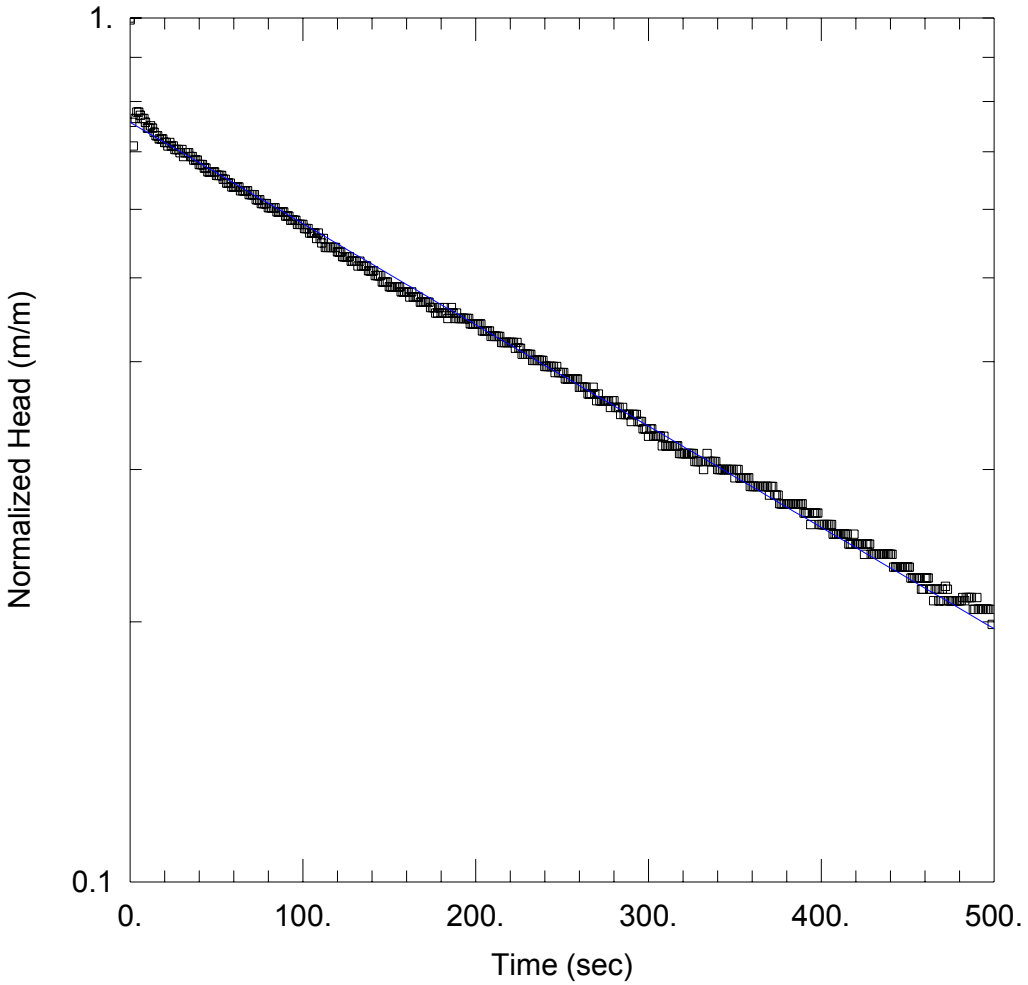

WELL TEST ANALYSIS

Data Set: W:\Grad Studies\Chalk River Field Work\AqteSOLV\Response Testing\LPH42-I_RH.aqt
Date: 12/08/14 Time: 14:10:55

PROJECT INFORMATION

Location: Chalk River: WMAF
Test Well: LPH25-I
Test Date: 27-Aug-14

AQUIFER DATA

Saturated Thickness: 11.12 m Anisotropy Ratio (Kz/Kr): 1.

WELL DATA (LPH42-I_RH)

Initial Displacement: 0.56 m
Total Well Penetration Depth: 11.12 m
Casing Radius: 0.03 m
Static Water Column Height: 10.59 m
Screen Length: 3.05 m
Well Radius: 0.03 m

SOLUTION

Aquifer Model: Unconfined
Solution Method: Hvorslev
K = 2.116E-6 m/sec
y0 = 0.4238 m

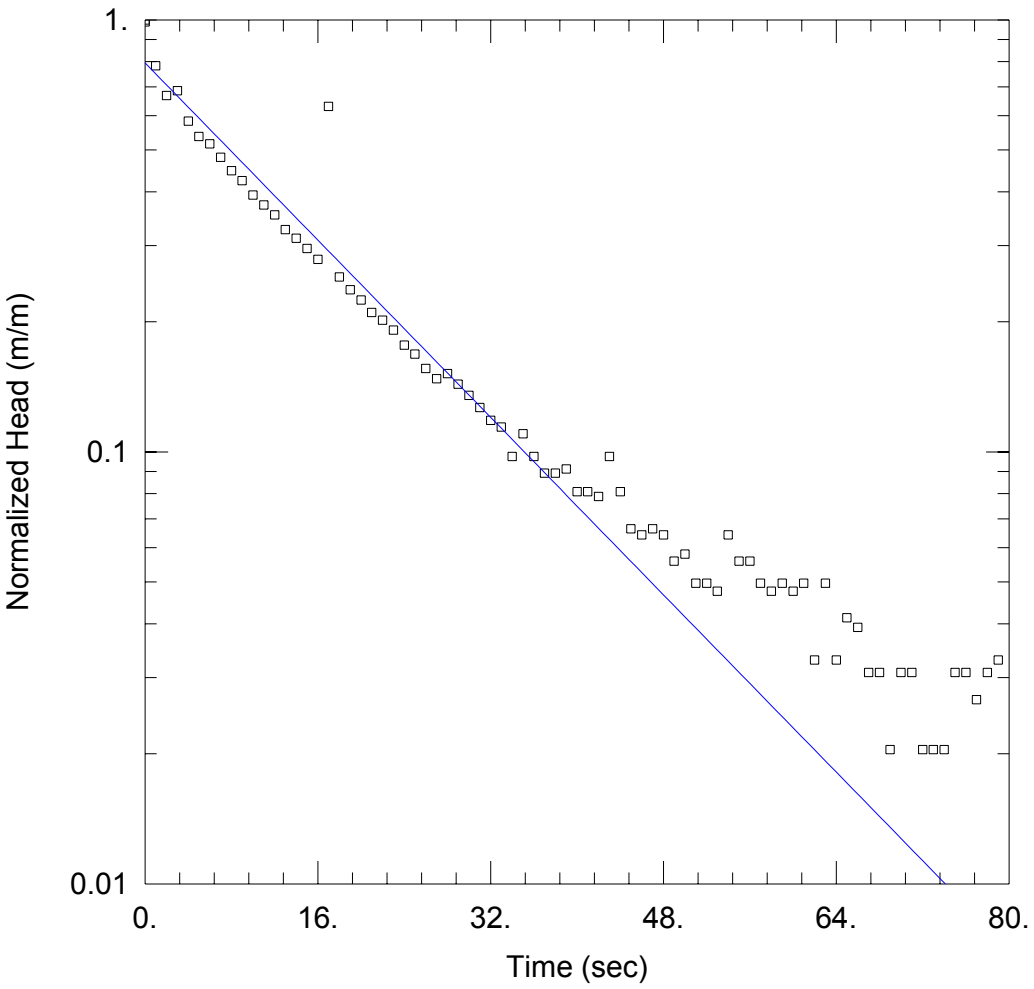

WELL TEST ANALYSIS

Data Set: W:\Grad Studies\Chalk River Field Work\AqteSOLV\Response Testing\LPH42-II_FH.aqt
Date: 12/08/14 Time: 14:11:23

PROJECT INFORMATION

Location: Chalk River: WMAF
Test Well: LPH25-I
Test Date: 27-Aug-14

AQUIFER DATA

Saturated Thickness: 1.8 m Anisotropy Ratio (Kz/Kr): 1.

WELL DATA (LPH42-II_FH)

Initial Displacement: 0.44 m
Total Well Penetration Depth: 1.8 m
Casing Radius: 0.03 m
Static Water Column Height: 0.83 m
Screen Length: 1.52 m
Well Radius: 0.03 m

SOLUTION

Aquifer Model: Unconfined
Solution Method: Hvorslev
K = 8.072E-5 m/sec
y0 = 0.3497 m

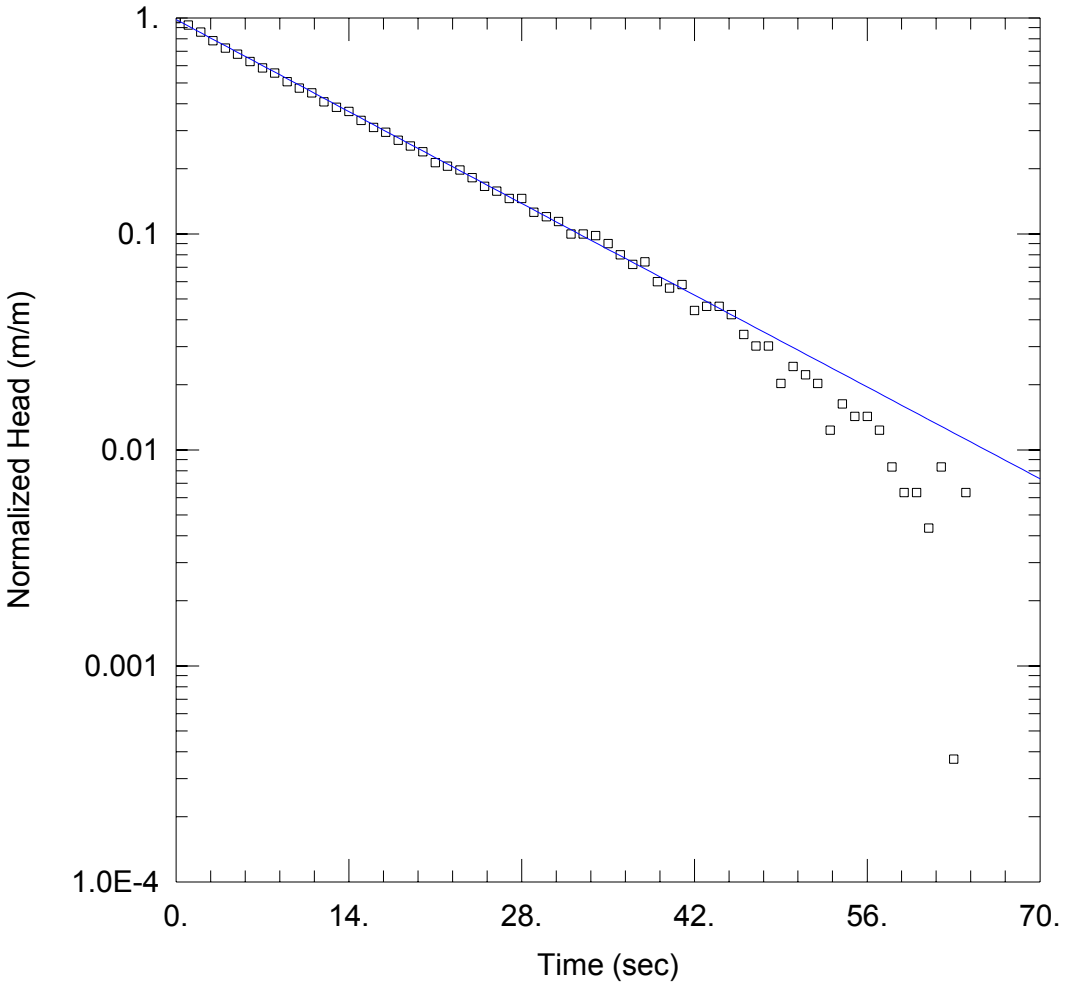

WELL TEST ANALYSIS

Data Set: W:\Grad Studies\Chalk River Field Work\AqteSOLV\Response Testing\LPH42-II_RH.aqt
Date: 12/08/14 Time: 14:11:50

PROJECT INFORMATION

Location: Chalk River: WMAF
Test Well: LPH25-I
Test Date: 27-Aug-14

AQUIFER DATA

Saturated Thickness: 1.8 m Anisotropy Ratio (Kz/Kr): 1.

WELL DATA (LPH42-II_RH)

Initial Displacement: 0.46 m
Total Well Penetration Depth: 1.8 m
Casing Radius: 0.03 m
Static Water Column Height: 0.83 m
Screen Length: 1.52 m
Well Radius: 0.03 m

SOLUTION

Aquifer Model: Unconfined
Solution Method: Hvorslev
K = 9.562E-5 m/sec
y0 = 0.4513 m

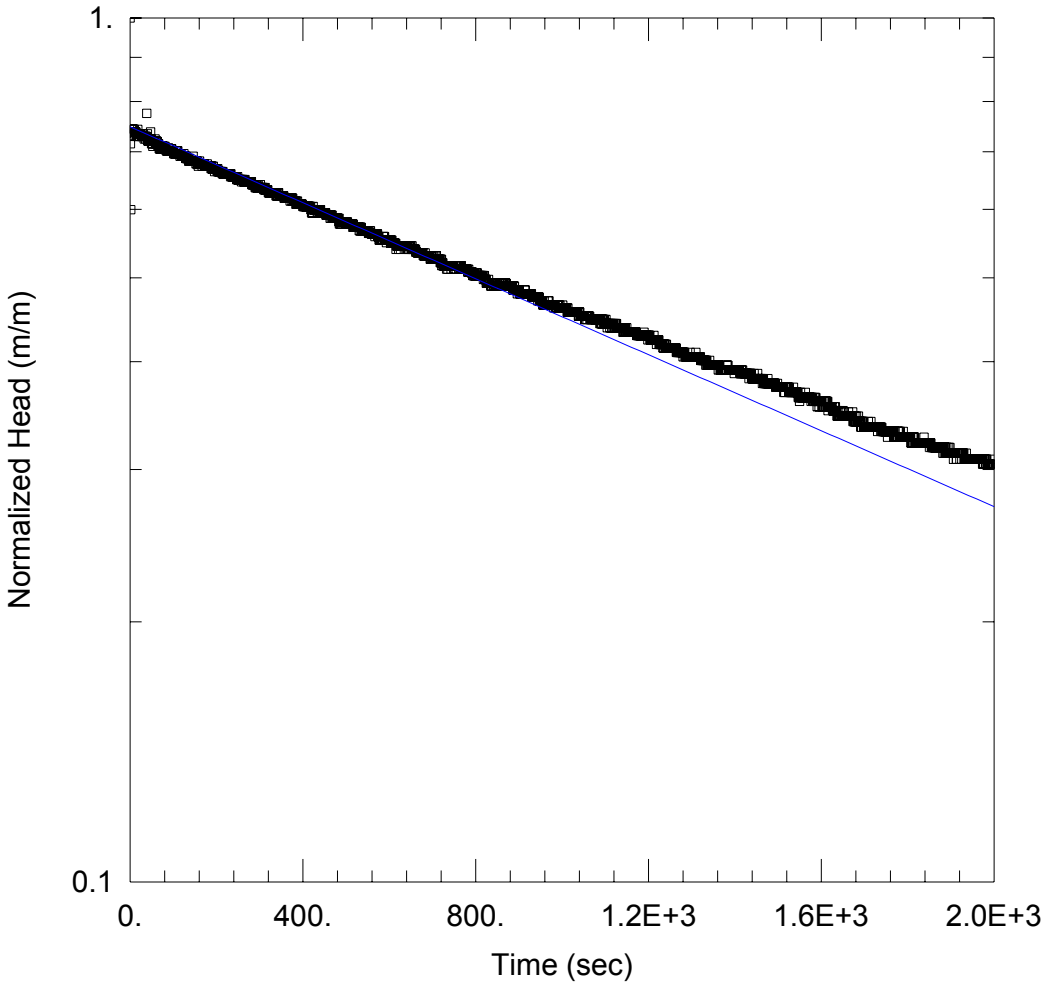

WELL TEST ANALYSIS

Data Set: W:\Grad Studies\Chalk River Field Work\AqteSOLV\Response Testing\LPH43-I_FH.aqt
Date: 12/08/14 Time: 14:13:13

PROJECT INFORMATION

Location: Chalk River: WMAF
Test Well: LPH25-I
Test Date: 27-Aug-14

AQUIFER DATA

Saturated Thickness: 2.28 m Anisotropy Ratio (Kz/Kr): 1.

WELL DATA (LPH43-I_FH)

Initial Displacement: 0.73 m
Total Well Penetration Depth: 19.76 m
Casing Radius: 0.03 m
Static Water Column Height: 18.64 m
Screen Length: 1.52 m
Well Radius: 0.03 m

SOLUTION

Aquifer Model: Unconfined
Solution Method: Hvorslev
K = 6.922E-7 m/sec
y0 = 0.5461 m

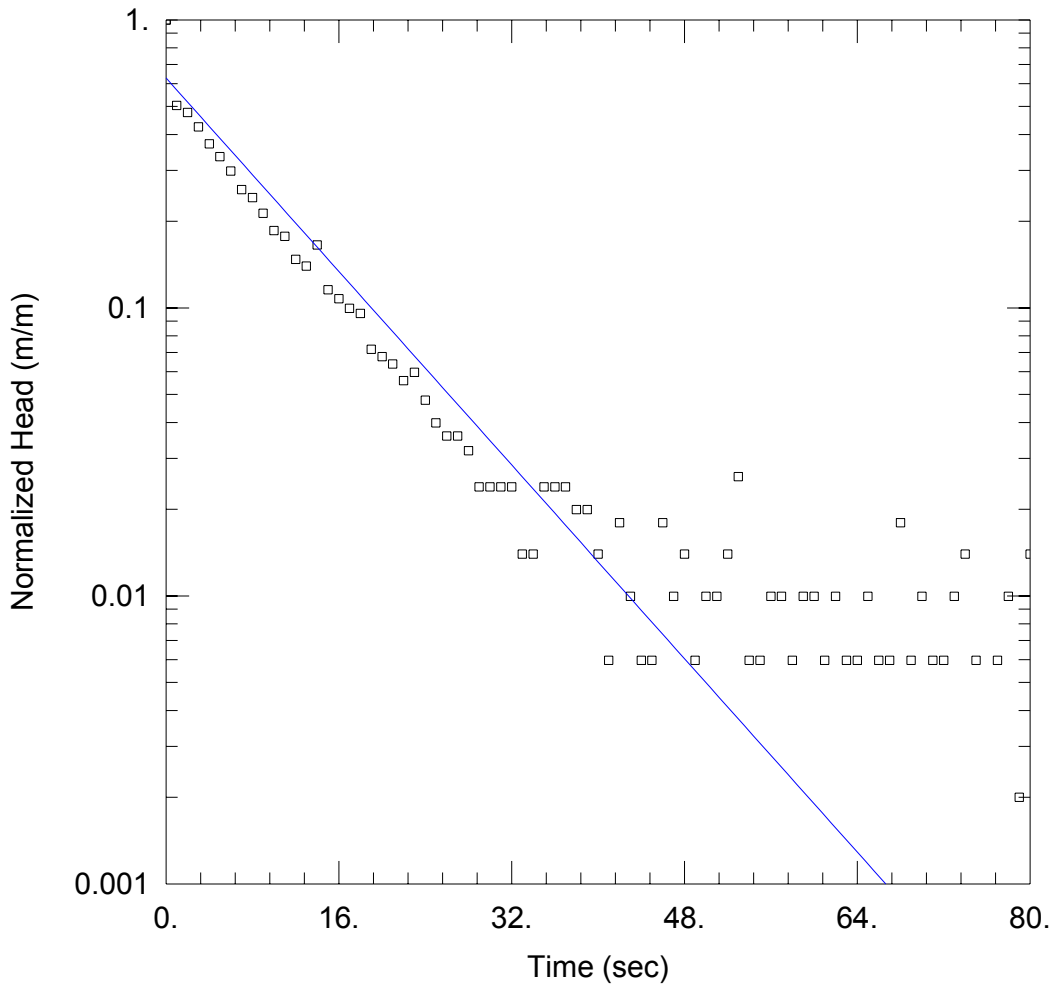

WELL TEST ANALYSIS

Data Set: W:\Grad Studies\Chalk River Field Work\AqteSOLV\Response Testing\LPH43-II_FH.aqt
Date: 12/08/14 Time: 14:14:03

PROJECT INFORMATION

Location: Chalk River: WMAF
Test Well: LPH25-I
Test Date: 27-Aug-14

AQUIFER DATA

Saturated Thickness: 3.36 m Anisotropy Ratio (Kz/Kr): 1.

WELL DATA (LPH43-II_FH)

Initial Displacement: 0.46 m
Total Well Penetration Depth: 3.36 m
Casing Radius: 0.03 m
Static Water Column Height: 5.16 m
Screen Length: 1.52 m
Well Radius: 0.03 m

SOLUTION

Aquifer Model: Unconfined
Solution Method: Hvorslev
K = 0.0001322 m/sec
y0 = 0.2888 m

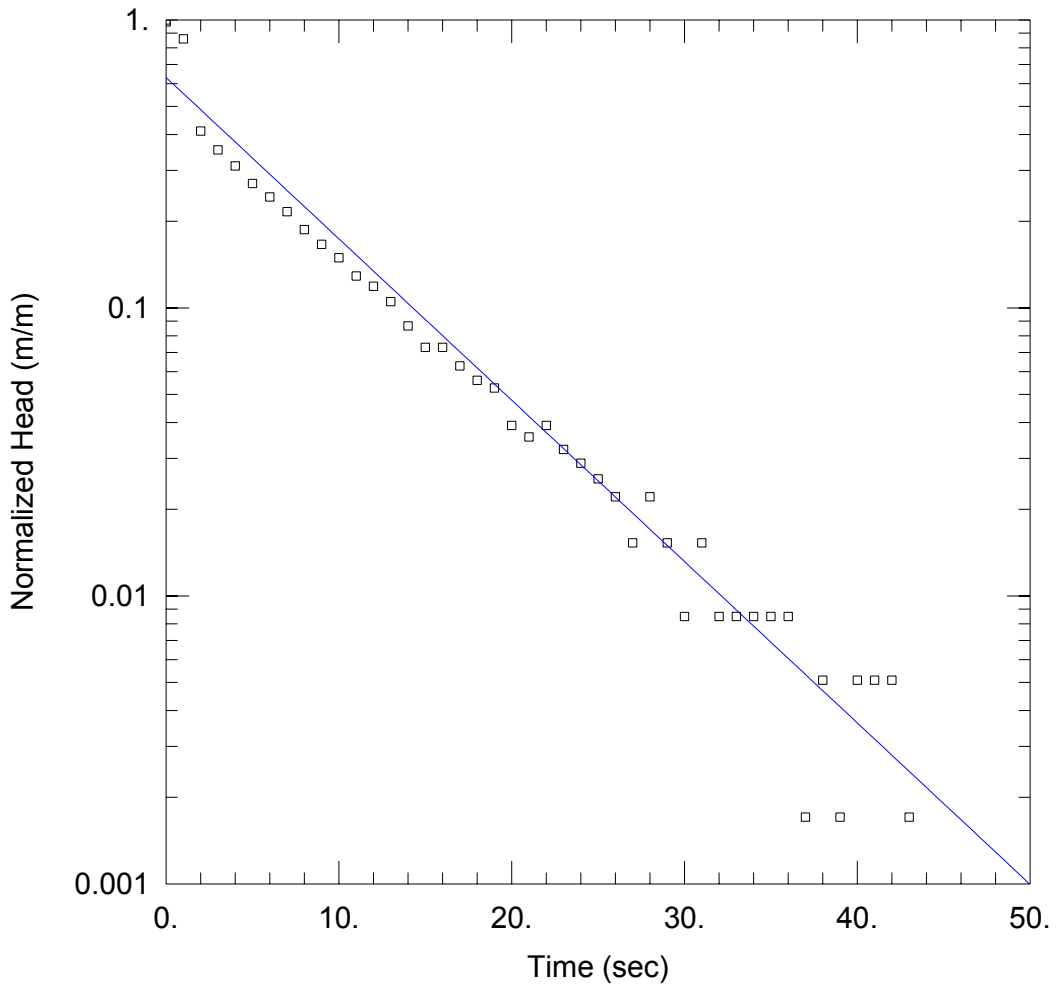

WELL TEST ANALYSIS

Data Set: W:\Grad Studies\Chalk River Field Work\AqteSOLV\Response Testing\LPH43-II_RH.aqt
Date: 12/08/14 Time: 14:14:45

PROJECT INFORMATION

Location: Chalk River: WMAF
Test Well: LPH25-I
Test Date: 27-Aug-14

AQUIFER DATA

Saturated Thickness: 3.36 m Anisotropy Ratio (Kz/Kr): 1.

WELL DATA (LPH43-II_RH)

Initial Displacement: 0.54 m
Total Well Penetration Depth: 3.36 m
Casing Radius: 0.03 m
Static Water Column Height: 5.16 m
Screen Length: 1.52 m
Well Radius: 0.03 m

SOLUTION

Aquifer Model: Unconfined
Solution Method: Hvorslev
K = 0.0001764 m/sec
y0 = 0.3407 m

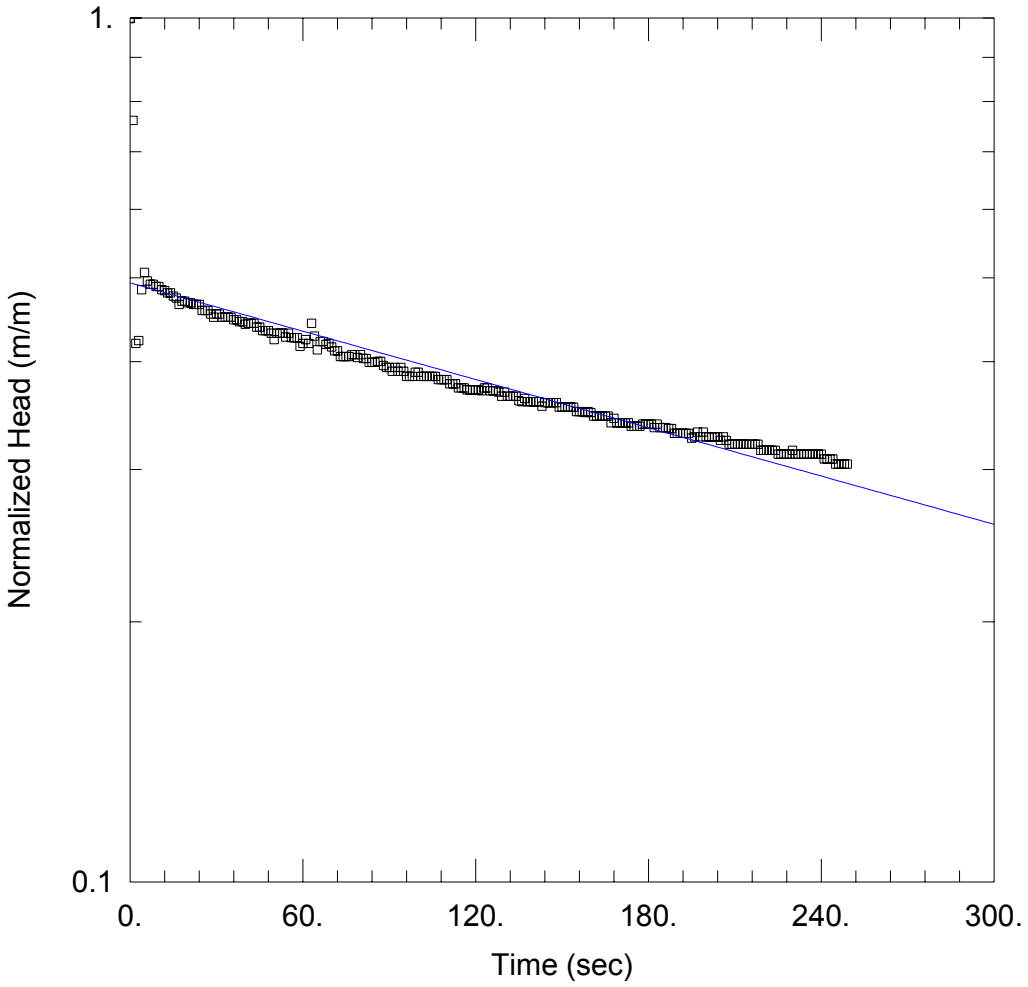

WELL TEST ANALYSIS

Data Set: W:\Grad Studies\Chalk River Field Work\AqteSOLV\Response Testing\LPH45-I_FH.aqt
Date: 12/08/14 Time: 14:17:58

PROJECT INFORMATION

Location: Chalk River: WMAF
Test Well: LPH25-I
Test Date: 27-Aug-14

AQUIFER DATA

Saturated Thickness: 9.67 m Anisotropy Ratio (Kz/Kr): 1.

WELL DATA (LPH45-I_FH)

Initial Displacement: 0.88 m Static Water Column Height: 7.89 m
Total Well Penetration Depth: 9.67 m Screen Length: 3.05 m
Casing Radius: 0.03 m Well Radius: 0.03 m

SOLUTION

Aquifer Model: Unconfined Solution Method: Hvorslev
K = 1.682E-6 m/sec y0 = 0.4342 m

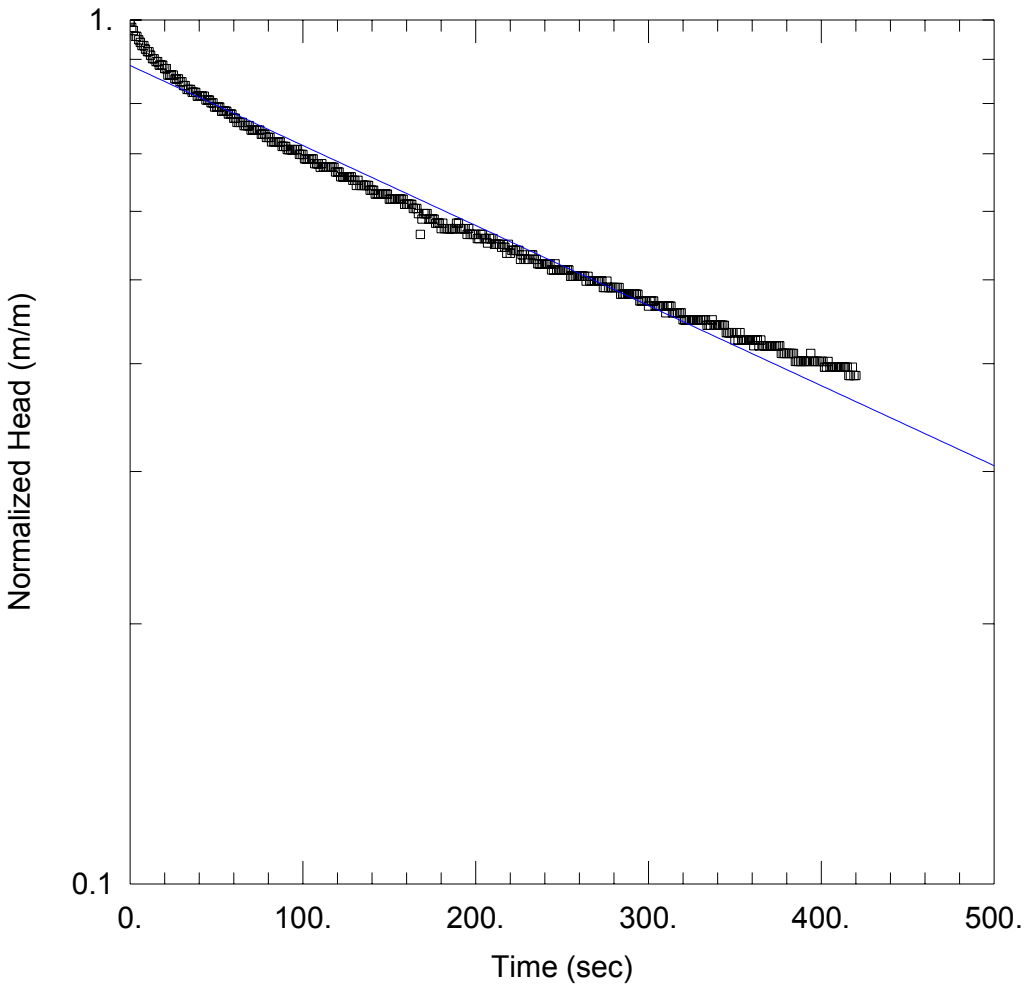

WELL TEST ANALYSIS

Data Set: W:\Grad Studies\Chalk River Field Work\AqteSOLV\Response Testing\LPH45-I_RH.aqt
Date: 12/08/14 Time: 14:18:39

PROJECT INFORMATION

Location: Chalk River: WMAF
Test Well: LPH25-I
Test Date: 27-Aug-14

AQUIFER DATA

Saturated Thickness: 9.67 m Anisotropy Ratio (Kz/Kr): 1.

WELL DATA (LPH45-I_RH)

Initial Displacement: 0.43 m
Total Well Penetration Depth: 9.67 m
Casing Radius: 0.03 m
Static Water Column Height: 7.89 m
Screen Length: 3.05 m
Well Radius: 0.03 m

SOLUTION

Aquifer Model: Unconfined
Solution Method: Hvorslev
K = 1.673E-6 m/sec
y0 = 0.3807 m

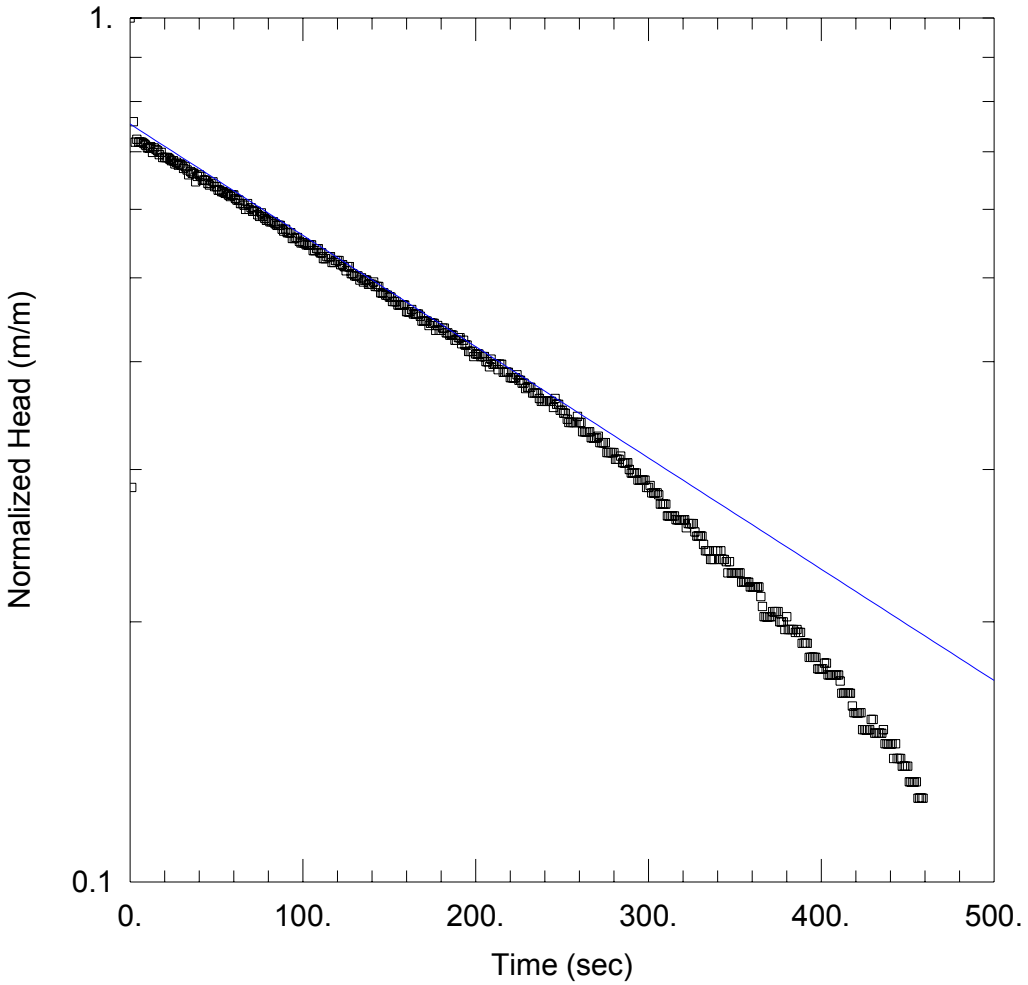

WELL TEST ANALYSIS

Data Set: W:\Grad Studies\Chalk River Field Work\AqteSOLV\Response Testing\LPH45-II_FH.aqt
Date: 12/08/14 Time: 14:19:15

PROJECT INFORMATION

Location: Chalk River: WMAF
Test Well: LPH25-I
Test Date: 27-Aug-14

AQUIFER DATA

Saturated Thickness: 5.74 m Anisotropy Ratio (Kz/Kr): 1.

WELL DATA (LPH45-II_FH)

Initial Displacement: 0.66 m
Total Well Penetration Depth: 5.74 m
Casing Radius: 0.03 m
Static Water Column Height: 1.5 m
Screen Length: 1.52 m
Well Radius: 0.03 m

SOLUTION

Aquifer Model: Unconfined
Solution Method: Hvorslev
K = 4.056E-6 m/sec
y0 = 0.4973 m

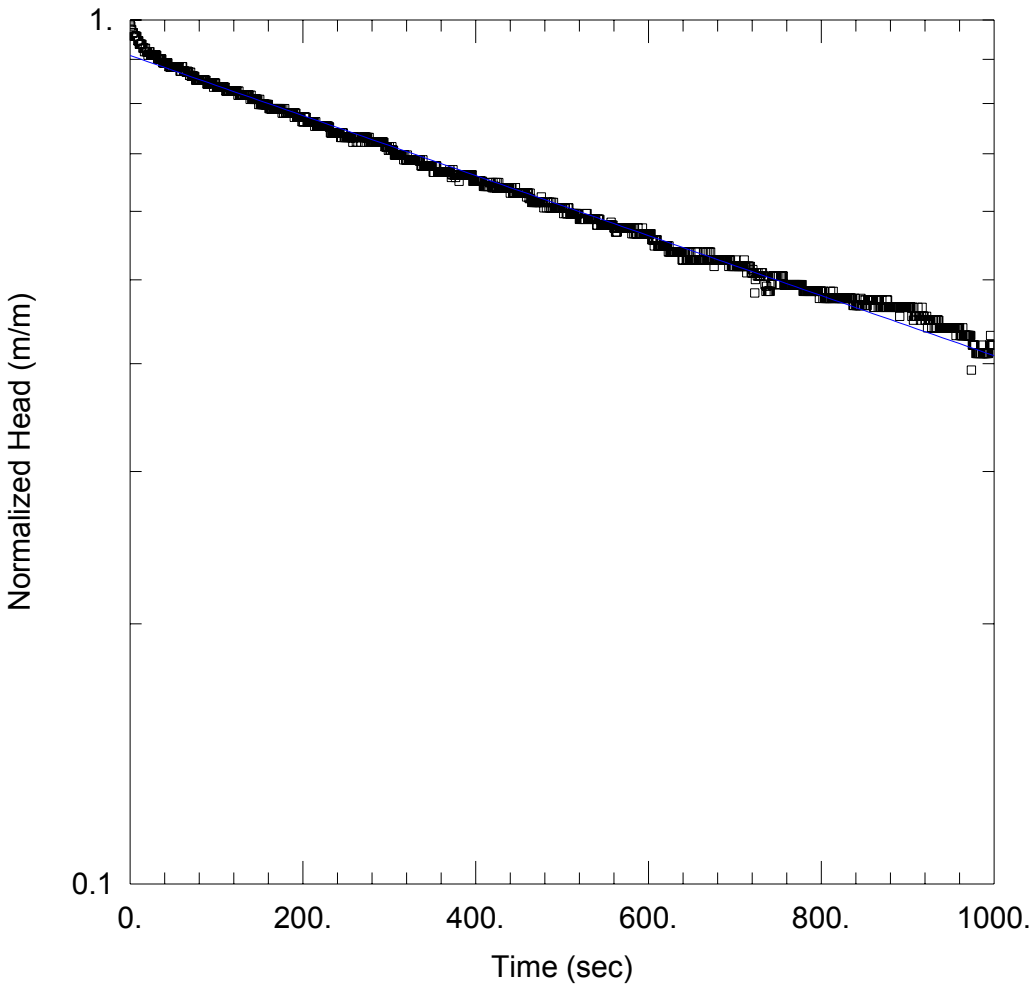

WELL TEST ANALYSIS

Data Set: W:\Grad Studies\Chalk River Field Work\AqteSOLV\Response Testing\LPH45-II_RH.aqt
Date: 12/08/14 Time: 14:19:47

PROJECT INFORMATION

Location: Chalk River: WMAF
Test Well: LPH25-I
Test Date: 27-Aug-14

AQUIFER DATA

Saturated Thickness: 5.74 m Anisotropy Ratio (Kz/Kr): 1.

WELL DATA (LPH45-II_RH)

Initial Displacement: 0.41 m Static Water Column Height: 1.5 m
Total Well Penetration Depth: 5.74 m Screen Length: 1.52 m
Casing Radius: 0.03 m Well Radius: 0.03 m

SOLUTION

Aquifer Model: Unconfined Solution Method: Hvorslev
K = 1.094E-6 m/sec y0 = 0.3728 m

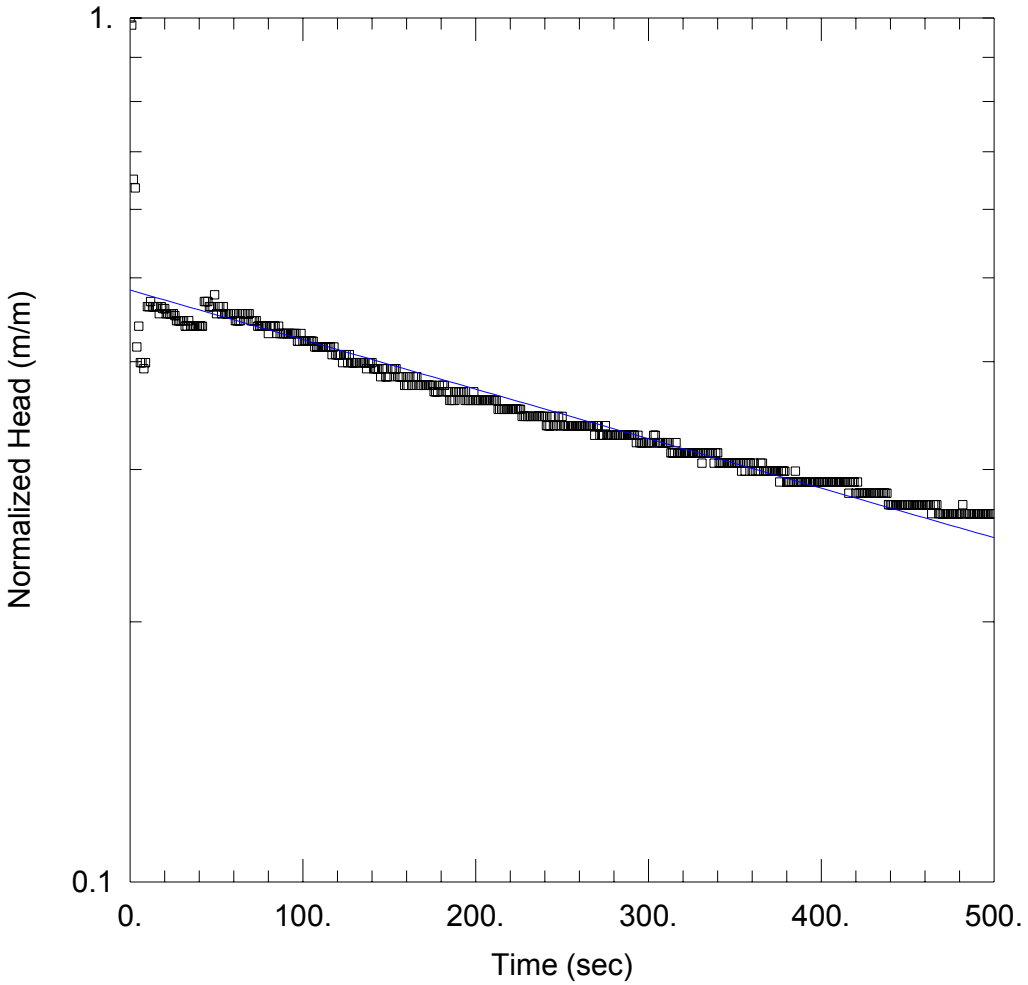

WELL TEST ANALYSIS

Data Set: W:\Grad Studies\Chalk River Field Work\AqteSOLV\Response Testing\LPH46-II_FH.aqt
Date: 12/08/14 Time: 14:20:20

PROJECT INFORMATION

Location: Chalk River: WMAF
Test Well: LPH25-I
Test Date: 27-Aug-14

AQUIFER DATA

Saturated Thickness: 19.34 m Anisotropy Ratio (Kz/Kr): 1.

WELL DATA (LPH46-II_FH)

Initial Displacement: 0.43 m
Total Well Penetration Depth: 19.34 m
Casing Radius: 0.03 m
Static Water Column Height: 0.17 m
Screen Length: 3.05 m
Well Radius: 0.03 m

SOLUTION

Aquifer Model: Unconfined
Solution Method: Hvorslev
K = 1.035E-6 m/sec
y0 = 0.2081 m

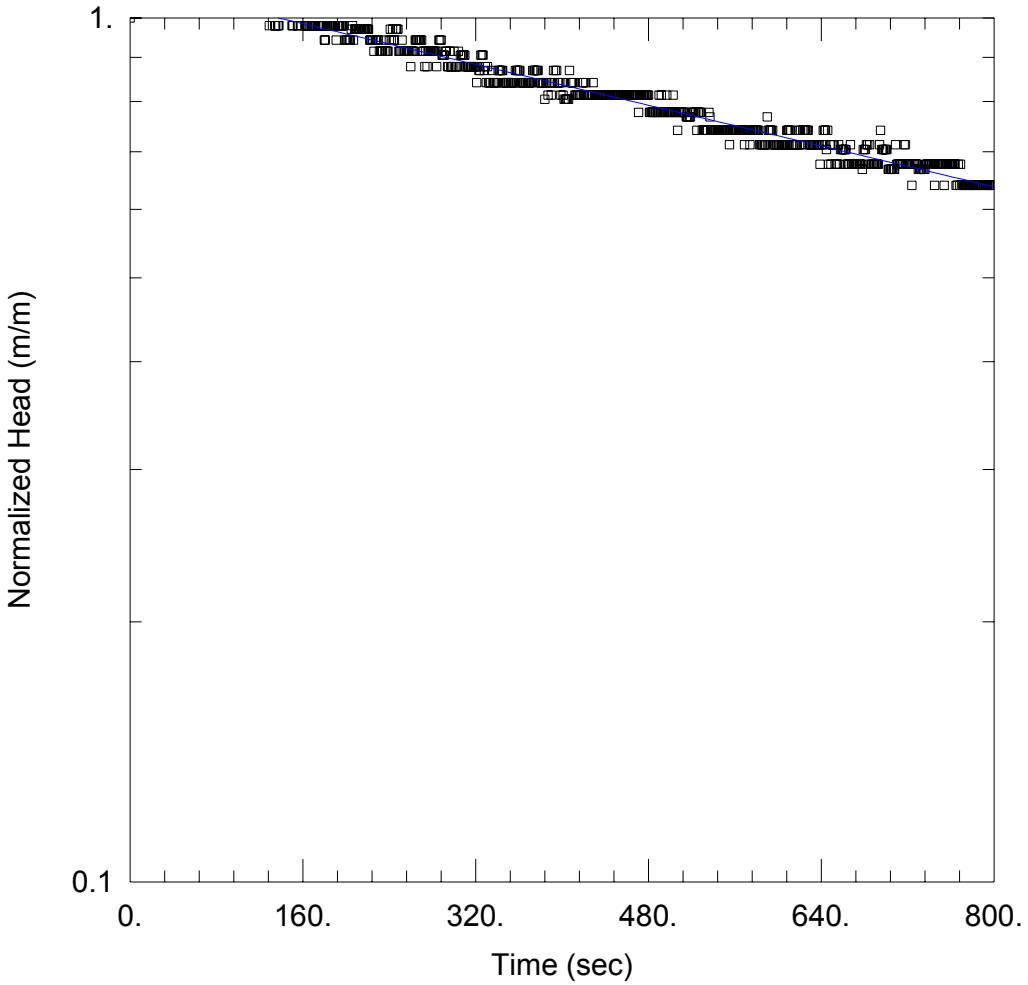

WELL TEST ANALYSIS

Data Set: W:\Grad Studies\Chalk River Field Work\AqteSOLV\Response Testing\LPH46-II_RH.aqt
Date: 12/08/14 Time: 14:20:56

PROJECT INFORMATION

Location: Chalk River: WMAF
Test Well: LPH25-I
Test Date: 27-Aug-14

AQUIFER DATA

Saturated Thickness: 19.34 m Anisotropy Ratio (Kz/Kr): 1.

WELL DATA (LPH46-II_RH)

Initial Displacement: 0.1 m Static Water Column Height: 0.17 m
Total Well Penetration Depth: 19.34 m Screen Length: 3.05 m
Casing Radius: 0.03 m Well Radius: 0.03 m

SOLUTION

Aquifer Model: Unconfined Solution Method: Hvorslev
K = 5.325E-7 m/sec y0 = 0.1098 m

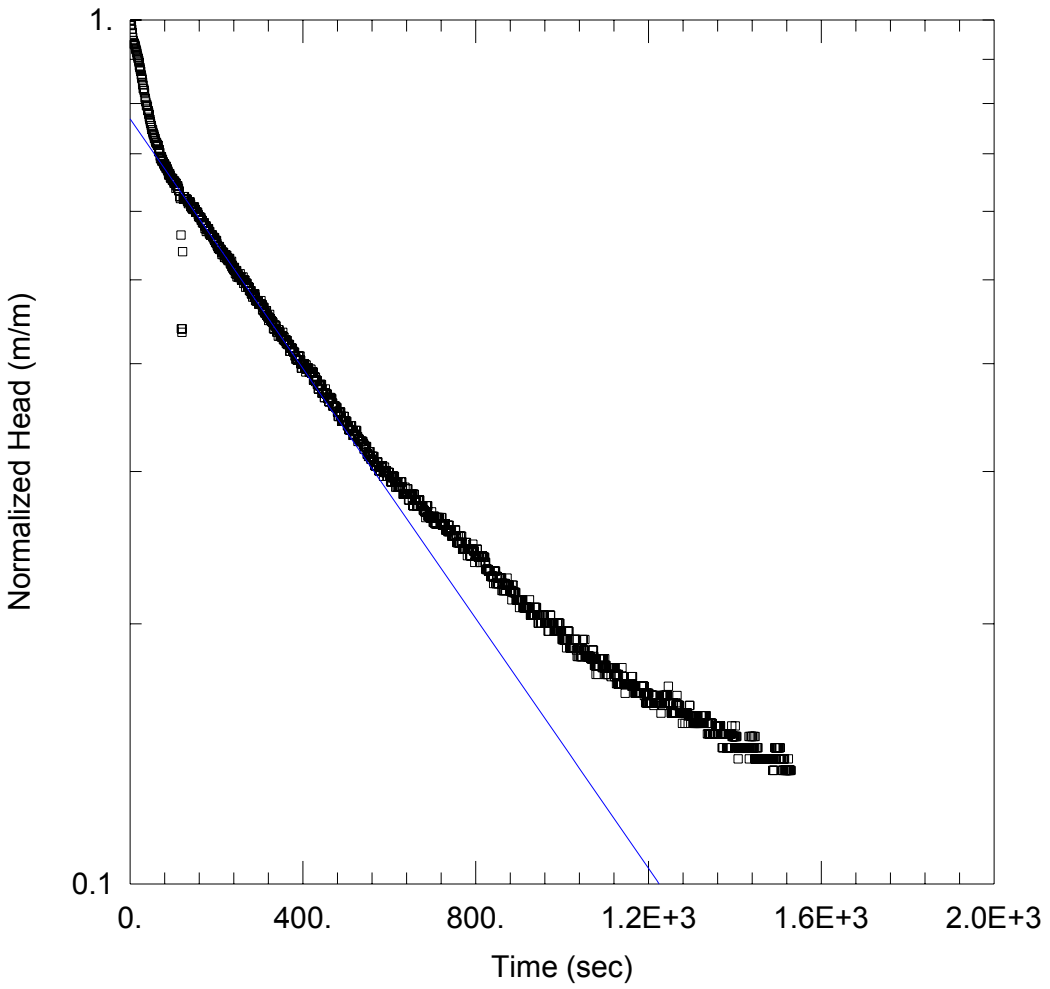

WELL TEST ANALYSIS

Data Set: W:\Grad Studies\Chalk River Field Work\AqteSOLV\Response Testing\LPH47-II_FH.aqt
Date: 12/08/14 Time: 14:21:30

PROJECT INFORMATION

Location: Chalk River: WMAF
Test Well: LPH25-I
Test Date: 27-Aug-14

AQUIFER DATA

Saturated Thickness: 2.71 m Anisotropy Ratio (Kz/Kr): 1.

WELL DATA (LPH47-II_FH)

Initial Displacement: 0.86 m Static Water Column Height: 0.13 m
Total Well Penetration Depth: 21.54 m Screen Length: 1.52 m
Casing Radius: 0.03 m Well Radius: 0.03 m

SOLUTION

Aquifer Model: Unconfined Solution Method: Hvorslev
K = 2.276E-6 m/sec y0 = 0.6606 m

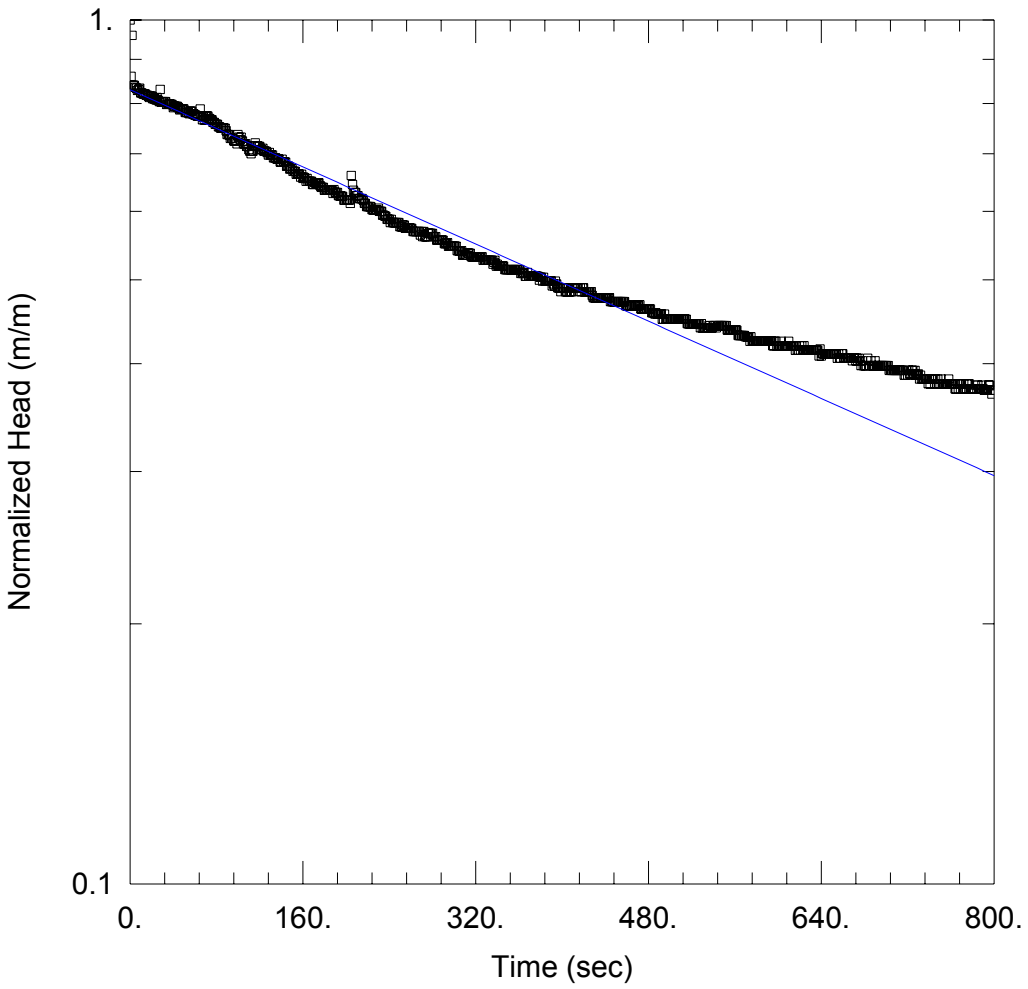

WELL TEST ANALYSIS

Data Set: W:\Grad Studies\Chalk River Field Work\AqteSOLV\Response Testing\LPH50-I_FH.aqt
Date: 12/08/14 Time: 14:22:09

PROJECT INFORMATION

Location: Chalk River: WMAF
Test Well: LPH25-I
Test Date: 27-Aug-14

AQUIFER DATA

Saturated Thickness: 10.83 m Anisotropy Ratio (Kz/Kr): 1.

WELL DATA (LPH50-I_FH)

Initial Displacement: 0.72 m Static Water Column Height: 1.18 m
Total Well Penetration Depth: 10.83 m Screen Length: 1.52 m
Casing Radius: 0.025 m Well Radius: 0.025 m

SOLUTION

Aquifer Model: Unconfined Solution Method: Hvorslev
K = 1.268E-6 m/sec y0 = 0.5975 m

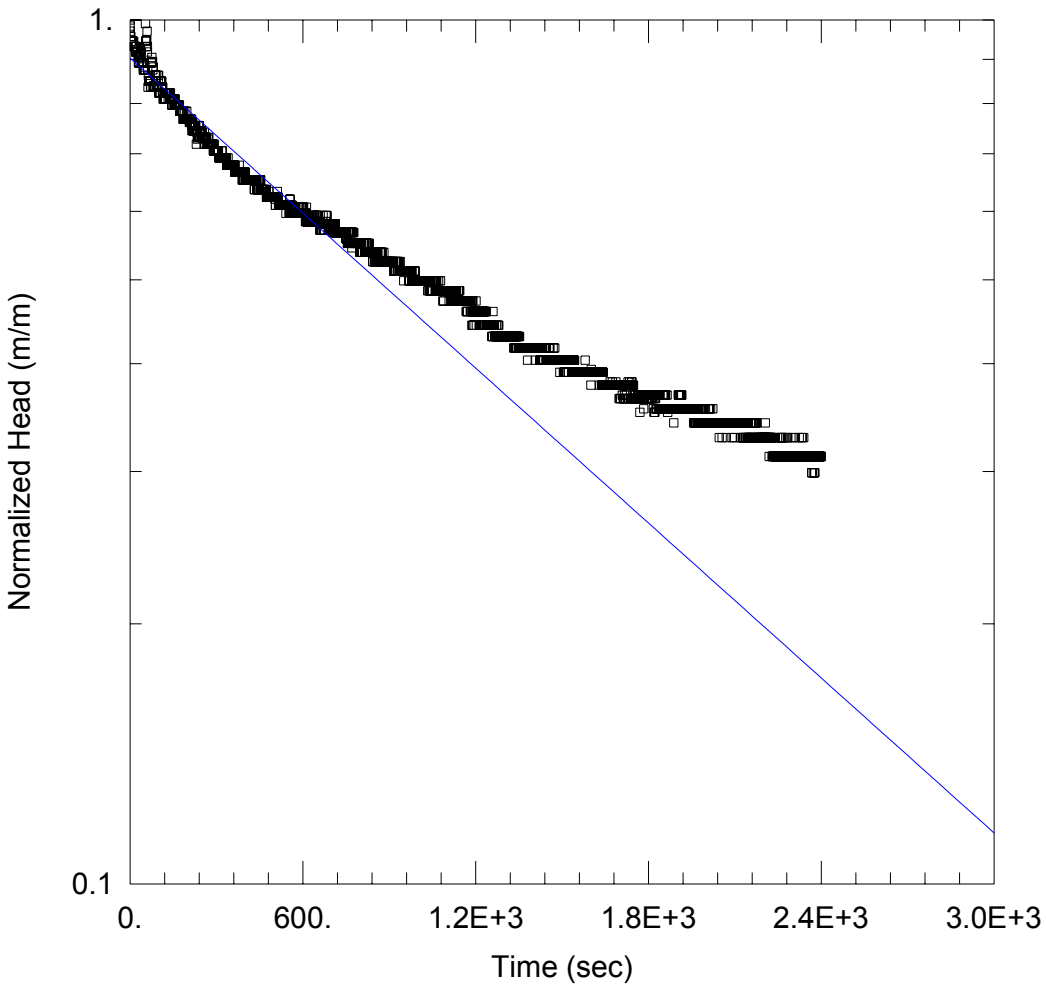

WELL TEST ANALYSIS

Data Set: W:\Grad Studies\Chalk River Field Work\AqteSOLV\Response Testing\LPH50-I_RH.aqt
Date: 12/08/14 Time: 14:24:26

PROJECT INFORMATION

Location: Chalk River: WMAF
Test Well: LPH25-I
Test Date: 27-Aug-14

AQUIFER DATA

Saturated Thickness: 10.83 m Anisotropy Ratio (Kz/Kr): 1.

WELL DATA (LPH50-I)

Initial Displacement: 0.28 m
Total Well Penetration Depth: 10.83 m
Casing Radius: 0.025 m
Static Water Column Height: 1.18 m
Screen Length: 1.52 m
Well Radius: 0.025 m

SOLUTION

Aquifer Model: Unconfined
Solution Method: Hvorslev
K = 6.793E-7 m/sec
y0 = 0.2528 m

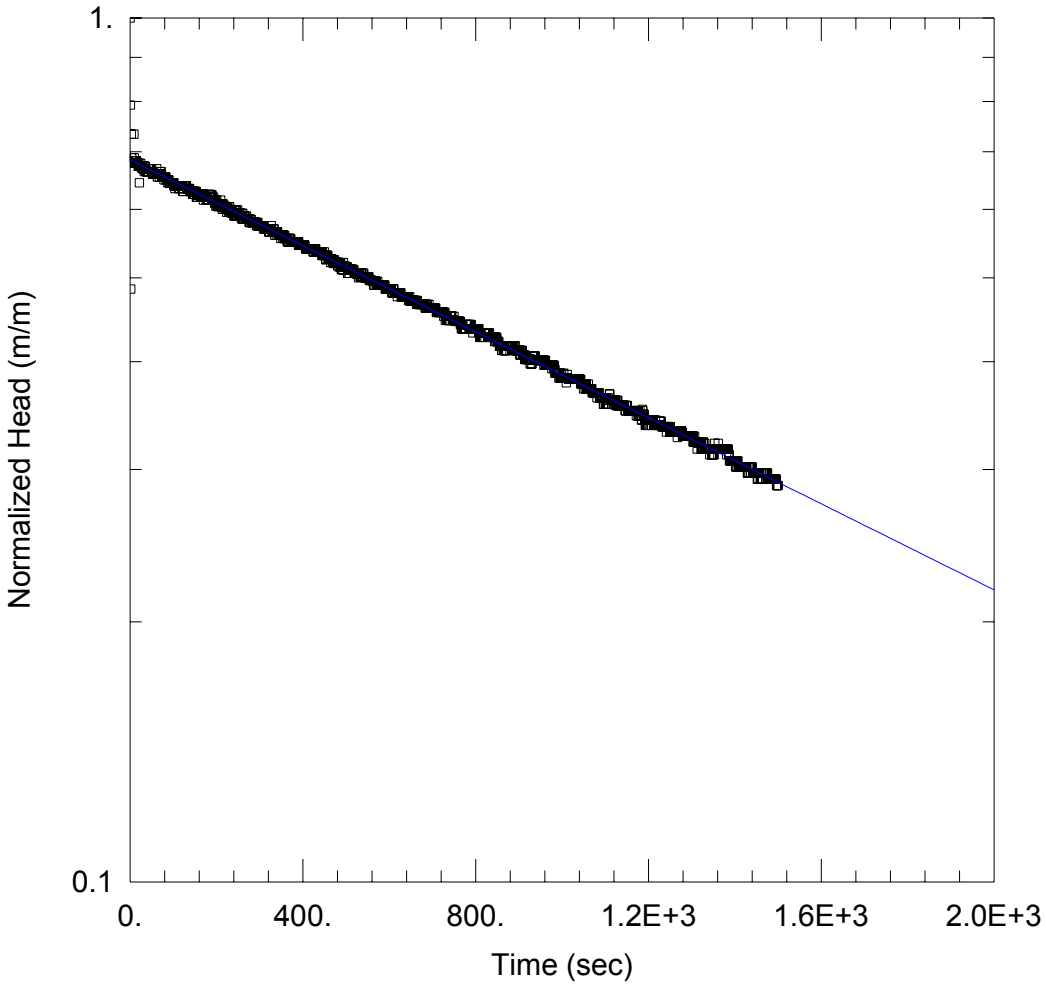

WELL TEST ANALYSIS

Data Set: W:\Grad Studies\Chalk River Field Work\AqteSOLV\Response Testing\LPH51-I_FH.aqt
Date: 12/08/14 Time: 14:24:58

PROJECT INFORMATION

Location: Chalk River: WMAF
Test Well: LPH25-I
Test Date: 27-Aug-14

AQUIFER DATA

Saturated Thickness: 2.44 m Anisotropy Ratio (Kz/Kr): 1.

WELL DATA (LPH51-I_FH)

Initial Displacement: 0.75 m Static Water Column Height: 6.6 m
Total Well Penetration Depth: 15.05 m Screen Length: 1.52 m
Casing Radius: 0.025 m Well Radius: 0.025 m

SOLUTION

Aquifer Model: Unconfined Solution Method: Hvorslev
K = 5.658E-7 m/sec y0 = 0.5139 m

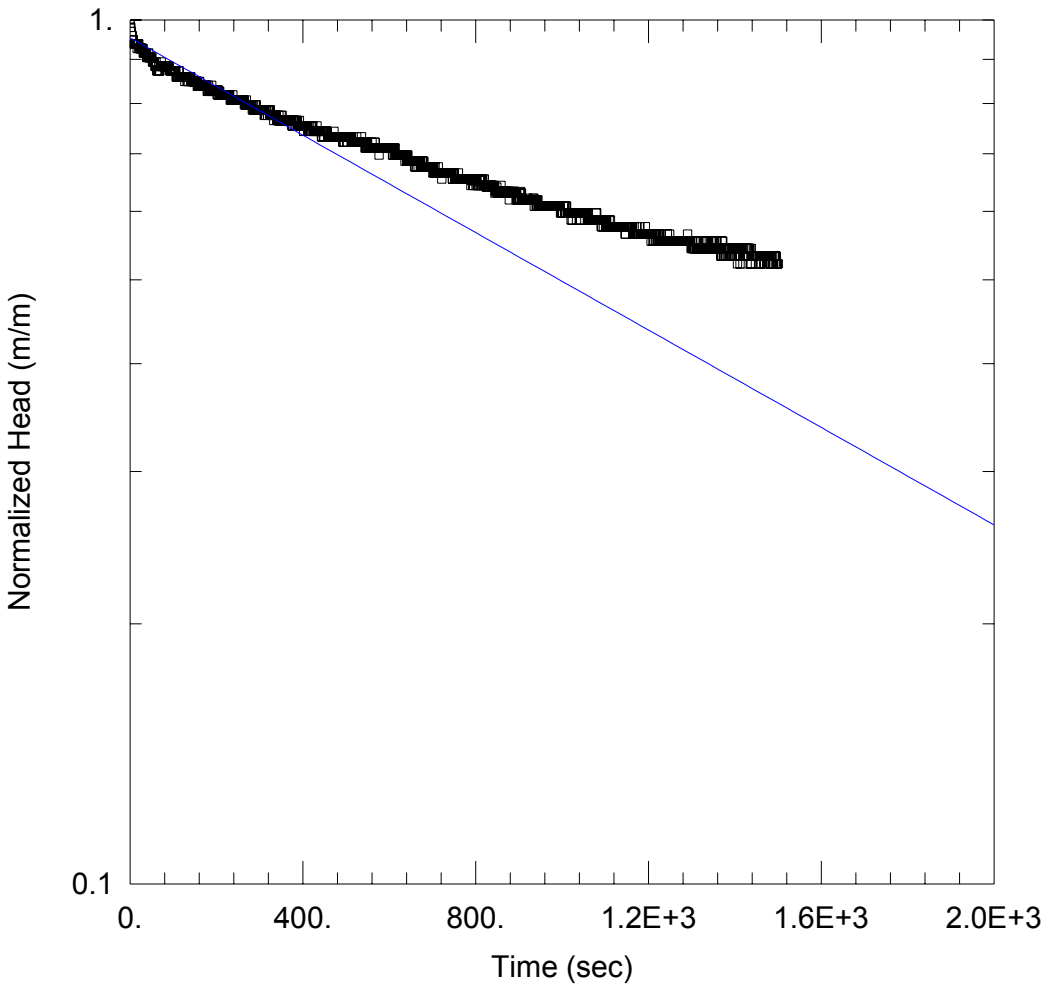

WELL TEST ANALYSIS

Data Set: W:\Grad Studies\Chalk River Field Work\AqteSOLV\Response Testing\LPH51-I_RH.aqt
Date: 12/08/14 Time: 14:25:27

PROJECT INFORMATION

Location: Chalk River: WMAF
Test Well: LPH25-I
Test Date: 27-Aug-14

AQUIFER DATA

Saturated Thickness: 2.44 m Anisotropy Ratio (Kz/Kr): 1.

WELL DATA (LPH-51_RH)

Initial Displacement: 0.34 m Static Water Column Height: 6.6 m
Total Well Penetration Depth: 15.05 m Screen Length: 1.52 m
Casing Radius: 0.025 m Well Radius: 0.025 m

SOLUTION

Aquifer Model: Unconfined Solution Method: Hvorslev
K = 6.406E-7 m/sec y0 = 0.3241 m

APPENDIX B

Modelling Scenario Parameter Matrix

Scenario	Multiplier			
	Hydraulic Conductivity	Dispersivity	Recharge (sloped area)	Recharge (waste area)
1	0.1	0.1	0.5	0.5
2	0.1	0.1	0.5	0.75
3	0.1	0.1	0.5	1
4	0.1	0.1	0.75	0.75
5	0.1	0.1	0.75	1.125
6	0.1	0.1	0.75	1.5
7	0.1	0.1	1	1
8	0.1	0.1	1	1.5
9	0.1	0.1	1	2
10	0.1	0.1	1.5	1.5
11	0.1	0.1	1.5	2.25
12	0.1	0.1	1.5	3
13	0.1	0.1	2	2
14	0.1	0.1	2	3
15	0.1	0.1	2	4
16	0.1	0.5	0.5	0.5
17	0.1	0.5	0.5	0.75
18	0.1	0.5	0.5	1
19	0.1	0.5	0.75	0.75
20	0.1	0.5	0.75	1.125
21	0.1	0.5	0.75	1.5
22	0.1	0.5	1	1
23	0.1	0.5	1	1.5
24	0.1	0.5	1	2
25	0.1	0.5	1.5	1.5
26	0.1	0.5	1.5	2.25
27	0.1	0.5	1.5	3
28	0.1	0.5	2	2
29	0.1	0.5	2	3
30	0.1	0.5	2	4
31	0.1	1	0.5	0.5
32	0.1	1	0.5	0.75
33	0.1	1	0.5	1
34	0.1	1	0.75	0.75
35	0.1	1	0.75	1.125
36	0.1	1	0.75	1.5
37	0.1	1	1	1
38	0.1	1	1	1.5
39	0.1	1	1	2

40	0.1	1	1.5	1.5
41	0.1	1	1.5	2.25
42	0.1	1	1.5	3
43	0.1	1	2	2
44	0.1	1	2	3
45	0.1	1	2	4
46	0.1	2	0.5	0.5
47	0.1	2	0.5	0.75
48	0.1	2	0.5	1
49	0.1	2	0.75	0.75
50	0.1	2	0.75	1.125
51	0.1	2	0.75	1.5
52	0.1	2	1	1
53	0.1	2	1	1.5
54	0.1	2	1	2
55	0.1	2	1.5	1.5
56	0.1	2	1.5	2.25
57	0.1	2	1.5	3
58	0.1	2	2	2
59	0.1	2	2	3
60	0.1	2	2	4
61	0.1	10	0.5	0.5
62	0.1	10	0.5	0.75
63	0.1	10	0.5	1
64	0.1	10	0.75	0.75
65	0.1	10	0.75	1.125
66	0.1	10	0.75	1.5
67	0.1	10	1	1
68	0.1	10	1	1.5
69	0.1	10	1	2
70	0.1	10	1.5	1.5
71	0.1	10	1.5	2.25
72	0.1	10	1.5	3
73	0.1	10	2	2
74	0.1	10	2	3
75	0.1	10	2	4
76	0.5	0.1	0.5	0.5
77	0.5	0.1	0.5	0.75
78	0.5	0.1	0.5	1
79	0.5	0.1	0.75	0.75
80	0.5	0.1	0.75	1.125
81	0.5	0.1	0.75	1.5

82	0.5	0.1	1	1
83	0.5	0.1	1	1.5
84	0.5	0.1	1	2
85	0.5	0.1	1.5	1.5
86	0.5	0.1	1.5	2.25
87	0.5	0.1	1.5	3
88	0.5	0.1	2	2
89	0.5	0.1	2	3
90	0.5	0.1	2	4
91	0.5	0.5	0.5	0.5
92	0.5	0.5	0.5	0.75
93	0.5	0.5	0.5	1
94	0.5	0.5	0.75	0.75
95	0.5	0.5	0.75	1.125
96	0.5	0.5	0.75	1.5
97	0.5	0.5	1	1
98	0.5	0.5	1	1.5
99	0.5	0.5	1	2
100	0.5	0.5	1.5	1.5
101	0.5	0.5	1.5	2.25
102	0.5	0.5	1.5	3
103	0.5	0.5	2	2
104	0.5	0.5	2	3
105	0.5	0.5	2	4
106	0.5	1	0.5	0.5
107	0.5	1	0.5	0.75
108	0.5	1	0.5	1
109	0.5	1	0.75	0.75
110	0.5	1	0.75	1.125
111	0.5	1	0.75	1.5
112	0.5	1	1	1
113	0.5	1	1	1.5
114	0.5	1	1	2
115	0.5	1	1.5	1.5
116	0.5	1	1.5	2.25
117	0.5	1	1.5	3
118	0.5	1	2	2
119	0.5	1	2	3
120	0.5	1	2	4
121	0.5	2	0.5	0.5
122	0.5	2	0.5	0.75
123	0.5	2	0.5	1

124	0.5	2	0.75	0.75
125	0.5	2	0.75	1.125
126	0.5	2	0.75	1.5
127	0.5	2	1	1
128	0.5	2	1	1.5
129	0.5	2	1	2
130	0.5	2	1.5	1.5
131	0.5	2	1.5	2.25
132	0.5	2	1.5	3
133	0.5	2	2	2
134	0.5	2	2	3
135	0.5	2	2	4
136	0.5	10	0.5	0.5
137	0.5	10	0.5	0.75
138	0.5	10	0.5	1
139	0.5	10	0.75	0.75
140	0.5	10	0.75	1.125
141	0.5	10	0.75	1.5
142	0.5	10	1	1
143	0.5	10	1	1.5
144	0.5	10	1	2
145	0.5	10	1.5	1.5
146	0.5	10	1.5	2.25
147	0.5	10	1.5	3
148	0.5	10	2	2
149	0.5	10	2	3
150	0.5	10	2	4
151	1	0.1	0.5	0.5
152	1	0.1	0.5	0.75
153	1	0.1	0.5	1
154	1	0.1	0.75	0.75
155	1	0.1	0.75	1.125
156	1	0.1	0.75	1.5
157	1	0.1	1	1
158	1	0.1	1	1.5
159	1	0.1	1	2
160	1	0.1	1.5	1.5
161	1	0.1	1.5	2.25
162	1	0.1	1.5	3
163	1	0.1	2	2
164	1	0.1	2	3
165	1	0.1	2	4

166	1	0.5	0.5	0.5
167	1	0.5	0.5	0.75
168	1	0.5	0.5	1
169	1	0.5	0.75	0.75
170	1	0.5	0.75	1.125
171	1	0.5	0.75	1.5
172	1	0.5	1	1
173	1	0.5	1	1.5
174	1	0.5	1	2
175	1	0.5	1.5	1.5
176	1	0.5	1.5	2.25
177	1	0.5	1.5	3
178	1	0.5	2	2
179	1	0.5	2	3
180	1	0.5	2	4
181	1	1	0.5	0.5
182	1	1	0.5	0.75
183	1	1	0.5	1
184	1	1	0.75	0.75
185	1	1	0.75	1.125
186	1	1	0.75	1.5
187	1	1	1	1
188	1	1	1	1.5
189	1	1	1	2
190	1	1	1.5	1.5
191	1	1	1.5	2.25
192	1	1	1.5	3
193	1	1	2	2
194	1	1	2	3
195	1	1	2	4
196	1	2	0.5	0.5
197	1	2	0.5	0.75
198	1	2	0.5	1
199	1	2	0.75	0.75
200	1	2	0.75	1.125
201	1	2	0.75	1.5
202	1	2	1	1
203	1	2	1	1.5
204	1	2	1	2
205	1	2	1.5	1.5
206	1	2	1.5	2.25
207	1	2	1.5	3

208	1	2	2	2
209	1	2	2	3
210	1	2	2	4
211	1	10	0.5	0.5
212	1	10	0.5	0.75
213	1	10	0.5	1
214	1	10	0.75	0.75
215	1	10	0.75	1.125
216	1	10	0.75	1.5
217	1	10	1	1
218	1	10	1	1.5
219	1	10	1	2
220	1	10	1.5	1.5
221	1	10	1.5	2.25
222	1	10	1.5	3
223	1	10	2	2
224	1	10	2	3
225	1	10	2	4
226	2	0.1	0.5	0.5
227	2	0.1	0.5	0.75
228	2	0.1	0.5	1
229	2	0.1	0.75	0.75
230	2	0.1	0.75	1.125
231	2	0.1	0.75	1.5
232	2	0.1	1	1
233	2	0.1	1	1.5
234	2	0.1	1	2
235	2	0.1	1.5	1.5
236	2	0.1	1.5	2.25
237	2	0.1	1.5	3
238	2	0.1	2	2
239	2	0.1	2	3
240	2	0.1	2	4
241	2	0.5	0.5	0.5
242	2	0.5	0.5	0.75
243	2	0.5	0.5	1
244	2	0.5	0.75	0.75
245	2	0.5	0.75	1.125
246	2	0.5	0.75	1.5
247	2	0.5	1	1
248	2	0.5	1	1.5
249	2	0.5	1	2

250	2	0.5	1.5	1.5
251	2	0.5	1.5	2.25
252	2	0.5	1.5	3
253	2	0.5	2	2
254	2	0.5	2	3
255	2	0.5	2	4
256	2	1	0.5	0.5
257	2	1	0.5	0.75
258	2	1	0.5	1
259	2	1	0.75	0.75
260	2	1	0.75	1.125
261	2	1	0.75	1.5
262	2	1	1	1
263	2	1	1	1.5
264	2	1	1	2
265	2	1	1.5	1.5
266	2	1	1.5	2.25
267	2	1	1.5	3
268	2	1	2	2
269	2	1	2	3
270	2	1	2	4
271	2	2	0.5	0.5
272	2	2	0.5	0.75
273	2	2	0.5	1
274	2	2	0.75	0.75
275	2	2	0.75	1.125
276	2	2	0.75	1.5
277	2	2	1	1
278	2	2	1	1.5
279	2	2	1	2
280	2	2	1.5	1.5
281	2	2	1.5	2.25
282	2	2	1.5	3
283	2	2	2	2
284	2	2	2	3
285	2	2	2	4
286	2	10	0.5	0.5
287	2	10	0.5	0.75
288	2	10	0.5	1
289	2	10	0.75	0.75
290	2	10	0.75	1.125
291	2	10	0.75	1.5

292	2	10	1	1
293	2	10	1	1.5
294	2	10	1	2
295	2	10	1.5	1.5
296	2	10	1.5	2.25
297	2	10	1.5	3
298	2	10	2	2
299	2	10	2	3
300	2	10	2	4
301	10	0.1	0.5	0.5
302	10	0.1	0.5	0.75
303	10	0.1	0.5	1
304	10	0.1	0.75	0.75
305	10	0.1	0.75	1.125
306	10	0.1	0.75	1.5
307	10	0.1	1	1
308	10	0.1	1	1.5
309	10	0.1	1	2
310	10	0.1	1.5	1.5
311	10	0.1	1.5	2.25
312	10	0.1	1.5	3
313	10	0.1	2	2
314	10	0.1	2	3
315	10	0.1	2	4
316	10	0.5	0.5	0.5
317	10	0.5	0.5	0.75
318	10	0.5	0.5	1
319	10	0.5	0.75	0.75
320	10	0.5	0.75	1.125
321	10	0.5	0.75	1.5
322	10	0.5	1	1
323	10	0.5	1	1.5
324	10	0.5	1	2
325	10	0.5	1.5	1.5
326	10	0.5	1.5	2.25
327	10	0.5	1.5	3
328	10	0.5	2	2
329	10	0.5	2	3
330	10	0.5	2	4
331	10	1	0.5	0.5
332	10	1	0.5	0.75
333	10	1	0.5	1

334	10	1	0.75	0.75
335	10	1	0.75	1.125
336	10	1	0.75	1.5
337	10	1	1	1
338	10	1	1	1.5
339	10	1	1	2
340	10	1	1.5	1.5
341	10	1	1.5	2.25
342	10	1	1.5	3
343	10	1	2	2
344	10	1	2	3
345	10	1	2	4
346	10	2	0.5	0.5
347	10	2	0.5	0.75
348	10	2	0.5	1
349	10	2	0.75	0.75
350	10	2	0.75	1.125
351	10	2	0.75	1.5
352	10	2	1	1
353	10	2	1	1.5
354	10	2	1	2
355	10	2	1.5	1.5
356	10	2	1.5	2.25
357	10	2	1.5	3
358	10	2	2	2
359	10	2	2	3
360	10	2	2	4
361	10	10	0.5	0.5
362	10	10	0.5	0.75
363	10	10	0.5	1
364	10	10	0.75	0.75
365	10	10	0.75	1.125
366	10	10	0.75	1.5
367	10	10	1	1
368	10	10	1	1.5
369	10	10	1	2
370	10	10	1.5	1.5
371	10	10	1.5	2.25
372	10	10	1.5	3
373	10	10	2	2
374	10	10	2	3
375	10	10	2	4